ULTRAVIOLET CURABLE ACRYLIC COPOLYMER BASED ELECTROLYTES FOR DYE-SENSITIZED SOLAR CELL APPLICATION

NURUL AKMALIAH BT DZULKURNAIN

INSTITUTE OF GRADUATE STUDIES
UNIVERSITY OF MALAYA
KUALA LUMPUR

2016

ULTRAVIOLET CURABLE ACRYLIC COPOLYMER BASED ELECTROLYTES FOR DYE-SENSITIZED SOLAR CELL APPLICATION

NURUL AKMALIAH BT DZULKURNAIN

THESIS SUBMITTED IN FULFILMENT OF THE REQUIREMENTS FOR THE DEGREE OF DOCTOR OF PHILOSOPHY/APPLIED SCIENCE

INSTITUTE OF GRADUATE STUDIES
UNIVERSITY OF MALAYA
KUALA LUMPUR

2016

UNIVERSITY OF MALAYA

ORIGINAL LITERARY WORK DECLARATION

Name of Candidate: **NURUL AKMALIAH BT DZULKURNAIN**

(I.C/Passport No:)

Registration/Matric No: **HHC 120006**

Name of Degree: **DOCTOR OF PHILOSOPHY**

Title of Project Paper/Research Report/Dissertation/Thesis ("this Work"):

ULTRAVIOLET CURABLE ACRYLIC COPOLYMER BASED ELECTROLYTES FOR DYE-SENSITIZED SOLAR CELL APPLICATION

Field of Study: **APPLIED SCIENCE**

I do solemnly and sincerely declare that:

(1) I am the sole author/writer of this Work;
(2) This Work is original;
(3) Any use of any work in which copyright exists was done by way of fair dealing and for permitted purposes and any excerpt or extract from, or reference to or reproduction of any copyright work has been disclosed expressly and sufficiently and the title of the Work and its authorship have been acknowledged in this Work;
(4) I do not have any actual knowledge nor do I ought reasonably to know that the making of this work constitutes an infringement of any copyright work;
(5) I hereby assign all and every rights in the copyright to this Work to the University of Malaya ("UM"), who henceforth shall be owner of the copyright in this Work and that any reproduction or use in any form or by any means whatsoever is prohibited without the written consent of UM having been first had and obtained;
(6) I am fully aware that if in the course of making this Work I have infringed any copyright whether intentionally or otherwise, I may be subject to legal action or any other action as may be determined by UM.

Candidate's Signature Date:

Subscribed and solemnly declared before,

Witness's Signature Date:

Name:

Designation:

ABSTRACT

New copolymers using methyl methacrylate (MMA) and ethyl methacrylate (EMA) monomers were randomly copolymerized via free-radical bulk polymerization method towards development as solid electrolyte in dye sensitized solar cell (DSSC). In this study, copolymer of 90MMA:10EMA showed the most promising characteristics to be used as host in polymer electrolytes due to its smooth cross sectional surface, lowest resistivity, low molecular weight, and glass transition temperature. Therefore, 90MMA:10EMA was incorporated with different weight ratios of lithium iodide and sodium iodide. The complexation between salts and copolymer host has been investigated using Fourier transform infrared spectroscopy. The ionic conductivity and thermal stability of the electrolytes were measured using impedance spectroscopy and differential scanning calorimetry, respectively. The highest ionic conductivities found for lithium iodide and sodium iodide systems were at 20 wt% with the value of 1.3×10^{-6} S cm^{-1} and 5.19×10^{-6} S·cm^{-1} respectively. The DSSCs employing the copolymer electrolytes with suitable working and counter electrodes were tested under AM 1.5 illumination at a light intensity of 100 mW·cm^{-2}. The DSSC exhibited photo-conversion efficiency of 0.45% for electrolytes containing lithium iodide and 0.62% for that containing sodium iodide. Furthermore, lithium and sodium iodide based polymer systems were added with 1-Methyl 3-propyl imidazolium iodide ionic liquid to study the characteristics of the electrolytes and to enhance the photo conversion efficiency of DSSCs. The electrolyte for both systems exhibited highest ionic conductivity at 6 wt% of ionic liquid with the value of 8.93×10^{-8} S cm^{-1} for lithium based and 4.43×10^{-5} S cm^{-1} for sodium based. The photo-conversion efficiency of DSSC employing ionic liquid based electrolytes demonstrated an increment of 1.19% for copolymer-lithium iodide-ionic liquid and 1.05% for copolymer-sodium iodide-ionic liquid. These performances strongly suggested that the polymer electrolytes are promising electrolytes for DSSC application.

ABSTRAK

Kopolimer baru menggunakan metil metakrilat (MMA) dan etil metakrilat (EMA) monomer telah dikopolimerasi secara rawak melalui kaedah radikal bebas pempolimeran pukal dan digunakan untuk pembuatan pepejal elektrolit di dalam pewarna sensitif sel solar (DSSC). Di dalam kajian ini, kopolimer 90MMA: 10EMA menunjukkan kriteria yang paling sesuai untuk digunakan sebagai perumah dalam elektrolit polimer kerana keratan rentas permukaan yang licin, nilai kerintangan yang paling rendah, berat molekular dan suhu peralihan kaca yang rendah. Oleh itu, 90MMA: 10EMA dicampurkan dengan nisbah berat litium iodida dan natrium iodida yang berbeza. Kompleksi antara garam dan perumah kopolimer telah dikaji menggunakan spektroskopi inframerah. Kekonduksian ionik dan kestabilan terma elektrolit diukur menggunakan spektroskopi impedans dan pengimbasan kalorimeter. Kekonduksian ionik tertinggi bagi sistem litium iodida dan natrium iodida adalah pada 20 wt% dengan nilai masing-masing adalah 1.3×10^{-6} S cm^{-1} dan 5.19×10^{-6} S cm^{-1}. DSSC yang terdiri daripada elektrolit polimer dengan elektrod kerja dan elektrod kaunter yang sesuai telah di uji di bawah pencahayaan AM 1.5 pada keaamatan cahaya 100 mW.cm^{-2}. DSSC tersebut mencapai kecekapan foto-penukaran sebanyak 0.45% untuk elektrolit yang mengandungi litium iodida dan 0.62% bagi yang mengandungi natrium iodida. Seterusnya, litium dan natrium iodida berasaskan sistem polimer telah ditambah dengan 1-Methyl 3-propyl imidazolium cecair ionik iodida untuk mengkaji ciri-ciri elektrolit tersebut dan penambahbaikan dalam kecekapan foto-penukaran DSSC. Elektrolit bagi kedua-dua sistem telah mencapai kekonduksian ionik tertinggi pada 6wt% cecair ionik dengan nilainya 8.94×10^{-8} S cm^{-1} untuk yang berasaskan lithium dan 4.43×10^{-5} S cm^{-1} untuk yang berasaskan natrium. Kecekapan foto-penukaran DSSC menggunakan elektrolit berasaskan cecair ionik menunjukkan peningkatan dengan 1.19% untuk kopolimer-litium iodida-cecair ionik dan 1.05% untuk kopolimer-natrium iodida-cecair ionik. Prestasi ini kuat menunjukkan bahawa elektrolit polimer ini adalah sesuai sebagai elektrolit untuk diaplikasi dalam DSSC

ACKNOWLEDGEMENTS

In the name of Allah S.W.T., the Most Gracious and the Most Merciful.

Alhamdulillah, a lot of thanks to Allah S.W.T for His blessings for me to complete this PhD thesis.

First and foremost, I would like to express my deepest gratitude to my supervisors, Prof. Dr. Nor Sabirin Mohamed and Prof. Dr. Azizan Ahmad for their support in my research and patiently corrected my thesis. My appreciation also goes to all my friends in Electrochemical Materials Devices research group and Polymer Ionic Group (UKM) for their moral support and guidance. It would have been lonely laboratory without them. I would also like to thank both of our research lab Science Officer and Assistant Science Officer for their help and cooperation. The University of Malaya Bright Spark scholarship and postgraduate research fund PPP (PG109-2013A) for making this research possible are also greatly acknowledged.

Very special thanks to my father, Mr. Dzulkurnain Mohd Isa, my mother, Mrs. Zaimah Mahamood, mother in law, Nelmawati Kadinan and my siblings for their prayers, encouragement, support and attention. I am also grateful to my husband and son, Mr. Syahrul Nellis and Muhammad Luqman Al-Hakim in cheering me up and stood by me through the good times and bad in order to complete this thesis.

TABLE OF CONTENTS

LIST OF FIGURES

LIST OF TABLES

LIST OF ABBREVIATIONS

AM	Air Mass
ATR	Attenuated Total Reflection
AIBN	Azobisisobutyronitrile
AZO	Aluminum doped ZnO
CB	Conduction Band
CdSe	Cadmium selenide
CZTS	Copper zinc tin sulfide
DC	Direct current
DEC	Diethyl carbonate
DMA	Dynamic Mechanical Analyzer
DMC	Dimethyl Carbonate
DMPA	2,2-Dimethoxy-2-phenylacetophenone
DSC	Differential Scanning Calorimetry
DSSC	Dye Sensitized Solar Cell
EA	Ethyl acrylate
EC	Ethylene Carbonate
EMA	Ethyl Methacrylate
EGMEM	Ethylene Glycol Methyl Ether Methacrylate
FTIR	Fourier transform Infrared spectroscopy
FTO	Fluorine doped Tin Oxide
GMA	Glycidyl Methacrylate
GPC	Gel Permeatography Calorimetry
H^+	Hydrogen ion
H_2O	Oxidane

I^-	Iodide ion
I_3^-	Triiodide ion
I_2	Iodine
IS	Impedance spectroscopy
ITO	Indium Tin Oxide
KOH	Potassium hydroxide
Li^+	Lithium ion
LiI	Lithium iodide
LSV	Linear Sweep Voltammetry
MMA	Methyl Methacrylate
N719	cis-diisothiocyanato-bis(2,2'-bipyridyl-4,4'-dicarboxylato) ruthenium(II) bis(tetrabutylammonium)
Na^+	Sodium ion
NaI	Sodium iodide
O_2	Oxygen
PC	Propylene carbonate
PEC	Polyestercarbonates
PEMA	Poly(ethyl methacrylate)
PEO	Poly(ethylene oxide)
PMMA	Poly(methyl methacrylate)
PMII	1-methyl 3-propyl imidazolium iodide
Pt	Platinum
PVA	Polyvinyl alcohol
PVC	Poly(vinyl chloride)
PVdF-HFP	Poly(vinlylidene fluoride hexafluoro propylene)
PVP	Poly(N-vinylpyrrolidone)

RAFT	Reversible Addition-Fragmentation chain Transfer
RI	Refractive Index
RT	Room temperature
SEM	Scanning Electron Microscopy
SnO_2	Tin (IV) oxide
SPE	Solid Polymer Elelctrolytes
$SrTiO_3$	Strontium Titanate
TCO	Transparent Conductive Oxide
THF	Tetrahydrofuran
TiO_2	Titanium oxide
UV	Ultraviolet
VB	Valence Band
ZnO	Zinc Oxide
ZnTe	Zinc telluride
Zn_2SnO_4	Zinc stannate
ZrO_2	Zirconium oxide

LIST OF SYMBOLS

A	Area of blocking electrode
R_b	Bulk resistance
ε	Dielectric constant
ε^*	Complex dielectric constant
E_a	Activation energy
FF	Fill factor
f_{max}	Relaxation frequency peak
σ	Conductivity
σ_i	Conductivity contributed by ions (cations/anions)
σ_e	Conductivity contributed by electrons/holes
σ_T	Total conductivity
ε	Dielectric constant
T_g	Glass transition temperature
T_m	Melting temperature
$Tan\ \delta$	Loss tangent
τ	Relaxation time
ΔH_m	Heat of fusion
Z_r	Real impedance
t_{ion}	Ionic transference number
M_w	Molecular weight
σ_o	Pre-exponential factor
Z_i	Imaginary impedance
ε_r	Real part of the dielectric constant
i_e	Residual current

I_0	Initial current
I_{ss}	Steady state current
J_{sc}	Short circuit current density
P_{in}	Incident light power density
R_0	Electrode resistance before polarization
R_{ss}	Electrode resistance after polarization
t	Thickness
t_e	Transference number of electron
t_i	Transference number of ion
i_T	Total current
C_o	Vacuum capacitance
wt %	Weight ratio
n	Refractive index
ΔV	Applied potential
V_{oc}	Open circuit voltage
V_{max}	Voltage maximum
J_{max}	Current density maximum

CHAPTER 1: INTRODUCTION

1.0 Background

Photovoltaic technology utilizing solar energy has received considerable attention as one of the environmentally sustainable energy technologies. One type of photovoltaic technology is dye-sensitized solar cell (DSSC) which provides a promising alternative to conventional p–n junction photovoltaic devices because of their relatively high photoelectric conversion efficiency, various choices of materials that can be used, and low environmental impact during fabrication (Lewis, 2007; Kim et al., 2008; Caramori et al., 2010; Preat et al., 2010; Hardin et al., 2012; Negro et al., 2012). DSSC consists of a dye-coated mesoporous nanocrystalline metal oxide photoanode electrode, modified platinum counter electrode and a thin polymer electrolyte layer sandwiched between the two electrodes. The polymer electrolyte membrane which is sealed between the two electrodes usually composed of I^-/I_3^- redox couple in organic solvents.

DSSC's prototype reported in 1991 achieved the power conversion efficiency about 11% by employing organic-solvent as the electrolyte (O'Regan & Grätzel, 1991; Nazeeruddin et al., 1993). Since then, DSSCs have received great attention and broad research over the world due to their high power conversion efficiency, low manufacturing cost and simple preparation technique. However, most of the cells that give high efficiency utilize liquid electrolytes, which cause some problems, such as leakage, volatilization, corrosion at the counter electrode, difficulty in fabrication and limited long-term performance (Nogueira et al., 2001; Kubo et al., 2002; Lin et al., 2011; Bari et al., 2012; Mastroianni et al., 2012). Replacing liquid electrolytes with solid polymer electrolytes (SPEs) has become one of the approaches to overcome those problems (Tennakone et al., 1995; Bach et al., 1998; Li et al., 2006). Besides, SPEs have been reported to show promising results for application in DSSCs (Nogueira et al., 2001; Günes & Sariciftci, 2008). SPEs are also safer, free from leakage problems, show good thermal stability and are easier to handle for device fabrication (Meng et al., 2003; Hirata et al., 2006; Yang et al., 2008; Imperiyka et al., 2014; Su'ait et al., 2015).

Even though solid polymer electrolytes (SPEs) render many advantages over liquid electrolyte systems, SPEs still have some limitations such as low room temperature ionic conductivity and poor mechanical stability (Ratner et al., 1987; Armand, 1990; Croce et al., 1998; Croce et al., 2000). There are several methods that have been proposed in order to improve the performance of SPEs such as modification of polymer hosts (Kim et al., 2005; Mobarak & Abdullah, 2010; Bella et al., 2013; Mobarak et al., 2013), addition of plasticizers or addition of fillers (Armand, 1990; Capuano et al., 1991; Tarascon et al., 1996). Among them, modification of polymer host becomes the main approach to enhance the properties of SPEs because polymer host plays an important role for ion transport mechanism in the SPEs (Bella & Bongiovanni, 2013; Weerasinghe et al., 2013; Shukla et al., 2014). Modification can be made by copolymerization technique (Decker, 1996; Bella et al., 2013; Imperiyka et al., 2014). Patel and coworkers have reported that copolymerization is the most successful technique to obtain materials with tailor made properties (Soykan et al., 2000; Andrzejewska, 2001; Strub, 2008; Patel et al., 2012). Oh et al (2001) and Balakrishnan et al (2013) have modified copolymers with two or more functional monomers as a solution to prevent the leakage problem of liquid electrolyte and improve the mechanical strength of gel polymer electrolytes (Oh et al., 2001; Balakrishnan et al., 2013). In addition, copolymerization were also reported to develop gel polymer electrolytes with enhanced ionic conductivity and charge-discharge cycle performance (Ichino et al., 1995; Yamazaki et al., 1995).

In recent years, many studies have been carried out on acrylic monomers because they are the most versatile family of monomers that can be used to form acrylate polymers based on the structure of acrylic acid, which consists of a vinyl group and a carboxylic acid terminus (Frechet et al., 1995; Yagci et al., 2010). For example, Reddy and coworkers have investigated the copolymerization of phenyl monomer (n-phenyl methacrylamide) with ethyl methacrylate (EMA) (Reddy et al., 2010). Roy and coworkers have investigated the RAFT copolymerization of N,N-(dimethylamino)ethyl methacrylate and methyl methacrylate (MMA) (Roy et al., 2013). Other than these works, many other researches have also done works on acrylic based polymer, but mostly for use in coating and paint (Balakrishnan et al., 2013; Lee et al., 2015). Only a few studies on acrylic based polymer electrolytes for application in DSSC have been done. However, the acrylic based polymer electrolytes have been prepared in the form of quasi solid electrolyte (Li et al., 2010; Tang et al., 2011).

Acrylic is thermoplastic resin which can be dissolved in suitable solvents such as aromatic hydrocarbons, acetone, alogenated hydrocarbons, and methyl ethyl ketone. Acrylic can cross-link by itself under ultraviolet exposure to a different extent as a function of specific type of polymer and temperature of exposure in respect to the glass transition of the polymer itself. In the case of acrylic, polymerization can be induced by UV curing technique. This technique has been recognized as a useful technology to transform instantly liquid photo reactive materials consisting of monomers and/or prepolymers into cured film in the presence of photoinitiators (Garnett, 1995; Decker, 1996; Bella & Bongiovanni, 2013). It has been shown to increase production speed, reduce reject rates, improve scratch and solvent resistance, and facilitate superior bonding. The technique is also important for the environmental preservation because of its high energy efficiencies and reduced emission of volatile organic compounds.

1.1 Problem Statement

A lot of research on acrylic based polymers has been carried out for application in paints, coatings, and others. Only a few researches on the acrylic-based polymer electrolytes for use in DSSC have been carried out but all the polymer electrolytes were prepared in the form of gel polymer electrolytes (Wu et al., 2007; Li et al., 2010; Boonsin et al., 2012; Bella et al., 2013). However, the main problems of usage acrylic based gel polymer electrolyte in DSSC are leakage for long term use and the needs of rigorous sealing procedure (Imperiyka et al., 2014). Therefore preparing acrylic based polymer electrolytes in solid form may offer alternative electrolyte materials to overcome these problems.

Preparing polymer electrolytes in solid form has main disadvantages which is low in ionic conductivity. Therefore, in order to overcome this problem, modification of the polymer host can be made. This is because polymer host plays an important role to for ions movement in the polymer electrolytes. There are a few types of modification of polymer host which are blending, plasticizing or copolymerizing (Li et al., 2010; Rudhziah et al., 2011; Boonsin et al., 2012; Imperiyka et al., 2013; Rudhziah et al., 2015). Among the techniques, copolymerization technique is the most useful technique to modify the polymers. This technique can be induced using UV curing technique which is the most effective techniques to produce instantaneously highly cross-linked materials in flexible film form (Gerbaldi et al., 2010; Bella & Bongiovanni, 2013). UV curing technique was used in the attempt to obtain acrylic copolymer film via an easy and fast technique. Besides that, the solvent-free, high-rate of curing reaction and ease of applicability are the main advantages of UV-curing technique. (Decker, 1996; Nair et al., 2008; Bella & Bongiovanni, 2013; Bella et al., 2013). This technique may offer some advantages to obtain free standing film of acrylic based copolymers suitable for polymer electrolytes.

Addition of salts is important for ions contributor in solid polymer electrolytes system. In this study, iodide based ions was chosen because it can influence the re-reduction of the oxidized state of the dye (redox system) as well as several other process in the DSSC (Singh et al., 2009; Bella et al., 2013). But, the addition of single iodide salt cannot increase too much the ionic conductivity of the solid polymer electrolytes. Therefore, in order to overcome this problem, binary iodide mixtures (iodide salts and iodide ionic liquids) was added in the solid polymer electrolytes system. According to some recent reports, the cation size of iodide salts and the binary iodide mixtures showed strong effect to the performance of DSSC (Bhattacharya et al., 2009; Dissanayake et al., 2013; Dissanayake et al., 2014). This can be understood by studying single and dual role of the cation in determining the short circuit current density through iodide ion conductivity as well as in influencing the charge injection mechanism at the electrolyte interface (Agarwala et al., 2011; Dissanayake et al., 2012). The problem is only a few published reports on the use of a binary iodide mixture in DSSC have been reported (Seo et al., 2011; Bandara et al., 2012). Therefore, in this research, the effects of single and binary iodide mixtures to the properties of copolymer based electrolytes and DSSC will be characterized and analyzed in order to understand well the DSSC mechanism.

1.2 Research Objectives

The main objective of this work is to prepare copolymer host designed for polymer electrolytes from two types of methacrylate monomers using UV curing technique and was further applied in the DSSC. Studies were carried out with the objectives as follows:

i. To obtain new copolymers using methacrylate monomers by copolymerizing the monomers via photo-polymerization technique for use as polymer host in polymer electrolytes.
ii. To investigate the effects of addition with various weight ratios of two types of iodide salts to the synthesized copolymers on the optical, thermal and electrical properties.
iii. To obtain copolymer electrolytes with enhanced properties by adding iodide ionic liquid. The characteristics of ionic liquid added polymer electrolytes were studied by comparing with the copolymer electrolytes without ionic liquid systems.
iv. To develop DSSC employing the copolymer electrolytes and suitable working and counter electrodes. The DSSC performance for each system (copolymer-salt and copolymer-salt-ionic liquid) was analyzed.

1.3 Materials Selection

In this work, methyl methacrylate, MMA and ethyl methacrylate, EMA monomers were used as host copolymer. Lithium iodide (LiI) and sodium iodide (NaI) have been used as the doping salts while 1-methyl 3-propyl imidazolium iodide (PMII) has been selected as additives.

1.4 Thesis organization

This thesis reports the research work with the objectives mentioned before. In chapter 2, an overview on polymer electrolytes is presented followed by an overview of the types of polymer electrolytes and techniques for their preparation. Chapter 3 covers the preparation method and characterization techniques of the P(MMA-co-EMA) based solid polymer electrolytes studied in this work. The solid polymer electrolytes were prepared using solution casting technique and the characteristics of the electrolytes were determined using Fourier transform infrared spectroscopy (FTIR), Dynamical mechanical analysis (DMA), Gel permeation calorimetry (GPC), Differential scanning calorimetry (DSC), Scanning electron microscopy (SEM), Impedance spectroscopy (IS), transference number measurement and linear sweep voltammetry (LSV). The preparation and characterization techniques of DSSC prepared using selected copolymer are explained at the end of Chapter 3.

Results and discussion of the synthesized copolymers, copolymer-salt electrolytes and ionic liquid added polymer electrolytes are discussed in Chapter 4, Chapter 5 and Chapter 6 respectively. Meanwhile, the results and discussion of DSSCs fabricated in this work are also discussed in Chapter 5 and Chapter 6. Finally, Chapter 7 gives the conclusions of this thesis and a few suggestions for future work.

CHAPTER 2: LITERATURE REVIEW

2.0 Introduction

Photovoltaic devices are based on the concept of charge separation at an interface of two materials of different conduction mechanism. To date, this field has been dominated by solid-state junction devices usually made of silicon. Besides, this field profiting from the experience and material availability resulting from the semiconductor industry (Mahesh & Rajesh, 2012). The dominance of the photovoltaic field by inorganic solid-state junction devices is now being challenged by the emergence of a third generation cells, based, for example, on nanocrystalline and conducting polymer films (Grätzel, 2001). The third generation cells based on nanocrystalline and conducting polymer films offer the prospective of low cost in fabrication and present attractive features that facilitate market entry. It is now possible to depart completely from the classical solid-state junction device, by replacing the contacting phase to the semiconductor by an electrolyte, liquid, gel or solid, thereby forming a photo-electrochemical cell (Grätzel, 2003).

The phenomenal progress realized recently in the fabrication and characterization of photo-electrochemical cell based on nanocrystalline materials has opened up vast new opportunities (Grätzel, 2005). Contrary to expectation, devices based on interpenetrating networks of mesoscopic semiconductors have shown strikingly high conversion efficiencies, which compete with those of conventional devices (Grätzel, 2001). The prototype of this family of devices is known as dye-sensitized solar cell, which realizes the optical absorption and the charge separation processes by the association of a sensitizer as light-absorbing material with a wide band gap semiconductor of nanocrystalline morphology (O'Regan & Grätzel, 1991; Hagfeldt & Grätzel, 2000).

2.1 Dye sensitized solar cell

DSSC is a third generation photovoltaic (solar) cell that converts any visible light into electrical energy. It was invented by Michael Grätzel and Brian O'Regan in 1991 (O'Regan & Grätzel, 1991). In the past two decades, dye sensitized solar cell (DSSC) formed by a combination of organic and inorganic components have gained great attention as the next generation of photovoltaic devices due to their potential low manufacturing costs, ease of preparation and relatively high electric conversion efficiency (O'Regan & Grätzel, 1991; Grätzel, 2001). It also offers the prospect of a cheap and versatile technology for large scale production of solar cells.

Previously, there is report on an impressive achievement of photo-conversion efficiency of about 11%. (Kuang et al., 2007). Although the efficiency is high, it utilized liquid electrolyte such as acetonitrile in the DSSC fabrication. Liquid electrolytes suffer from the typical drawback such as leakage, volatilization, corrosion of the electrodes and difficulties in cell fabrication therefore limiting the long-term performance and practical use of the DSSC (Seo et al., 2011). Therefore, an attempt to overcome these problems has been made by replacing the liquid electrolytes with solid polymer electrolytes. The solid polymer electrolytes based DSSC have some advantages over liquid electrolyte based DSSC as they show good mechanical stability and are leak proof, do not contain volatile solvents and are therefore free from evaporation of the electrolyte component in the DSSC (Yang et al., 2008). Besides that, solid polymer electrolytes based DSSC have showed promising photo-conversion efficiency results (Qin & Peng, 2012).

2.2 DSSC structure

A typical DSSC consists of two main electrodes, namely; photoelectrode and counter electrode at the back contact of the photovoltaic cell as the catalyst surface (Thomas et al., 2014) deposited onto the thin layer of transparent conducting oxide (TCO). TCO allows light to pass through to the active material beneath (where carrier generation occurs) and acting as an ohmic contact for charge carrier to transport out of the photovoltaic devices (Ashton, 2013). There are a few types of TCO glass substrate that are commonly used in DSSC such as indium-doped tin oxide (ITO), fluorine doped tin oxide (FTO), or aluminum-doped zinc oxide (AZO) (Coutts et al., 1999; Kong et al., 2007; Liu et al., 2010; Stadler, 2012; Su’ait et al., 2015). Photoelectrode was spread with metal oxide semiconductor and then covered with an organic dye which act as a photo-absorber material. While counter electrode plays a role in transferring electrons, since charge transfer resistance from FTO surface to the electrolyte is high, the use of a suitable catalyst helps in the reduction of the charge transfer resistance at counter electrode, and thus helps in pushing the reaction toward a forward direction (Thomas et al., 2014). There are several types of counter electrodes available such as platinum, carbon based materials, nitrides and sulfides based materials that are extensively studied by the researchers (Hagfeldt et al., 2010; Jena et al., 2012; Thomas et al., 2014). Among them, Platinum (Pt) is the most common counter electrode used in DSSC due to its high catalytic activity and high power conversion efficiency. Both of the electrodes are then separated with an electrolyte containing redox mediators such as iodide based, thiocyanate based, and cobalt based electrolytes (Fukui et al., 2006; Wu et al., 2007; Yella et al., 2011) as shown in Figure 2.2.

Metal oxide semiconducting materials act as electron acceptor and electronic conduction path to facilitate photoexcited electrons because of their conductive electronic structure, referred to as the valence band (VB) and conduction band (CB) (O'Regan & Grätzel, 1991; Gong et al., 2012). There are a few types of metal oxide semiconductors that have gained a lot of attentions due to their wide bandgap such as TiO_2, ZnO, SnO_2, ZrO_2 and Nb_2O_5 (Zhang et al., 2005; Li et al., 2014; Omar & Abdullah, 2014; Jamil et al., 2015). Besides these simple oxides, ternary oxides, such as $SrTiO_3$ and Zn_2SnO_4, also have been investigated, as well as core–shell structures, such as ZnO-coated SnO_2 (Lenzmann et al., 2001; Hagfeldt et al., 2010; Yang et al., 2010). Since the discovery of DSSC in 1991 by O'Regan and Grätzel (1991), mesoporous TiO_2 made up of arrays of nanoparticles photoelectrode has an unbeatable record of the highest efficiencies in DSSC till today (Jena et al., 2012). It is because, the n-type of TiO_2 photoelectrode nanoparticles offer some unique properties that make it a possible semiconductor for DSSC such as low intrinsic conductivity of the film, small size of the nanocrystalline particles which does not support a built-in electric field and the electrolyte diffuse into the porous film all the way to the back-contact will create the semiconductor/electrolyte interface essentially three-dimensional (Grätzel, 2003). TiO_2 normally occurs in three phase modification structures, namely; rutile, anatase and brookite phases.

Rutile is the thermodynamically stable phase while anatase is preferable phase for dye sensitized solar cells application, due to its larger band gap (E_g = 3.2 eV for anatase compared to E_g = 3.0 eV for rutile, corresponding to an absorption edge of kg 390 nm and kg 410 nm, respectively) (Schwanitz, 2008; Lee et al., 2011). Besides that, the high refractive index of TiO_2 (n = 2.5 in anatase phase) results in efficient diffuse scattering of the light inside the porous photoelectrode, which significantly enhances the light absorption (Sao, 2009). Furthermore, mesoporous TiO_2 photoelectrode has a high internal surface area to support the monolayer of a dye sensitizer and its conduction band edge lies slightly below the excited state energy level positioned of many dyes sensitizer. This condition is required for efficient electron injection in the conduction band to transport across TiO_2 film by diffusion toward the TCO (Grätzel, 2003; Sao, 2009; Jena et al., 2012). The high dielectric constant of TiO_2 ($\varepsilon = 80$ in anatase phase) also provides good electrostatic shielding of the injected electrons from the oxidized dye molecule attached to the TiO_2 surface, thus reduced their recombination before reduction of the dye by the redox electrolyte (Narayan, 2012). However, the capabilities of TiO_2 anatase phase to absorb solar spectrum in the range of ultraviolet or near-ultraviolet radiation can only capture about 4% of the solar light. Thus, dye sensitization of wide band-gap semiconductor surfaces by anchored dyes has provided a successful solution to extending the absorption range of the cells to long wavelength region (Chen et al., 2011).

Dye sensitizer layer serves as the solar energy absorber in DSSC which absorbs the solar photons and produced electron–hole pairs. Since the electrons and holes in the dye layer have very small mobilities, this layer must be very thin for the charge carriers to reach the membranes within their lifetimes (Würfel & Würfel, 2009). There are many different types of dyes that have been extensively studied for DSSC application and it can be classified into two main types; organic dyes and inorganic dyes according to the structure (Kong et al., 2007). Organic dyes include natural organic dyes such as coumarin (Hara et al., 2003; Hara et al., 2003; Liu et al., 2012) perylene (Zafer et al., 2007; Cappel et al., 2009) and synthetic dyes. While, inorganic complexes dyes includes metal complex, such as polypyridyl complexes of transition metals, metalloporphyrins, metallo-phathalocyanines and inorganic quantum dots (CdS, CdSe, CZTS, ZnTe) which has high thermal and chemical stability as compared to organic dyes (Hagfeldt et al., 2010; Yella et al., 2011; Giribabu & Kanaparthi, 2013).

Electrolyte is one of the important part for regeneration of the dye sensitizer from its oxidized state by receiving ground-state electrons from redox mediators in DSSC (Grätzel, 2003). The chemical composition of the electrolyte is a particularly crucial parameter in photovoltaic systems. The electrolyte needs to meet the requirements of having a long-term stability, including chemical, optical, electrochemical, thermal and interfacial stability, which does not cause desorption and degradation of the dye from the oxide surface. The electrolyte must reduce the oxidized dye rapidly and guarantee the fast diffusion of charge carriers between porous nanocrystalline layer and the counter electrode in order to sustain the light energy conversion (Bella et al., 2013).

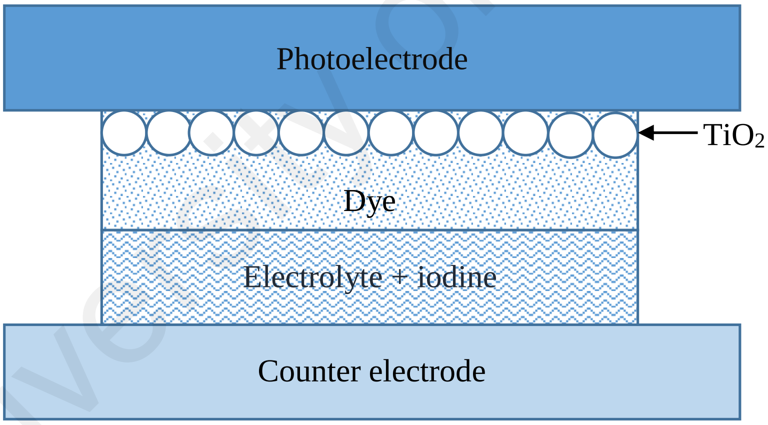

Figure 2.1: DSSC components

2.3 Working principle of DSSC

Energy conversion from light source to electricity in DSSC is based on the injection of electrons from a photoexcited dye molecules into the conduction band of the nanocrystalline TiO_2 semiconductor (Nogueira et al., 2004). The electrons then enter the external circuit and return to the de-excited ionized dye molecules through the redox mediator. The complete photoelectrochemical cycle of the DSSC can be outlined as follows (Sariciftci et al., 1992; Hagfeldt & Grätzel, 2000; Benkö et al., 2002; Wu et al., 2008):

(1) Upon illumination of light through the photoelectrode, dye molecules absorb photons ($h\nu$) forming excitations in the dye molecule (electron-hole pairs).

$$D + h\nu \rightarrow D^{*} \quad \text{(photoexcitation)} \qquad (1)$$

(2) The excited dye molecules then release the electrons and inject them into the conduction band (CB) of TiO_2 leaving a hole on each dye molecule.

$$D^{*} + TiO_2 \rightarrow D^{+} + e^{-}\,(TiO_2)\ \text{(electron injection)} \qquad (2)$$

(3) Subsequently, the injected electrons in CB are transported across the TiO_2 by diffusion toward the TCO substrate, and then to the external circuit resulting in a flow of current.

$$e^{-}\,(TiO_2) + Electrode \rightarrow TiO_2 + e^{-}(Electrode) + energy \qquad (3)$$

(4) The holes in the dye molecules are filled back with electrons from redox reaction. The dye is subsequently regenerated from its oxidized state by electron transfer from iodide (I^{-}) ions in the electrolyte containing (I^{-}/I_3^{-}) redox couple.

$$D^{+} + e^{-}(I^{-}) \rightarrow D + I_3^{-}\text{(sensitizer generation)} \qquad (4)$$

(5) The triiodide (I_3^{-}) ions formed in this regeneration process diffuse to the platinum-coated electrode, where they are reduced rapidly to I^{-}.

$$I_3^{-} + 2e^{-}\,(Pt) \rightarrow 3I^{-}\ \text{(electron donor regeneration)} \qquad (5)$$

The circuit being completed via electron migration through the external load. Photo-injected electrons should escape from any recombination process in order to have a unit charge collection efficiency at the photoelectrode back contact. Therefore, appropriate selection and optimization of the materials constituting the cell components is essential both for obtaining high photovoltaic performance and to ensure their durability over time.

One of the main criticality of DSSC is related with the use of an organic solvent-based liquid electrolyte (Wu et al., 2008). To overcome these critical issues, SPEs have been recently proposed as electrolytes in DSSC fabrication. Solid polymer electrolytes with combination of non-volatility, good performance, flexibility on the structure design, chemical and electrochemical stability, are the best candidates to ensure high and durable sunlight conversion efficiencies of the corresponding DSSC (Lee & Yang, 2011; Bella & Bongiovanni, 2013).

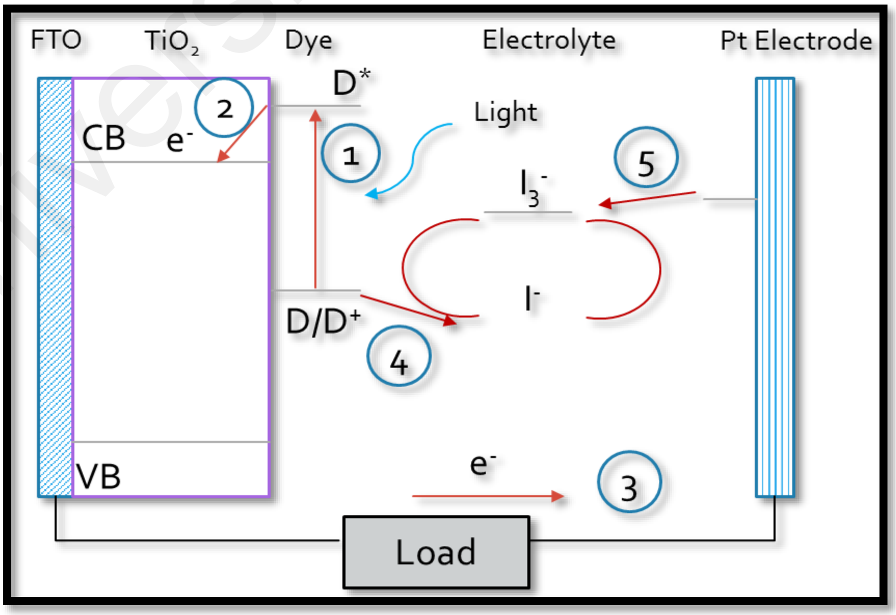

Figure 2.2: Working principle of DSSC

2.4 Solid polymer electrolytes

SPEs are complexes of polymers with metal salts which can be prepared by dissolving the ionic salts into the coordinating polar polymer hosts. The film of SPEs are usually prepared using solution casting technique. Recently, SPEs have received considerable attention due to potentially promising applications of such electrolytes, not only in all solid-state rechargeable batteries, but also in other electrochemical devices such as supercapacitors, fuel cell, electrochromic windows, and sensors (Gray, 1991; Scrosati et al., 1997; Ng & Mohamad, 2008; Eh et al., 2015). For an example, Smitha et al (2005) reviewed the basic characteristics of membranes polymer electrolytes for application in fuel cell (Smitha et al., 2005). Besides that, Lewandoski and co-workers (2001) have successfully used PEO–KOH–H_2O solid polymer electrolyte for fabricating supercapacitor and the electrolyte showed good compatibility which enhanced the performance of the supercapacitor (Lewandowski et al., 2001). Furthermore, Lin et al (2015) have synthesized PEO-MUSiO_2 using in situ hydrolysis method and successfully fabricated in all-solid-state Li batteries with significantly enhanced performance (Lin et al., 2015).

SPEs possess many advantages such as better mechanical stability, good electrode-electrolyte contact, easy for devices fabrication, free from leakage and wide operating temperature range (Agapov & Sokolov, 2011; Balducci et al., 2011). Although they possess many advantages, SPEs still exhibit low conductivity at room temperature (Kang et al., 2002; Rajendran et al., 2008). There are a few methods have been employed to improve the properties of SPEs (mechanical stability, ionic conductivity, thermal behavior, etc), such as modifying the polymer host of polymer electrolytes (Kim et al., 2005; Bella et al., 2013), addition of suitable salts (Kalaignan & Kang, 2006;

Bhattacharya et al., 2009) and also addition of plasticizers or ionic liquids (Kawano & Watanabe, 2003; Bai et al., 2008; Seo et al., 2011).

2.5 Modification of the polymer host

There are a few techniques that can be used to modify the polymer hosts such as blending, plasticization and copolymerization technique (Li et al., 2008; Basri et al., 2011; Rudhziah et al., 2011; Bella et al., 2014; Imperiyka et al., 2014; Rudhziah et al., 2015).

2.5.1 Blend Technique

Blend technique is a physical mixtures of polymers that combining the useful properties of the constituent components to achieve economic or property advantage (Yu et al., 2006). This technique is commonly used in order to obtain polymers with improved thermal, mechanical and electrical properties (Luo et al., 2003; Rudhziah et al., 2015). According to Sundaram and co-workers (2008), blending of PVdF-HFP with PVA decreased the glass transition temperature (T_g), melting temperature (T_m) and heat of fusion (ΔH_m) (Sundaram et al., 2008). On the other hand, Hatta and co-workers (2005) observed that the conductivity of PVA blend PVP-KOH increased with the increase of PVP content in the polymer electrolytes system (Hatta et al., 2005). Besides that, Ding and co-workers (2009) reported an improvement in ionic conductivity and mechanical property of electrospun PVdF-HFP/PMMA blend membranes (Ding et al., 2009). Furthermore, Rudhziah et al (2015) successfully enhanced the ionic conductivity of polymer electrolytes by blending κ-carrageenan with cellulose derivative. The new derivatives of κ-carrageenan and cellulose will have more number of oxygen atoms that may provide vacancies for cations to coordinate. This will lead to the enhancement of ionic conductivity and excellent thermal and chemical stability (Rudhziah et al., 2015). However, in polymer blends, the individual polymers are chemically different and do not form covalent bonds as in copolymers. The blends often characterized by their phase behaviour as being miscible or immiscible (Kannan, 2012).

2.5.2 Plasticization technique

Plasticization technique is a technique with addition of low molecular weight and high dielectric constant polymer into the polymer host in order to enhance the conductivity of the polymer electrolytes. According to Imperiyka et al (2014), ionic conductivity of P(GMA-MMA) + $LiClO_4$ improved up to two orders of magnitude upon addition of ethylene carbonate (EC) into the polymer electrolytes (Imperiyka et al., 2014). Besides that, Ahmad and co-workers (2011) reported that with addition of plasticizers such as propylene carbonate (PC) and EC to the MG49/PMMA based polymer electrolytes, the conductivity of polymer electrolytes was enhanced. The enhancement was ascribed to increased amorphous content as well as increase in ion concentration (Ahmad et al., 2011). Cowie and co-workers (1987; 1998) prepared hybrid polymer electrolyte films by dissolving PAN and $LiClO_4$ in a plasticizer such as PC and EC. The plasticizers reduced the viscosity of the electrolytes which in turn facilitated the movement of charge carriers along the polymer backbone (Cowie et al., 1987; Cowie & Spence, 1998). Some examples of typical plasticizers together with their properties are listed in Table 2.1. However, plasticization technique also have some drawbacks such as solvent volatility, poor mechanical properties due to a high degree of plasticization and reactivity of polar solvent with electrode (Hou & Siow, 2000; Fan et al., 2002; Saikia et al., 2011).

Table 2.1: Some typical plasticizers and their physical properties (Song et al., 2000)

Plasticizer	**Melting point, M_p (˚C)**	**Boiling point, B_p (˚C)**	**Density, ρ (g cm^{-3})**	**Dielectric constant, *ε***	**Molecular weight, M_w (g mol^{-1})**	**Solubility parameter (J cm^{-3})$^{1/2}$**
DMC	2.4	90	1.06	3.12	90.08	20.3
DEC	-43.0	126	0.98	2.82	118.13	18.0
BL	-43.3	204	1.13	39.0	86.09	25.8
PC	-48.8	242	1.20	66.14	102.09	27.2
EC	36.4	248	1.32	89.78	88.06	30.1

2.5.3 Copolymerization technique

Copolymerization technique is a technique that combine chemically two or more types of different monomers to produce a new copolymer. It is the most successful technique to obtain materials with tailor made properties such as the improvement of mechanical stability and ionic conductivity (Soykan et al., 2000; Kang et al., 2002; Patel et al., 2012). According to Oh et al., copolymers have been proposed as a solution to prevent the leakage problem of liquid electrolyte and improve the mechanical strength of gel polymer electrolytes (Oh et al., 2001). Besides that, copolymers were also used to develop gel polymer electrolytes with enhanced ionic conductivity and charge-discharge cycle performance (Ichino et al., 1995; Yamazaki et al., 1995). Moreover, by copolymerization technique, the mechanical properties of polymeric materials suitable as electrolytes also makes them the right candidates for flexible DSSCs (Bella et al., 2013; Imperiyka et al., 2013). In this study, the copolymerization was prepared using free radical photo-polymerization technique.

Free-radical polymerization is normally recognized as addition polymerization which is one of the chemical processes used to alter monomer into long chain segments. It is a well-established technique that takes place at room temperature under UV radiation. This technique has an advantage over conventional routes as it gives freedom to design polymeric networks and their final properties (Decker, 1996). It is also versatile, easy to handle, fast and environmental friendly, as energy consumption is low and there is no emission of volatile organic compounds, as the use of solvent is almost avoided (Gerbaldi et al., 2010). The polymerization occurred by introducing free radicals in the acrylic monomers. Free radical polymerization composed with three kinds of chemical reactions which are initiation, propagation, and termination. Monomers polymerized by this process must contain an unsaturated site in their structure. The reactivity exhibited by the two electrons in the π-bond found on the doubly-bound carbon atoms is the fundamental factor that gives monomers the ability to experience chain growth phenomena (Campbell, 1994). In order for polymerization to occur, a free radical initiator must break into free radicals to begin the process. Once monomer units add rapidly, high molecular weights of polymers build up in a short time.

As noted earlier free-radical polymerization is separated into three distinct steps. The first step occurs when the free radical initiator dissociates to produce free radicals. Initiation involves another reaction, the addition of the first monomer unit to form the initiating species. The next step is the addition of monomer units to the initiating species until the radical reactive centre is transferred to the end of the propagating chain. This portion of the polymerization is ascribed to as the propagation step. The third step of free radical polymerization is termination step which is finally, the special chains will stop growing (Charlesby, 1965; Hutchinson & Penlidis, 2008; Drobny, 2010). Two growing chains contain radicals may react with each other by combination resulting in “dead” polymer. The term of dead polymer represents the stopping of growth for the propagating radical.

2.6 Types of copolymers

Copolymers can be divided into a few types namely alternating copolymers, block copolymers, graft copolymers and random copolymers.

2.6.1 Alternating copolymers

Alternating copolymer is a type of polymer that consists of two different repeating monomer units in which the monomer units alternate positions within the chain of the molecule.

A-B-A-B-A-B-A-B-A-B-A-B-A-B-A-B

2.6.2 Block copolymers

Block copolymer is a mixed distribution of monomer units which is a long sequence or block of one monomer is joined to a block of the second monomer.

A-A-A-B-B-B-A-A-A-B-B-B-A-A-A

2.6.3 Graft copolymers

Graft copolymer is a special type of branched copolymer in which the side chains of a given monomer are attached to the main chain of the second monomer.

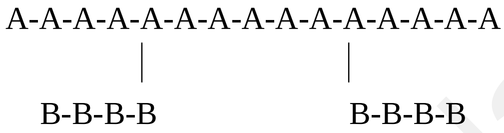

$$\begin{array}{c}\text{A-A-A-A-A-A-A-A-A-A-A-A-A-A-A}\\ \qquad|\qquad\qquad\qquad|\qquad\\ \text{B-B-B-B}\qquad\qquad\text{B-B-B-B}\end{array}$$

2.6.4 Random copolymers

Random copolymer is a copolymer where the different types of monomer units are distributed randomly, and sometimes unevenly, in the polymer chain.

A-B-A-A-B-B-A-B-B-A-B-A-A-B-A

In this study, random copolymer structure is chosen because among all types of copolymers, random copolymers are much easier to be synthesized. Besides that, this type of copolymers can also self-assemble various structures (Liu et al., 2005; Yan et al., 2006; Guo et al., 2008).

2.7 Basic characteristics of acrylic monomers

The main reason of utilizing acrylic monomers to produce new copolymer is its stability against UV radiation. Acrylic monomers also provide the final coating with flexibility, hardness, water resistance, scratch resistance, exterior durability, tensile properties, solvent resistance and adhesion. A typical structure of an acrylic monomer is shown in Figure 2.1 below:

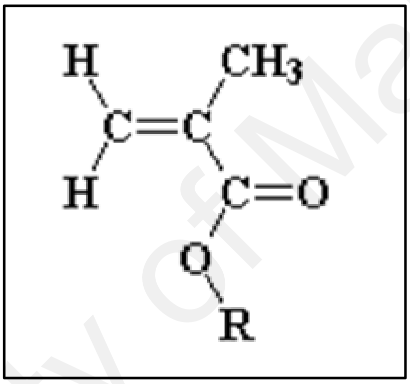

*R = atom or group of atom

Figure 2.3: A typical structure of an acrylic monomer

There are few types of acrylic monomers such as acrylate, methacrylate, acrylamide acrylonitrile, etc. Among all these types of acrylic monomers, methacrylate monomer is a versatile monomer group. Its physical and chemical properties depend upon the “R' ” group, the molecular weight and the tacticity (Yagci et al., 2005), the number of carbon atoms present in the backbone and the nature of the substituent present on the α position of the vinyl group polymer (Martens, 1961). This methyl group helps in the stability, hardness and stiffness of the polymers formed from the methacrylate monomers. Most researchers used methacrylate monomers to produce copolymers because of its very reactive double bond and easily to polymerize with other methacrylate or acrylic monomers. Besides that, methacrylate monomer also has carbonyl group (C=O) which provides oxygen atom and it is expected to form coordinate bond with the cations from the incorporated salt.

2.7.1 Methyl Methacrylate

Methyl methacrylate (MMA) monomer is a colourless and volatile organic compound in liquid form. It has a relatively high vapour pressure (51.3 hPa at 20°C) and moderate water solubility (15 g/litre). The empirical formula for methyl methacrylate is $C_5H_8O_2$. The structural formula for methyl methacrylate is illustrated in Figure 2.4.

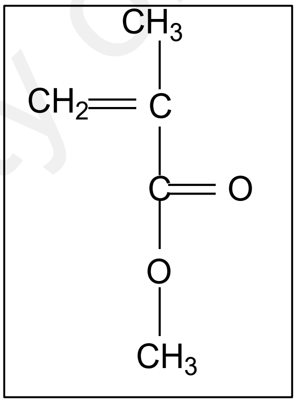

Figure 2.4: Chemical structure of MMA

MMA monomer has a polar functional group with high affinity for cations which makes it a potential candidate for polymer electrolyte material. Besides that, MMA also have reactive vinyl group (C=C) which can easily polymerize with other methacrylate monomer.

2.7.2 Ethyl Methacrylate

Ethyl methacrylate (EMA) monomer characteristics is about same as MMA monomer. It is also a colourless liquid and volatile organic compound. EMA has moderate vapour pressure which is 20 hPa at 20°C and low water solubility (4.69 g/litre at 20 °C). The empirical formula for ethyl methacrylate is $C_6H_{10}O_2$. The structural formula for ethyl methacrylate is shown in Figure 2.5 below.

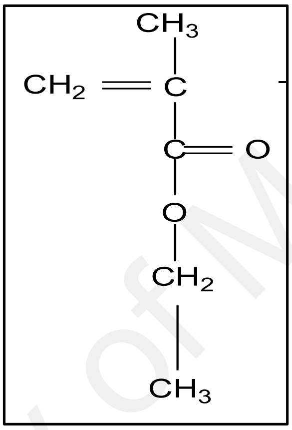

Figure 2.5: Chemical structure of EMA

EMA monomer also has a polar functional group and reactive double bond so that when it copolymerizes with MMA monomer, the active site for cations interactions will increase.

2.8 Copolymerization of MMA with EMA

Owning to several benefits of both MMA and EMA, various chemical modifications have been attempted to modify their properties and extend their usage.

The random copolymerization of MMA and EMA have merge their properties in a cooperation way. Generally, copolymerizing acrylics monomers into a new polymers have been reported to have improved properties such as:

1) Improved mechanical properties of SPE,
2) Increased adhesion to the electrodes,
3) Enhanced conductivity,
4) Improve the formation of flexible films, and
5) Lower the glass transition temperature,

There are various reports on copolymerizing either MMA or EMA with other acrylic monomers. Reddy et al. (2010) which have been successfully investigated the copolymerization of different ratio of phenyl monomer (n-phenyl methacrylamide) with ethyl methacrylate (EMA) using free radical solution polymerization (Reddy et al., 2010). Roy and co-workers (2013) reported that, they have successfully copolymerized N,N-(dimethylamino)ethyl methacrylate with MMA using reversible addition-fragmentation chain transfer (RAFT) copolymerization technique (Roy et al., 2013). Kalal et al. (1974) research involved a detailed study of thermodynamic properties and characterization of poly (glycidyl methacrylate-co-ethyl methacrylate) (P(GMA-co-EMA)) obtained by α-α′azobisisobutyronitrile (AIBN) (Kalal et al., 1974). Moreover, Nasirtabrizi et al. (2011) have reported the homopolymerized of GMA and copolymerize of GMA with other acrylate monomers such as EMA, MMA and ethyl acrylate (EA) using free radical polymerization initiated by AIBN (Nasirtabrizi et al., 2011). Imperiyka and Bella et al. have copolymerized GMA monomer with MMA, EMA and ethylene glycol methyl ether methacrylate (EGMEM) for use as polymer host for polymer electrolytes (Imperiyka et al., 2013; Bella et al., 2014; Imperiyka et al., 2014). These polymer electrolytes were then applied in photo-electrochemical devices. However, the use of MMA with EMA copolymer as host in polymer electrolytes have never been reported in the literature. In this study, new copolymer of EMA/MMA was synthesized using free radical photo-polymerization technique and then used as host for polymer electrolytes for application in DSSC.

CHAPTER 3: RESEARCH METHODOLOGY

3.0 Introduction

This chapter describes the preparation and characterization techniques of the polymer host, solid polymer electrolytes and DSSC. The characterization techniques employed in this study are FTIR, DMA, GPC, DSC, SEM, IS, Transference number measurement and LSV. The technique of solar cell performance analysis is also included in this chapter.

3.1 Samples Preparation

3.1.1 Preparation of polymer host

For the polymer host preparation, two types of monomers have been chosen which are MMA and EMA. (100-x) wt% of MMA and (x) wt% of EMA solutions (where x = 10, 30, 50, 70 and 90) was added with 2, 2-dimethoxy-2-phenylacetophenone (DMPA) which was used as a photo-initiator, with the ratio of 16:1 (polymer host: photo-initiator) (Imperiyka et al., 2013). The mixture was stirred until a clear solution was formed. The mixture was then poured into a teflon petri dish and exposed under UV radiation with continuous flow of nitrogen gas for a few minutes to avoid the sample from reacting with oxygen in the air. Then, the formed transparent copolymer was washed using methanol to remove the residual materials. This method was previously reported by Imperiyka et al., 2013. The flow diagram of the copolymer preparation technique is illustrated in Figure 3.1. Three grams (this amount is sufficient enough to produce a few copolymer films) of the synthesized copolymers was then dissolved in 30 ml of tetrahydrofuran (THF) and stirred for 24 hours at 40 ˚C until homogenous solution was obtained. The solution was then cast into glass petri dishes and left to dry at room temperature in a fume hood (for slowly evaporation) to form free standing films. The preparation of host polymer have been repeated 5 times for each ratio.

3.1.2 Preparation of solid polymer electrolytes

In order to prepare polymer electrolyte films, the copolymer that showed potential properties to be as host polymer for polymer electrolytes was used. Three grams of the selected ratio of P(MMA-co-EMA) copolymer, LiI salt of varying weight ratio (10, 20, 30 and 40) was dissolved in 30 ml of THF at 40 ˚C. The weight ratio (wt%) of salt was calculated using the following equation:

$$wt_{salt}(gram) = (wt\ \%\ of\ salt) \times (wt\ of\ P(MMA - co - EMA)\ \ (gram)) \quad (3.1)$$

This preparation technique was also applied for NaI salt system. Figure 3.2 shows the flow diagram of the preparation process of the solid polymer electrolyte. All the preparation of the polymer electrolytes (LiI and NaI) films was repeated for 5 times.

3.1.3 Preparation of ionic liquid added solid polymer electrolytes

The mixtures of 90MMA-co-10EMA copolymer with LiI were added with 1-methyl-3-propylimidazolium iodide (PMII) that was used as the second additives and dissolved with THF solution in separate beakers for 24 hours at 40 ˚C. PMII was chosen due to its interesting characteristics such as molten salt at room temperature, low volatile and nonflammable ionic liquid. Therefore, the PMII not only can act as a plasticizer, but also as ions contributor (Wang et al., 2004; Mohmeyer et al., 2006; Singh et al., 2008; Noor et al., 2013). The obtained homogenous solution was then poured into a glass petri dish and left to dry at room temperature for 8 hours to form free standing film. The weight percentage of PMII was limited up to 8 wt% since high loading of the ionic liquid produce electrolytes of poor film stability (gel-like electrolyte). The wt% of PMII addition was calculated using the following equation:

$$wt_{PMII} = (wt\,\%\,of\ PMII) \times (wt\ of\ P(MMA - co - EMA)\,) \qquad (3.2)$$

This technique was also applied for P(MMA-co-EMA) + NaI salt system. Figure 3.3 shows the flow diagram of the preparation process of solid polymer electrolyte ionic liquid systems in this study.

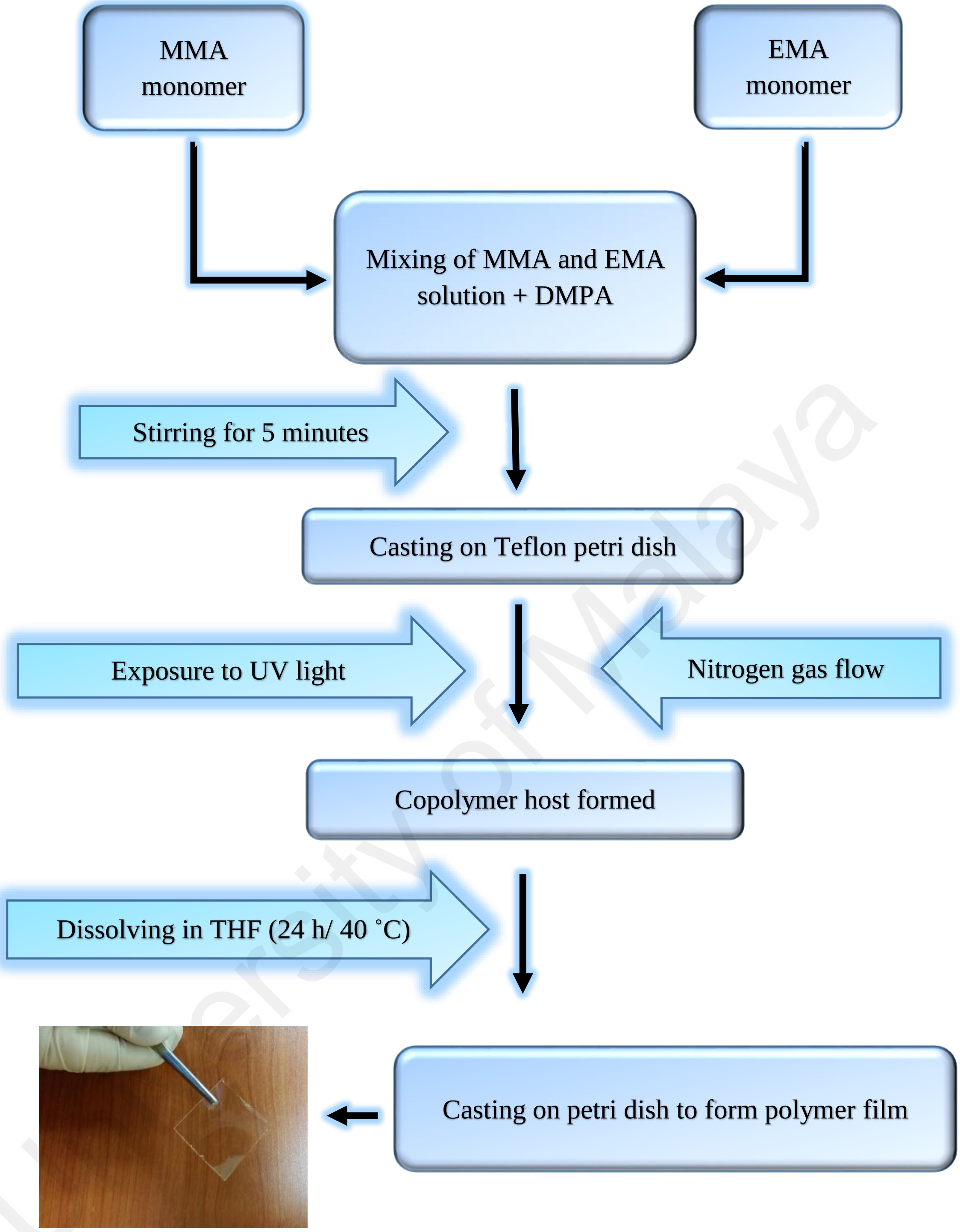

Figure 3.1: Flow diagram of preparation procedure of polymer host film

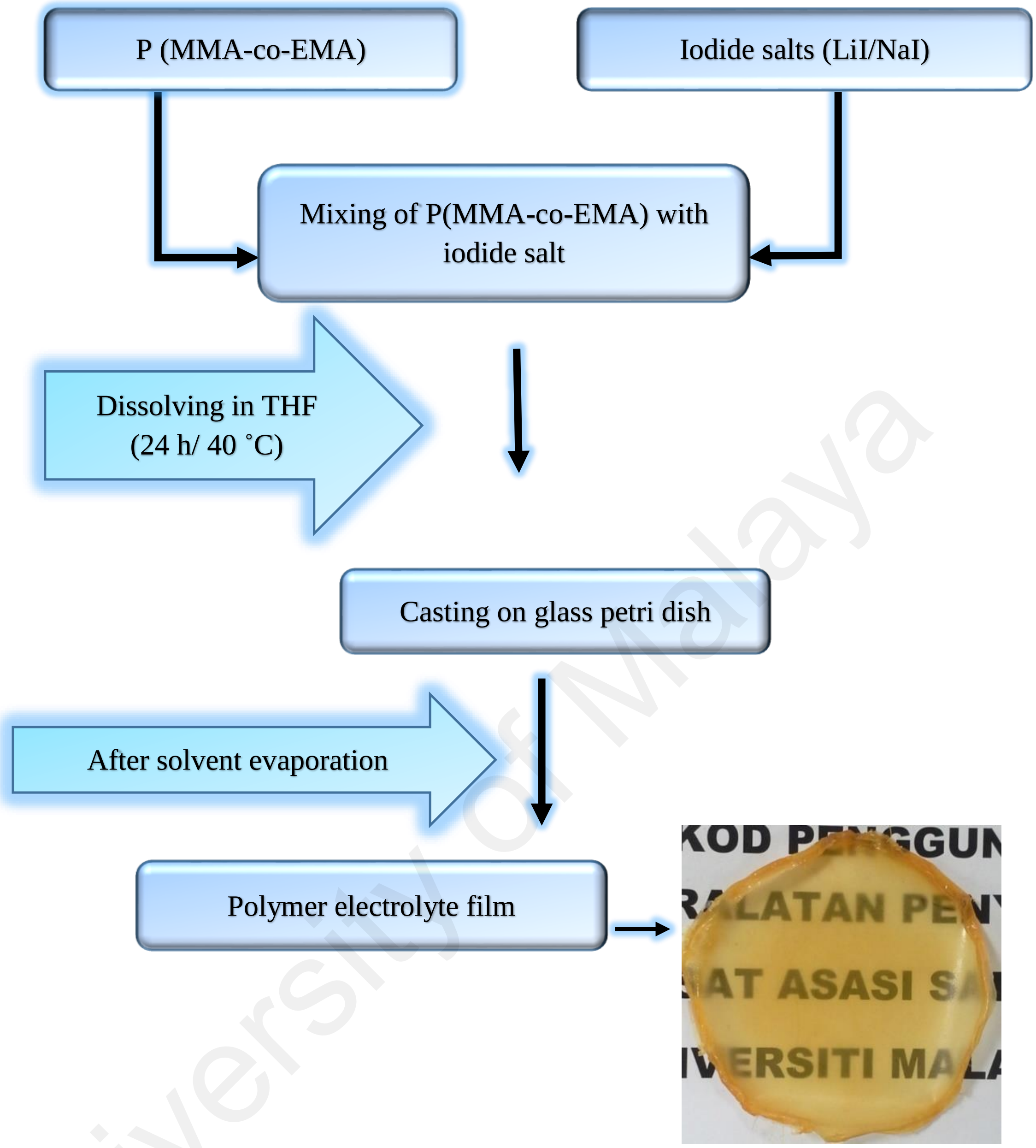

Figure 3.2: Flow diagram of preparation procedure of polymer electrolyte films

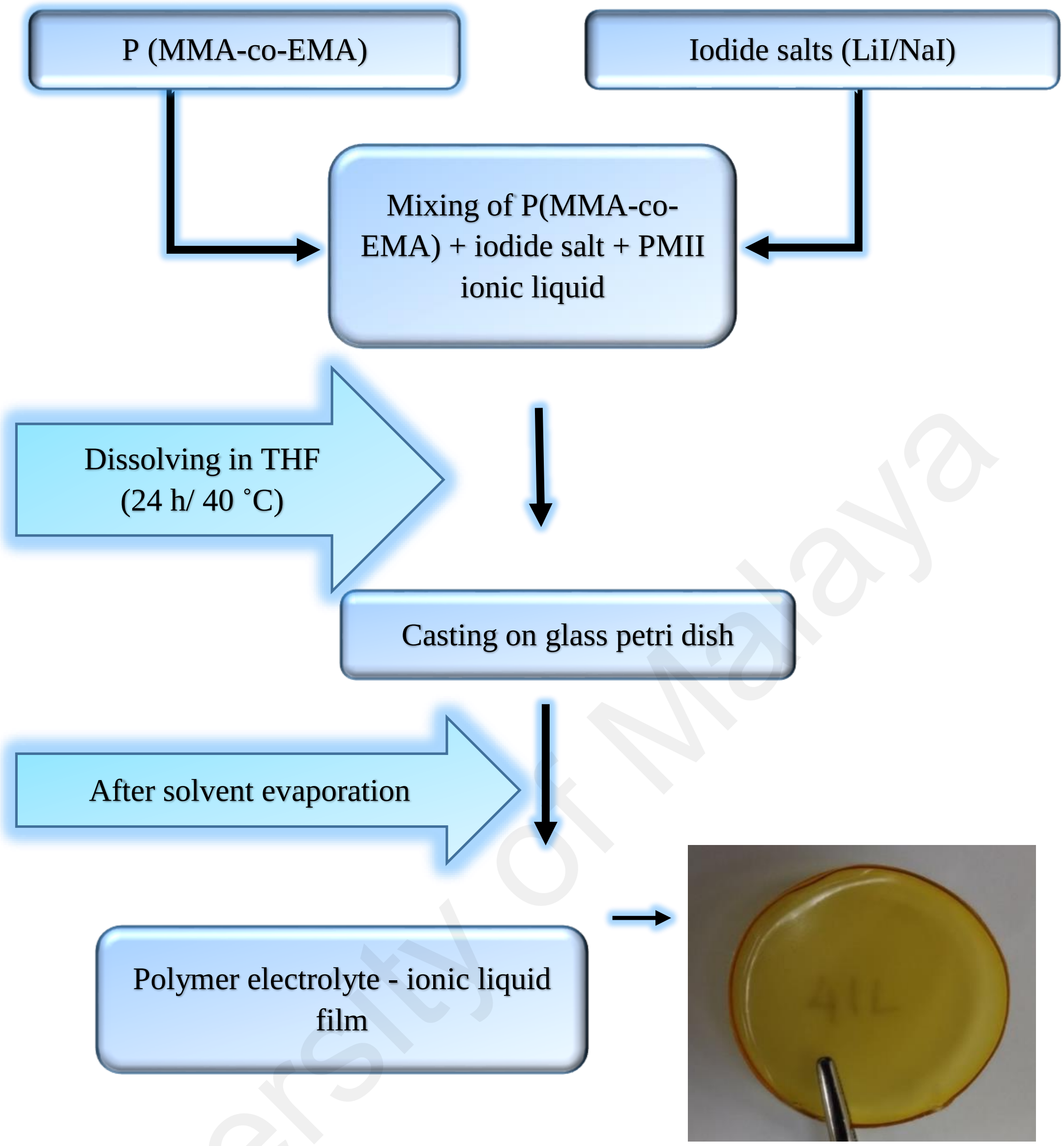

Figure 3.3: Flow diagram of preparation procedure of ionic liquid added polymer electrolyte films

3.1.4 Preparation of Dye Sensitized Solar Cell

Photoanode glass, with the support of adhesive tapes that was used to prevent it from moving, was spread with titanium dioxide (TiO_2) paste (DSL 18NR-AO) using doctor blade technique while, fluorine-doped tin oxide (FTO) counter electrode was platinized with platinum (Pt) paste under commercial name Platisol T by brushing-painting technique. Both TiO_2 photoanode and platinized FTO counter electrode were then annealed at 450 ˚C for 30 minutes in order to change the anatase phase into the rutile phase and activate quasi transparent platinum layer respectively (Bella et al., 2013; Su'ait et al., 2014). The TiO_2 photoanode was sensitized in 0.3 mM of *cis*-diisothiocyanato-bis(2,2’-bipyridyl-4,4’-dicarboxylato ruthenium(II) bis(tetrabutylammonium) dye (N719 dye) solution at room temperature for 24 hours (to ensure the the TiO_2 photoanode was fully sensitized by N719 dye). The highest conducting polymer-salt (with and without ionic liquid) systems were then added with iodine (10:1) for 24 hours and cast on the TiO_2 photoanode electrodes and left to dry at room temperature for a few minutes (Su'ait et al., 2014). The assembling procedure of FTO/TiO_2-dye/polymer electrolytes membrane-I_2/Pt dye sensitized solar cell is shown in Figure 3.4

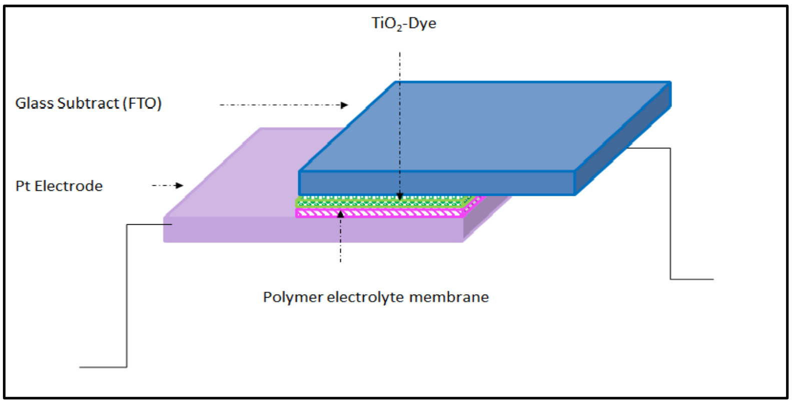

Figure 3.4: Fabrication of FTO/TiO_2-dye/polymer electrolytes membrane-I_2/Pt dye sensitized solar cell

3.2 Characterization of samples

3.2.1 Fourier Transform Infrared Spectroscopy

FTIR is an analytical tool used for identifying chemical interaction that occurred in polymer electrolytes (Noor et al., 2013; Su'ait et al., 2014). The IR spectra may show the occurrence of interactions in the polymer electrolytes which change the vibrational modes of atoms or molecules in the materials (Rajendran & Uma, 2000). In this research, universal attenuated total reflectance (ATR) accessory was used for FTIR analysis because it is more suitable to analyze polymer electrolyte samples in solid form. ATR-FTIR spectra were recorded by computer interfaced with Perkin Elmer Frontier FTIR spectrophotometer. The prepared sample was placed on the top plate of universal ATR and a pressure was applied to push the sample onto the diamond surface. The analysis was carried out in the range of 4000 to 550 cm^{-1} with a scanning resolution of 2 cm^{-1}.

3.2.2 Differential Scanning Calorimetry

DSC measures the temperature and heat flow associated with transitions in materials as a function of time and temperature. It is widely used to characterize thermal transitions of materials and provides useful information about melting point, glass transition temperature, crystallinity, heat capacity, thermal stability and phase transition temperature. It can also be used to check the absence of significant amounts of new phases in a sample (Bershteĭn & Egorov, 1994; Danley et al., 1998; Noor et al., 2013). In this work, about 5-6 mg were placed in an aluminum crucible with the heating temperature range from 30 to 250 ^{o}C at a scanning rate of 10 $^{o}C/min$. The analysis was performed using DSC 131 EVO instrument (SETARAM Instruments) and the results were evaluated with the STARe Software.

3.2.3 Scanning Electron Microscopy

SEM is a useful tool to observe samples morphology. It utilizes electrons in the formation of a microscopic image (Harrison et al., 1998; Zadora & Brożek-Mucha, 2003). The electrons are usually emitted from a tungsten filament that is heated by running a current through it. The emitted primary electrons beam are accelerated towards the sample and focused with electromagnetic lenses. Once the primary electrons beam hits the sample, atoms from the sample are ejected. The interaction between electrons from the beam and atoms from the sample will produce signal that contains topographical information of the sample. The cross sectional morphological images of the prepared host copolymer samples in this study was observed using Zeiss EVO MA10 scanning electron microscope at a magnification of 100× with an accelerating voltage of 10.0 kV. Each of the sample was prepared by breaking into a small rectangular shape by using liquid nitrogen and was coated with gold under vacuum condition.

3.2.4 Gel Permeation Chromatography

GPC is one of the most powerful and versatile analytical techniques available for understanding and predicting polymer performance. It is the most convenient technique for characterizing the complete molecular weight distribution of a polymer. GPC can determine several important parameters such as average number of molecular weight, average weight of molecular weight, average Z weight of molecular weight, and the most fundamental characteristic of a polymer its molecular weight distribution (Imperiyka et al., 2014; Su'ait et al., 2014; Ibrahim et al., 2015). In this study, the molecular weight analysis of copolymer host was performed using GPC system that consists of a Water 717 plus Autosampler and a Water 2414 differential refractive index (RI) detector. The samples were prepared by dissolving 0.03 g of sample in 10 ml of THF at 40°C for 24 hours to achieve equilibrium before injected to the GPC system. The injection volume is 100 ml and operation time taken was 55 minutes for each sample.

3.2.5 Dynamic Mechanical Analyzer

DMA is a tool that can be used to characterize a material’s properties as a function of temperature, time, frequency, stress and other parameters. DMA measurements can be carried out in all standard deformation modes such as bending, tension, compression and shear mode. DMA measures stiffness and damping that can also be reported as modulus and tan delta (Rani et al., 2014; Ibrahim et al., 2015; Rudhziah et al., 2015). From the measurement results, glass transition temperature value of each sample can be determined. In this study, Perkin Elmer DMA 8000 instrument was used to get the glass transition temperatures of the copolymer host samples. The analysis was done in tension mode. The samples used were of 20 mm length, 10mm width, and a thickness between 0.1 to 0.5 mm. The temperature range was from 30 to 100 ºC at heating rate of 1 ºC/min at the frequency of 1 Hz.

3.2.6 Electrochemical Impedance Spectroscopy

EIS is a powerful tool for the characterization of many electrical properties of materials and their interfaces with electron conducting electrodes. This spectroscopic technique refers to the measurement of the real and imaginary parts of impedance over a wide range of frequency (Chandra and Pandey; 1992, Bonanas et al, 1987).

The data of the impedance analyzer are commonly presented in Nyquist plot which consists of imaginary (Z_i) and real (Z_r) impedance components as shown in Figure 3.5. Each point in the plot corresponds to impedance at a particular frequency. From the plot, the value of bulk resistance, R_b of a sample could be obtained and the conductivity, σ could then be calculated using the equation:

$$\sigma = \frac{t}{R_b A} \tag{3.3}$$

where t is the thickness of the electrolyte and A is the electrolyte – electrode contact area (Bard & Faulkner, 1980; Arof et al., 2000; Macdonald & Barsoukov, 2005).

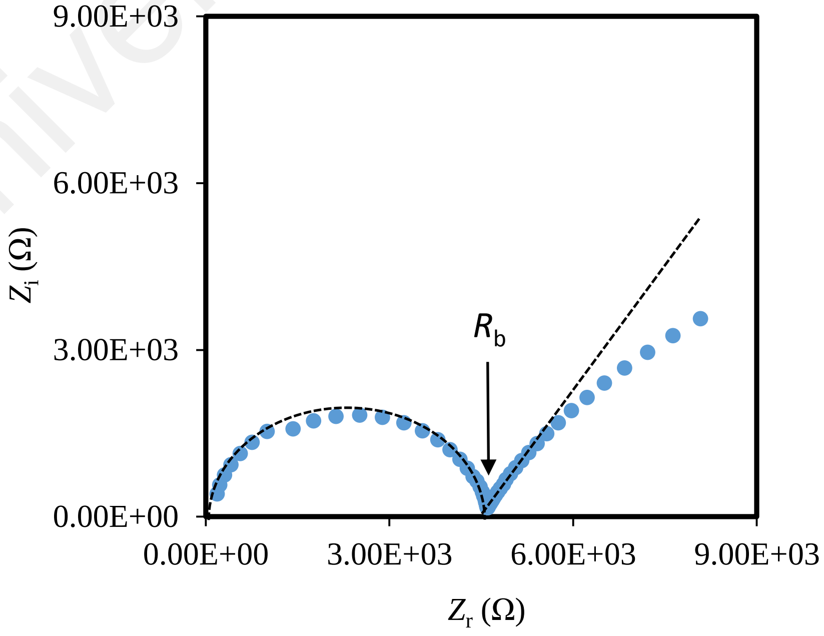

Figure 3.5: Typical complex impedance plot for polymer electrolytes

In this study, the ionic conductivity and other electrical properties were measured using Solartron 1260 impedance analyzer over the frequency range from 10 Hz to 5 MHz with 100 mV voltage amplitude. In order to investigate the effect of temperature changes to the ionic conductivity, the temperature dependence- ionic conductivity was carried out in a temperature range from 30 ˚C to 100 ˚C (Solartron was connected to the sample that was placed in a temperature chamber).

3.2.7 Transference number measurement

Transference number which is also known as transport number in solid electrolytes is due to both ions and electrons. Both ionic transference number (t_{ion}) and electronic transference number (t_e) may be found from the equation as follows:

$$\sigma_T = \sigma_i + \sigma_e \tag{3.4}$$

where σ_i and σ_e are the conductivities contributed by ions (cations/anions) and electrons/holes respectively (Arof et al., 2000). The transference number of an ion (t_i) or an electron (t_e) in a solid electrolyte is the ratio of the conductivity due to the ionic species to the total conductivity of the electrolyte i.e.

Ionic transference number,

$$t_{ion} = \frac{\sigma_i}{\sigma_T} \tag{3.5}$$

Electronic transference number,

$$t_e = \frac{\sigma_e}{\sigma_T} \tag{3.6}$$

Every type of electrolytes has their own ionic or electron transference number, t_i and t_e which must be always positive and between zero and one. If the solid electrolyte is purely ionic, then t_{ion} = 1 while for an electronic conductor t_e = 1. For mixed conductors, t_{ion} may have value from 0 to 1 (Bhargav et al., 2007).

Therefore, to determine the majority of charge carrier that contribute for the conductivity of P(MMA-co-EMA)-salt and P(MMA-co-EMA)-salt-ionic liquid films, the transference number were measured using DC polarization technique. For this technique, the solid polymer electrolyte sample was sandwiched between stainless steel electrodes with applied potential difference of 1 V. The value of current was monitored until it reached the steady state condition (Wagner & Wagner, 1957).

The transference number was calculated from polarization current versus time plot using equation:

$$\tau_{ion} = \frac{I_{initial} - I_{final}}{I_{initial}} \tag{3.7}$$

where $I_{initial}$ is the initial current and I_{final} is the final residual current (constant current). If the charge transport in the sample is ionic, the current through an ion blocking electrode decreases rapidly with time as shown in Figure 3.6.

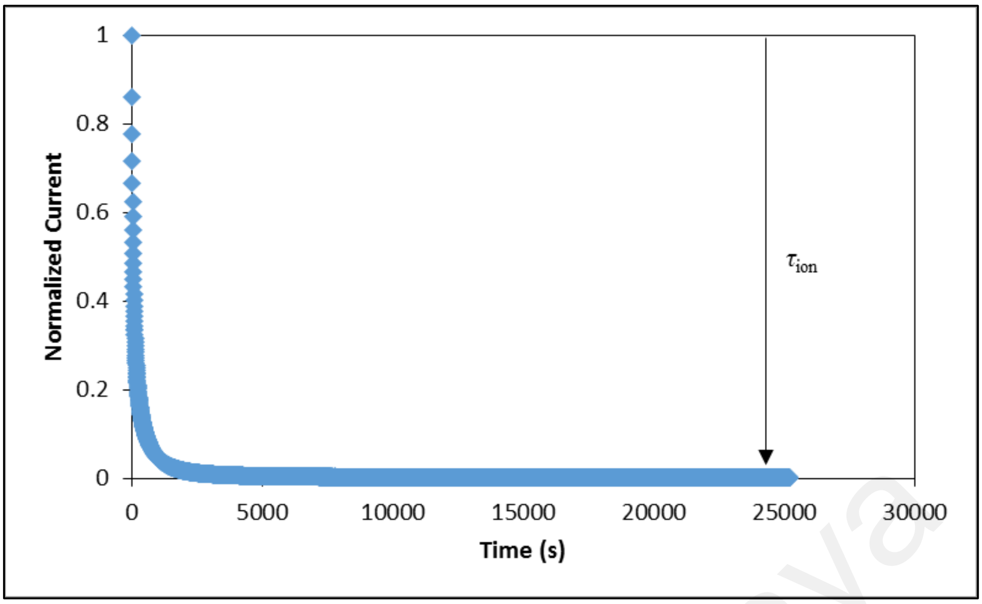

Figure 3.6: Normalized current versus time

In order to determine the actual type of charge carrier in the electrolytes, cation transference number measurement was done based on the analysis of combined dc and ac on the symmetrical cell with non-blocking cation electrodes such as lithium or sodium which allowed Li^+ and Na^+ ions to transfer respectively. For this measurement, the samples were sandwiched between lithium metal or sodium metal electrodes and all measurement was done in an argon filled glove box with $O_2 < 0.1$ ppm and $H_2O < 0.1$ ppm. The cation transference number measurement was done using Bruce and Vincent method in order to determine the actual type of charge carriers. This method requires characterization of cell before and after polarization (after reaching the steady state) by using combination of EIS and DC polarization technique (Bruce et al., 1988).

For small polarization potentials, the transference number for the cation, X^+ (where X = Li or Na) is given by:

$$X^+ = \frac{I_{ss}(\Delta V - I_0 R_0)}{I_0(\Delta V - I_{ss} R_{ss})} \tag{3.8}$$

where I_{ss} is the steady-state current, I_0 the initial current, ΔV the applied potential, R_{ss} and R_0 the electrode resistances after and before the polarization, respectively (Bruce et al., 1988; Riley et al., 2002; Bhargav et al., 2009). The impedance plot before and after polarization and variation of the current with time are shown in Figure 3.7 and 3.8 respectively.

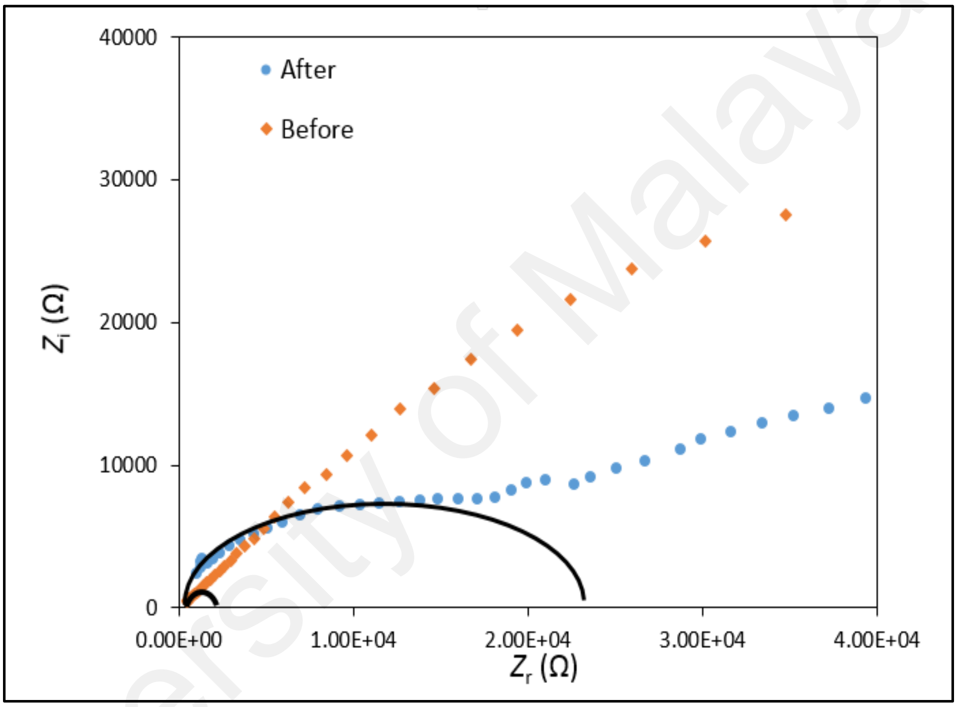

Figure 3.7: Impedance plot before and after polarization of Li metal/ P(MMA-co-EMA)/Li metal

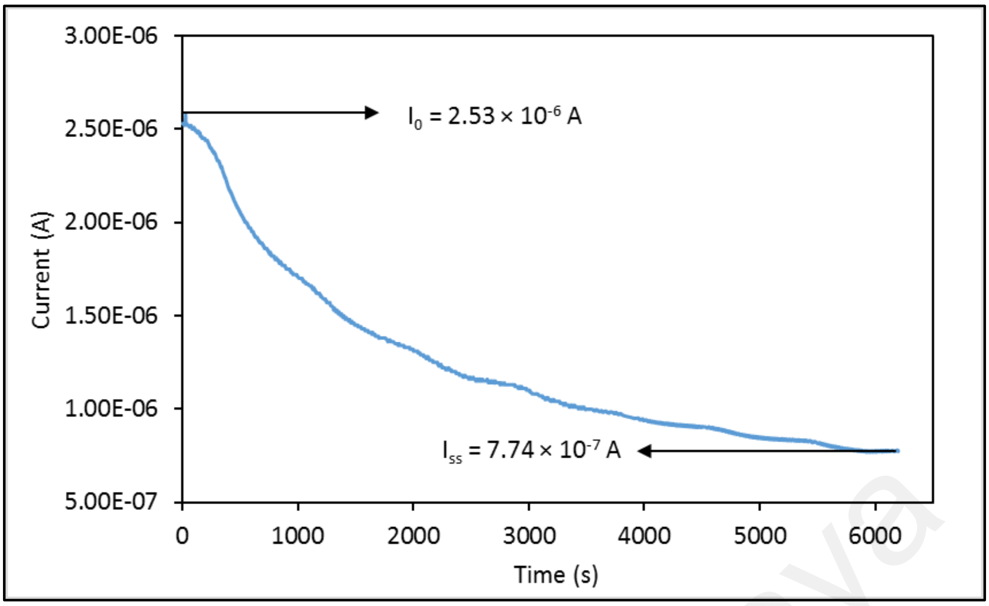

Figure 3.8: Current versus time plot for Li metal/P(MMA-co-EMA) + 20 LiI/Li metal

3.2.8 Linear Sweep Voltammetry

LSV is a technique where the current at a working electrode is measured while the potential between the working electrode and a reference electrode is swept linearly in time (Bard & Faulkner, 1980). Oxidation or reduction of species is registered as a peak or through in the current signal at the potential at which the species begins to be oxidized or reduced (Figure 3.9).

The LSV measurement in this study was obtained using a multichannel electrochemical workstation (Zive MP2 Multichannel) which was operated at a scanning rate of 100 mVs^{-1} over the potential range from 0 to 5 V, with stainless steel as both working and reference electrodes at room temperature.

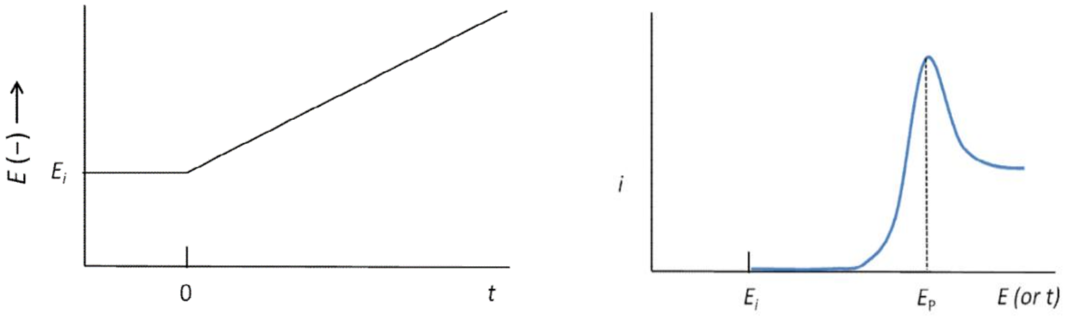

(a) (b)

Figure 3.9:(a) Linear potential sweep starting at E_i . (b) Resulting *I*–*E* curve adapted from (Wang, 2006)

3.2.9 Current density-voltage measurements

Current density-voltage (*J*–V) measurement was recorded using Wonatech Zive MP2 multichannel electrochemical analyzer with a xenon light source under AM (air mass) 1.5 illumination (100 mW·cm^{-2}) controlled by a radiometer. The measurement was carried out at room temperature and the illumination cell area was set to 1 cm^2 to study the performance of DSSC. The performances was evaluated by calculating the fill factor, FF and energy conversion efficiency, η. FF is defined as the ratio of the maximum power from the DSSC to the product of open circuit voltage and short current density. Meanwhile, the η is efficiency of energy conversion from light to electricity. The values of FF and η were calculated using Equations (3.9) and (3.10), respectively:

$$\mathrm{FF} = \frac{V_{max} \times J_{max}}{V_{OC} \times J_{SC}} \tag{3.9}$$

$$\eta = \frac{V_{OC} \times J_{SC} \times \mathrm{FF} \times 100}{P_{in}} \tag{3.10}$$

where V_{OC} is the open circuit voltage (V), J_{SC} is the short circuit current density (mA cm^{-2}), P_{in} is the incident light power density (mW cm^{-2}) while V_{max} (V) and J_{max} (mA cm^{-2}) are the voltage and the current density in the J-V curves, respectively, at the point of maximum power output (Bella et al., 2013; Su'ait et al., 2014)

CHAPTER 4: P(MMA-CO-EMA) RANDOM COPOLYMER SYNTHESIZED USING FREE-RADICAL BULK POLYMERIZATION METHOD

4.0 Introduction

In this study, P(MMA-co-EMA) copolymers were prepared using free-radical bulk polymerization technique with different ratios of MMA and EMA. One of the photographs of the flexible copolymer film is shown in Figure 4.1 (a). The ratio of copolymer films prepared in this study are listed in Table 4.1. The difference of copolymerization ratio of the two monomers cannot be too small because there is no significant effect to the polymer chain (Pomposo et al., 1996; Kim et al., 1998; Roy et al., 2013). In order to identify the most potential copolymer ratio to be used as host for polymer electrolytes, FTIR, DMA, GPC, SEM and IS measurement were carried out. The characterization was done on the copolymer with EMA ratio up to 50 wt% since the films containing EMA > 50 wt% poor in mechanical properties. EMA has low mechanical strength compared to MMA due to its longer chain length. Therefore, the mechanical strength of the P(MMA-co-EMA) decreases when the MMA ratio is decreased (Kim & Oh, 2000; Latif et al., 2006). As such the copolymers containing high wt% of EMA become gel-like (Figure 4.1 b), hence they are not suitable use for preparation of SPEs. The results of these studies are presented in the following sections.

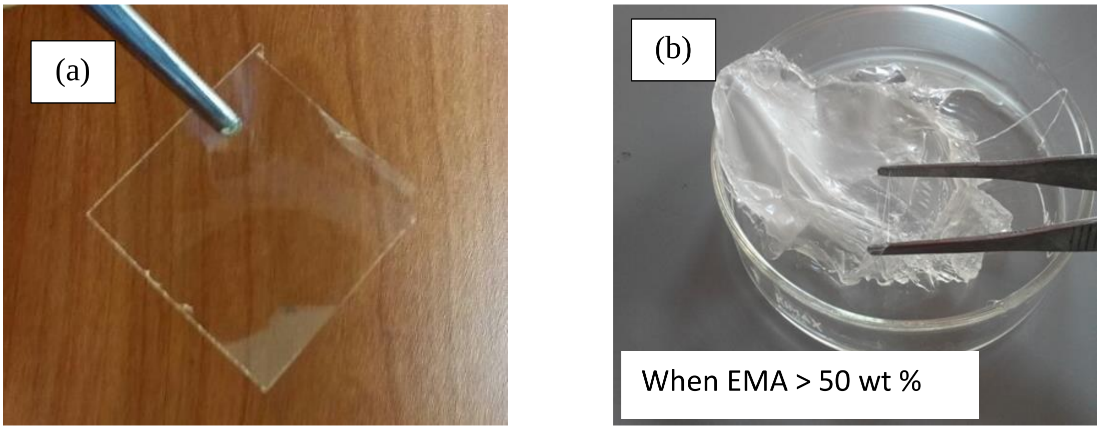

Figure 4.1: Photograph of (a) free standing film of P(MMA-co-EMA) and (b) gel-like film of P(MMA-co-EMA)

Table 4.1: MMA and EMA copolymer films prepared in this study.

MMA (wt% ratio)	EMA (wt% ratio)	Sample Designation	Sample
90	**10**	90MMA:10EMA	Free standing film
70	**30**	70MMA:30EMA	Free standing film
50	**50**	50MMA:50EMA	Free standing film
30	**70**	30MMA:70EMA	Not free standing film
10	**90**	10MMA:90EMA	Not Free standing film

4.1 FTIR Analysis

Figure 4.2 shows FTIR spectra for MMA and EMA monomers, and MMA-co-EMA copolymers of different MMA:EMA ratios. The chemical structure of EMA is quite similar to that of MMA where the only differences between them are the chain length and alkyl group bonded to methacrylate group. MMA contains methoxy group (-OCH_3) that is bonded to the carbonyl (C=O) carbon while the ethoxy group ($-OC_2H_5$) is found in EMA. The main evidence to prove that the monomers have been successfully copolymerized is the disappearance of the absorption peaks at 939 cm^{-1} which is assigned to C-H bonding in the $C=CH_2$ group and the stretching vibration band of C=C at 1638 cm^{-1} (Patel et al., 2008) as can be seen in Figure 4.2. According to Han et al (2013) and Szczepanski et al (2012; 2015), the disappearance of the double bond peaks (C=C and $C=CH_2$) indicates that the monomers had participated in the synthesis reaction (Szczepanski et al., 2012; Han et al., 2013; Szczepanski & Stansbury, 2015). The chemical structure of P(MMA-co-EMA) after copolymerization is illustrated in Figure 4.3.

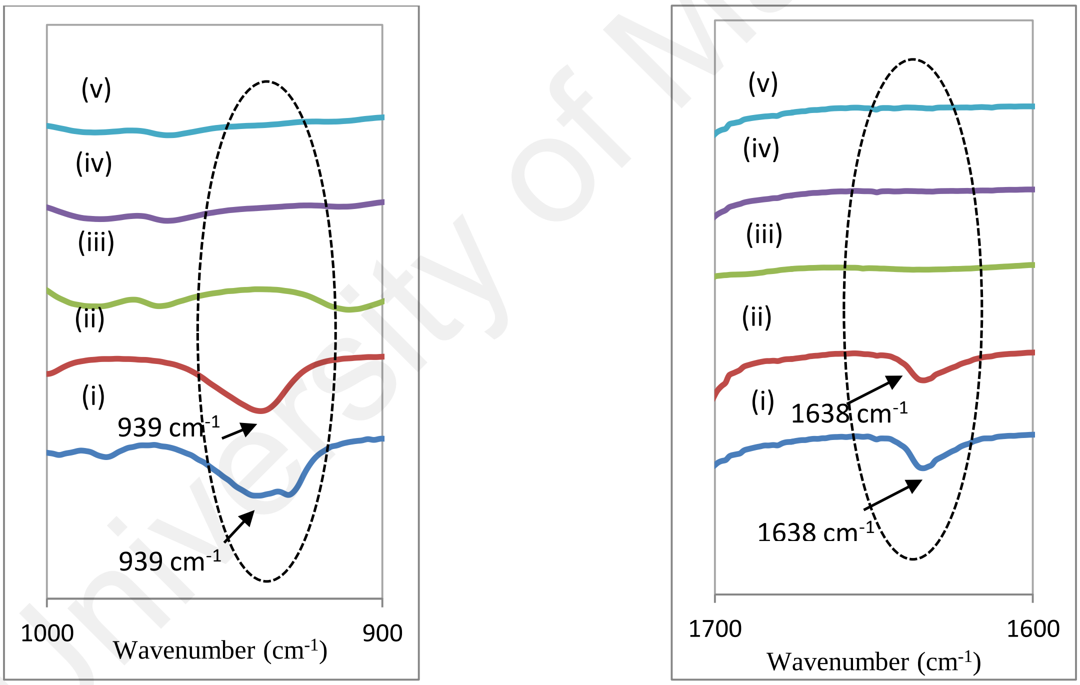

Figure 4.2: FTIR spectra of (i) MMA, (ii) EMA, (iii) 90MMA:10EMA, (iv) 70MMA:30EMA (v) 50MMA:50EMA copolymers in the wavenumber regions of (a) $C=CH_2$ bonding (b) C=C bonding

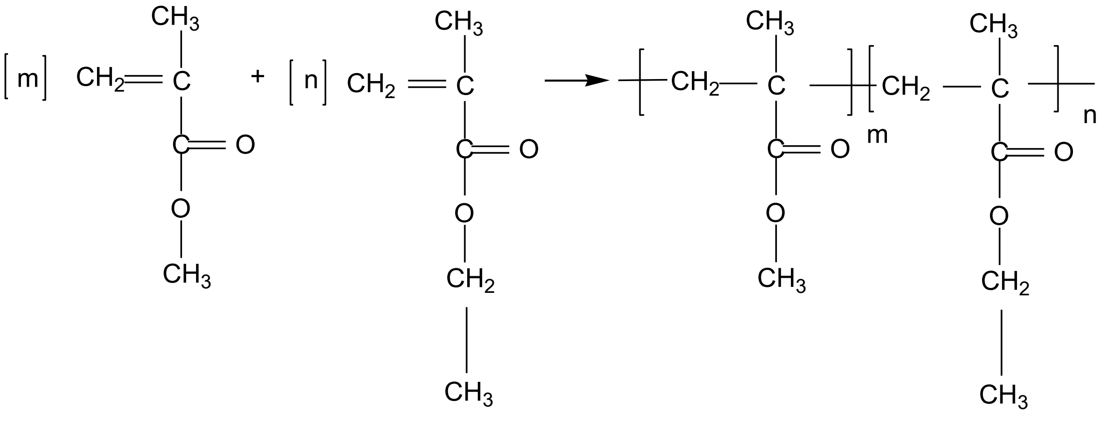

Figure 4.3: Structure of P(MMA-co-EMA)

Illustrated in Figure 4.4 are the strong absorption peaks observed within range 1720 - 1740 cm^{-1}, 1140 - 1160 cm^{-1} and 1240 - 1300 cm^{-1} which are assigned to carbonyl group (C=O), ether group (C-O-C), and epoxy group (C-O-C) respectively (Su'ait et al., 2009; Ahmad et al., 2011; Imperiyka et al., 2013). In the region of 2900 to 3000 cm^{-1}, the peaks at 2986, 2945, 2910 cm^{-1} are due to the C-H stretching vibration of the methylene (C-CH_3) and ethylene (O-C_2H_5) groups. Similar observation has been reported by Venkatesh and co-workers (Venkatesh et al., 1985; Abdelrazek, 2007; Sivakumar et al., 2007; Reddy et al., 2010). From the figure, it can be seen that there are only single bands occurred for all functional groups indicating that MMA and EMA was successfully copolymerized. Besides that, the bands for the focus functional groups such as carbonyl, ether and epoxy are shifted to lower wavenumbers by > 2 cm^{-1} suggesting the occurrence of interactions between the two monomers. Similar observations were reported by other researchers. (Imperiyka et al., 2013; Ibrahim et al., 2015; Rudhziah et al., 2015).

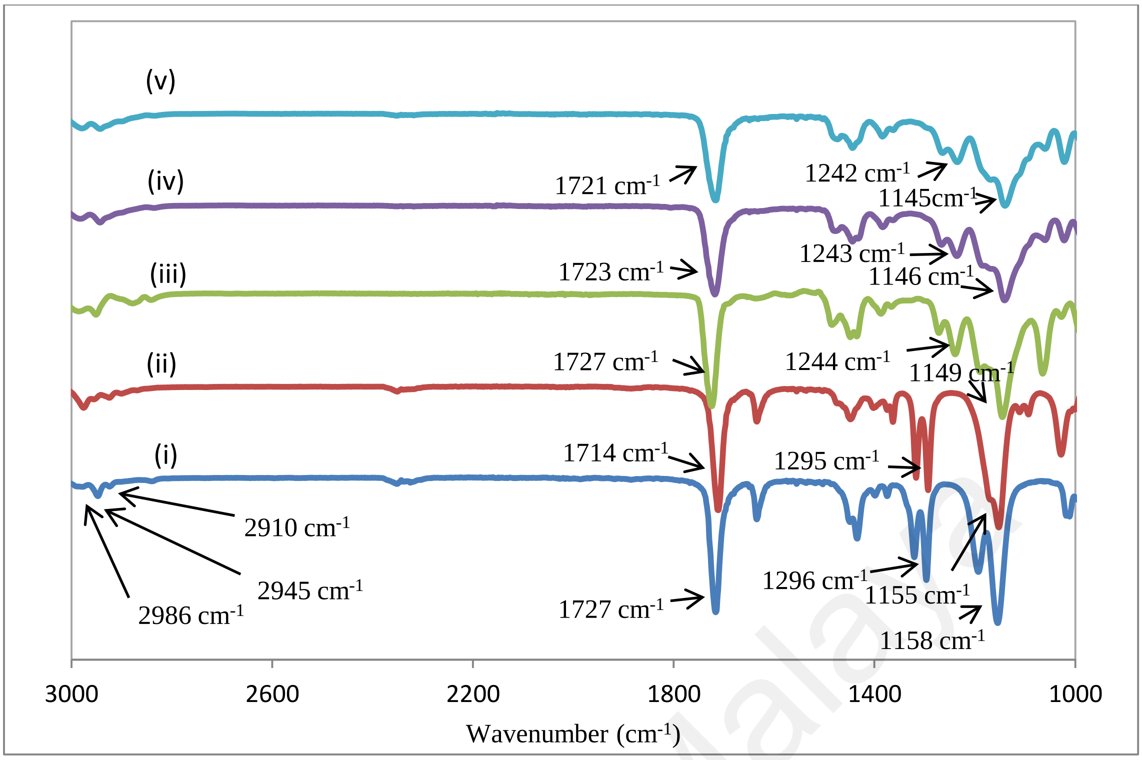

Figure 4.4: FTIR spectra of (i) MMA, (ii) EMA, (iii) 90MMA:10EMA, (iv) 70MMA:30EMA and (v) 50MMA:50EMA copolymers

4.2 Thermal Analysis

Presented in Figure 4.5 are tan δ – temperature curves for the three MMA:EMA copolymers. Temperature corresponding to the maximum peak of tan δ is attributed to T_g while height of tan δ curves is related to the mechanical nature of the copolymers (Elmér et al., 2003; Szczepanski et al., 2012; Szczepanski & Stansbury, 2015). The values of T_g determined from the plots are 33.8, 67.8 and 55.9 °C for the samples of 90MMA:10EMA, 70MMA:30EMA and 50MMA:50EMA respectively. The T_g values shows no specific trend with the EMA concentration. Logically, EMA has longer side chain compared to MMA which allows greater chain mobility and spaces between the chains leading to reduction in entaglement interactions and T_g (Szczepanski et al., 2012). But in this study, there is no correlation between T_g and EMA content. According to some researchers, the relationship between T_g and composition is not always linear for random copolymer and the presence of a single T_g confirms the homogeneity of the copolymers (Sichina, 2000; Slobodian et al., 2012; Pal et al., 2014). From the tan δ curves, it can be seen that 90MMA: 10EMA exhibit the lowest T_g value compared to the other ratio indicating that the polymeric network become looser, hence enhance the flexibility of the polymer chain (Bella et al., 2014).

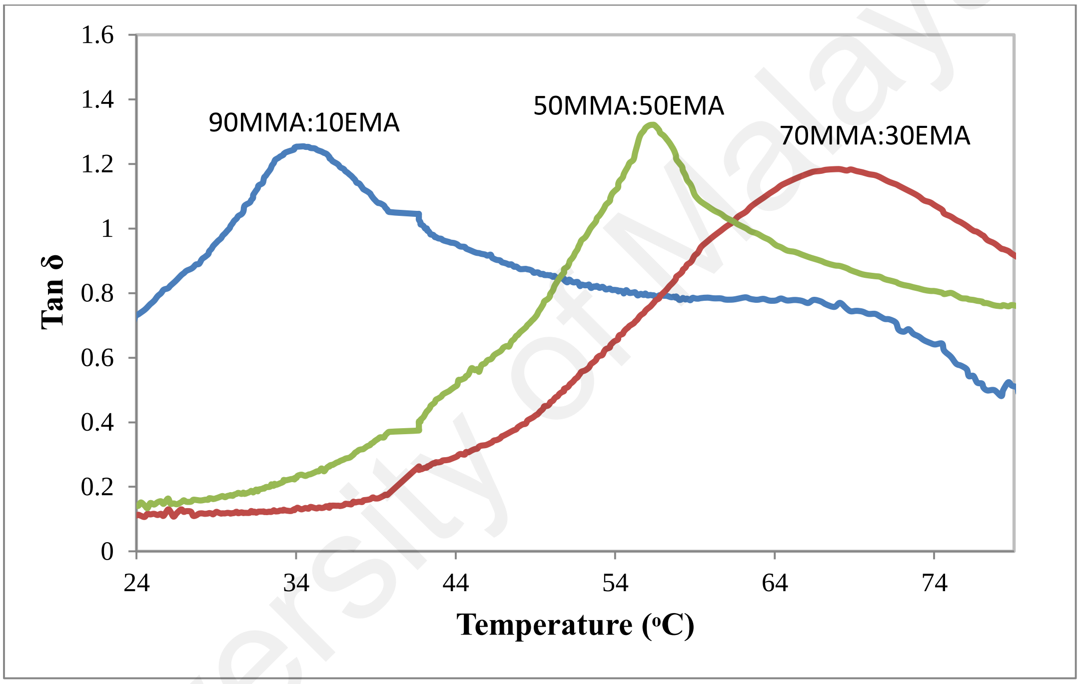

Figure 4.5: DMA spectra for MMA:EMA copolymers

4.3 GPC study

Table 4.2 shows the molecular weights for MMA:EMA copolymers which have been analyzed using GPC. From the table, it can be seen that 90MMA: 10EMA copolymer possesses the lowest molecular weight value followed by 50MMA: 50EMA and 70MMA: 30EMA. This results are consistent with the T_g values that reported earlier which shows that, the lowest molecular weight exhibit the lowest T_g. This is because, when the molecular weight is lower, the chain flexibility of the polymer host will be greater. This will helps in enhancing ion transport in the polymer host and hence enhanced the ionic conductivity (Scrosati, 1993; Szczepanski et al., 2012; Szczepanski & Stansbury, 2015). This agreement was also supported by Shi and Vincent (1993) which reported that the ionic conductivity increases with decrease of molecular weight (Shi & Vincent, 1993).

Table 4.2: Molecular weight values for (100-*x*)MMA:(*x*)EMA copolymers

Sample name	Molecular weight (g/mol)
90MMA:10EMA	46941
70MMA:30EMA	64605
50MMA:50EMA	57566

4.4 Morphology study

The SEM micrographs of the three MMA:EMA copolymer films depicted in Figure 4.6 were characterized at the cross sectional area. As can be seen, the surface of 70MMA:30EMA and 50MMA:50EMA in Figure 4.6 (b and c) shows unsmooth and cracked surface. Whereas, the surface morphology for 90MMA:10EMA in Figure 4.6 (a) is smooth. According to previous reports, the smoother surface will helps to improve the better interfacial properties at the electrode electrolytes interface hence enhance the performance of DSSC (Xia et al., 2006; Prabakaran et al., 2015)

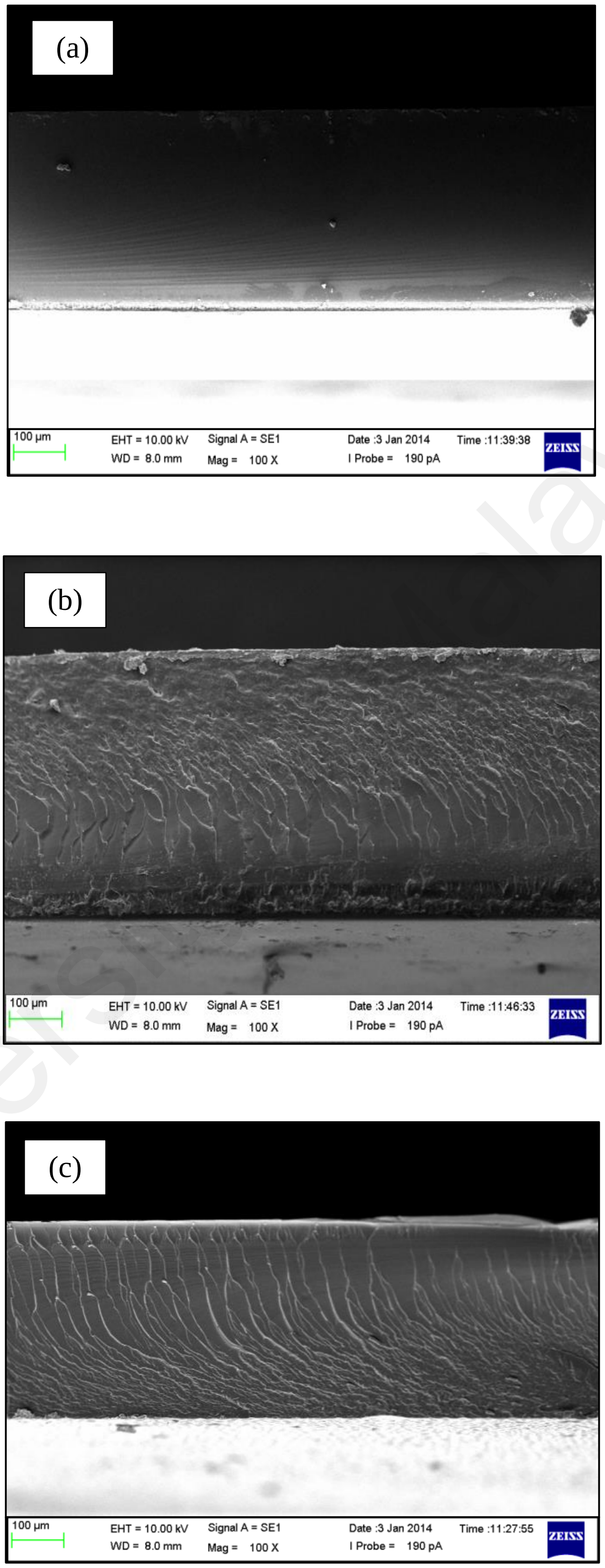

Figure 4.6: Cross section morphology of (a) 90MMA:10EMA, (b) 70MMA:30EMA, and 50MMA:50EMA samples

4.5 Electrical study

The room temperature bulk resistivity, R_b of MMA: EMA copolymer films with different EMA concentrations are listed in Table 4.3. Bulk resistance is the material property which shows how strongly the material opposes the flow of electric current. From the table, 90MMA:10EMA shows the lowest R_b value followed by 70MMA:30EMA and 50MMA:50EMA. As in Equation 3.3, R_b of a sample is inversely proportional to the conductivity, σ. The lower R_b value indicating the smaller resistance of ions to flow between electrode-electrolytes interfaces. As a results, it helps the ions move easier inside the polymer host hence enhance the conductivity (Wright, 1975; Ratner & Shriver, 1988). Therefore, it shows that 90MMA: 10EMA is the most potential of copolymer ratio to be as host in polymer electrolytes.

Table 4.3: Conductivity values for (100-*x*)MMA:(*x*)EMA copolymer

Copolymer	Bulk resistivity (Ω)
90MMA:10EMA	$(6.16 \pm 0.42) \times 10^8$
70MMA:30EMA	$(3.11 \pm 0.46) \times 10^9$
50MMA:50EMA	$(1.51 \pm 0.16) \times 10^9$

The results obtained in this section show that the copolymer ratio of 90MMA:10EMA is the most potential for application in polymer electrolytes due to its better in physical and electrical properties such as greater chain flexibility, smooth surface and lower bulk resistivity. This indicates that 90MMA:10EMA can helps the ions move freely inside the polymer host system.

CHAPTER 5: P(MMA-co-EMA) – IODIDE SALTS (LiI and NaI) POLYMER ELECTROLYTE FILMS

5.0 Introduction

As mentioned in Chapter 4, the copolymer ratio of 90MMA:10EMA has been identified as the most suitable to be used as a polymer host. Therefore, in order to prepare copolymer electrolytes, 90MMA:10EMA was added with various amounts of LiI and NaI salts forming two systems which are P(MMA-co-EMA) + LiI system and P(MMMA-co-EMA) + NaI system respectively. For the purpose of determining suitable ratio polymer electrolytes to be applied in DSSC, the prepared samples were characterized using FTIR, DSC, IS, transference number and LSV measurement. The obtained flexible polymer electrolytes films are shown in Figure 5.1 (a) and (b). From the figures, it can be seen that P(MMA-co-EMA) + NaI (Figure 5.1 b) form films that are more transparent compared to P(MMA-co-EMA) + LiI (Figure 5.1 a) films. The results of characterization are revealed in the following sections.

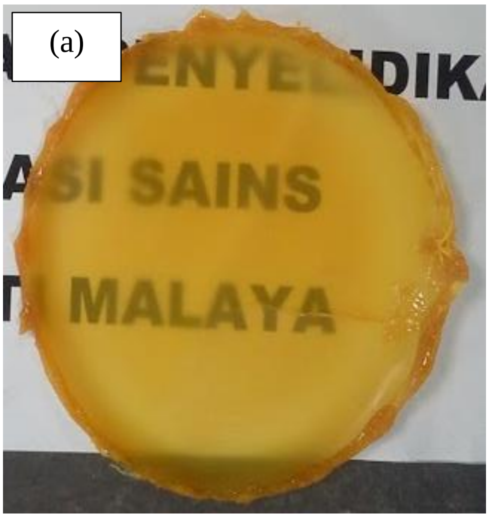

Figure 5.1: Flexible films of (a) P(MMA-co-EMA) + LiI and (b) P(MMA-co-EMA) + NaI polymer electrolytes

5.1 P(MMA-co-EMA) + LiI POLYMER ELECTROLYTE SYSTEM

Table 5.1 lists the composition and designation of each P(MMA-co-EMA) + LiI polymer electrolyte film prepared in this study.

Table 5.1: P (MMA-co-EMA) + LiI polymer electrolytes prepared in this study.

P(MMA-co-EMA) + (*x*) LiI (wt% ratio)	**Sample Designation**
10	10 LiI
20	20 LiI
30	30 LiI
40	40 LiI

5.1.1 FTIR analysis

According to Sako et al. (2001) and other researchers, iodide salts has been widely used for the cleavage of the C-O bonds in esters and ethers with the presence of polar solvent. (Sako et al., 2001; Chakraborti et al., 2002; Dick et al., 2004), Therefore, the dissociation of lithium and iodide ion in the polymer host leads to the coordination of lithium ions to the carbonyl and C-O bond at the ether group and iodide ions to the methyl group. This is due to the lithium ions which are more attractive to the oxygen (O) atoms that have lone pair of electrons and iodide ions to the CH_3 group that have been as polar group after cleavage with C-O bonds in esters and ethers. Figure 5.2 shows the FTIR spectra of the specific functional groups of P(MMA-co-EMA) which are carbonyl group (C=O) located around the wavenumber of 1750-1730 cm^{-1}, ether (C-O-C) and methyl group (CH_3) located around the wavenumber of 1500-1000 cm^{-1} (Su'ait et al., 2009; Ahmad et al., 2011). Figure 5.2 (a) presents the symmetrical stretching of the carbonyl group, ν(C=O) spectra for the polymer host added with various concentrations of LiI salt. With addition of 10 wt%, 20 wt%, 30 wt% and 40 wt% of lithium salt, the carbonyl peak was down shifted from 1724 cm^{-1} to 1719 cm^{-1}.

Figure 5.2 (b, c and d) shows the vibration mode for ether and methyl group. Specific vibrational mode of ether group (C-O-C) can be observed at a stretching mode of –COO- and ν(C-O) which are symmetrical stretching mode (ν_s(C-O-C)), asymmetrical stretching mode (ν_{as}(C-O-C)) and asymmetric deformation of the MMA-co-EMA group, $\delta(O\text{-}CH_3)$ at the wavenumber of 1271, 1147 and 1448 cm^{-1} respectively (Su'ait et al., 2009; Imperiyka et al., 2013). With addition of salt, these bands are shifted to the lower wavenumbers of 1269, 1142 and 1444 cm^{-1}. The $–CH_3$ asymmetric bending at 1435 cm^{-1} and $–CH_3$ symmetric bending at 1241 cm^{-1} were shifted to the lower wavenumbers of 1431 cm^{-1} and 1235 cm^{-1} respectively. The bands for all three specific functional groups

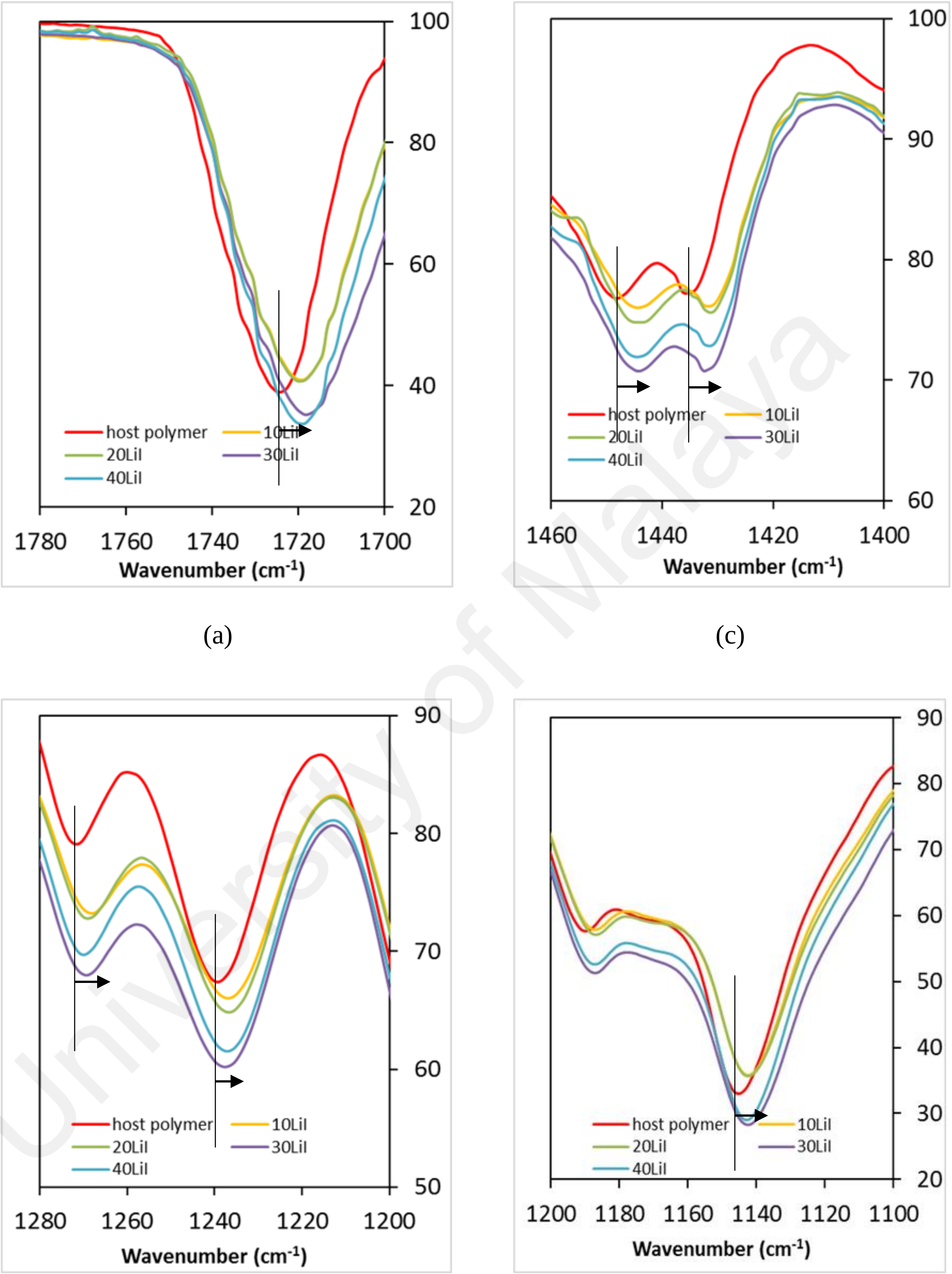

(a)

(c)

(b)

(d)

Figure 5.2: FTIR spectra of P(MMA-co-EMA) + LiI polymer electrolytes in the (a) carbonyl (b, c and d) vibration of ether and methyl group spectral region

are shifted more than 2 cm^{-1}, indicates interactions between cation and anion from the doping salt with the functional group in the host polymer (Mauritz, 1989; Sagane et al., 2005; Ahmad et al., 2011; Imperiyka et al., 2013; Imperiyka et al., 2014). The effects on the intensity of FTIR spectra after addition of different wt% of LiI could not be studied since the force applied by the knob of ATR-FTIR analyzer towards the samples is controlled by the equipment (the applied force is different from one to the other). The proposed mechanism of the complexation between lithium and iodide ions with the polymer host is shown in Figure 5.3.

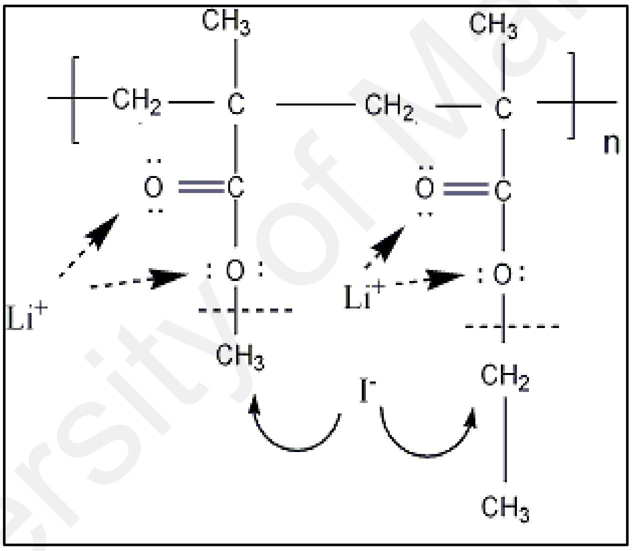

Figure 5.3: Proposed interaction in P(MMA-co-EMA) + LiI polymer electrolytes

5.12 Conductivity Measurement

Figure 5.4 shows the variations of ionic conductivity and glass transition temperature with wt% ratio of LiI. From the figure, it can be seen that the ionic conductivity increase and achieves an optimum value of 1.3 × 10^{-6} S cm^{-1} at 20 wt% of LiI. This may be due to the increase of mobility of Li^{+} and I^{-} ions. However, when the concentration of LiI increased above than 20 wt%, the dissociation of Li^+ and I^- ions might have reached an optimum value resulting in a decrease in ionic conductivity. The increase of Li^+ and I^- ions may form ion pairs or ion clusters which reduce the number of free ions leading to the decrease in ionic conductivity (Karan et al., 2008; Kunze et al., 2012). Figure 5.4 also demonstrates that the ionic conductivity generally is also related to the glass transition temperature (T_g) of the polymer electrolytes. When the T_g value decreases, the flexibility of the polymeric chain increases leading to the increase of Li^+ and I^- transportation in the polymeric chain (Chaurasia et al., 2014; Ng et al., 2015). As a result, the ionic conductivity value is enhanced (Nagaoka et al., 1984; Kobayashi et al., 1985). This is another factor for the higher ionic conductivity value of 20LiI compared to other electrolyte films.

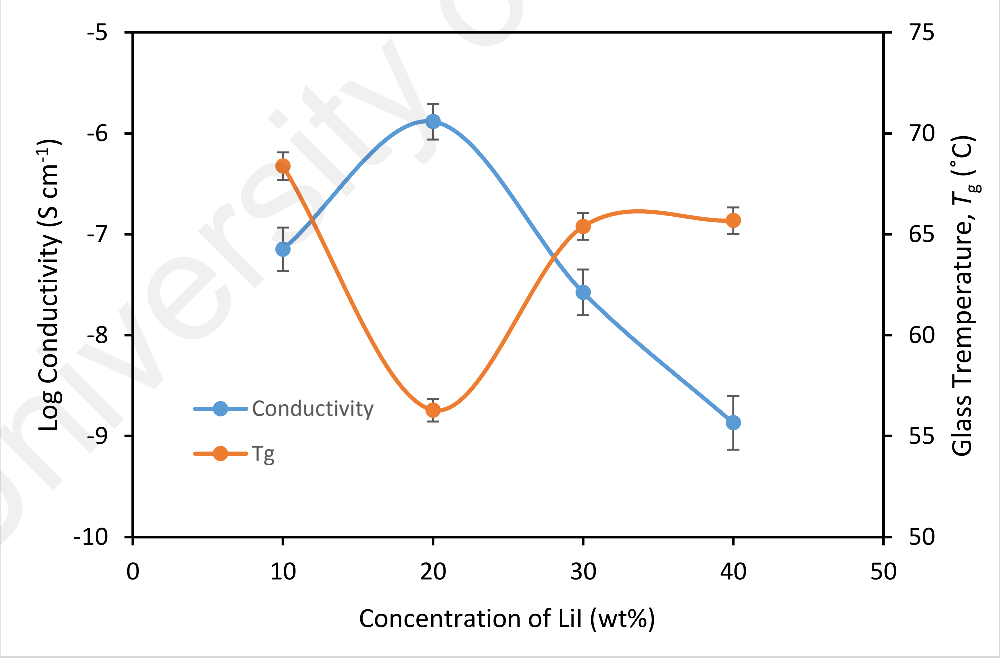

Figure 5.4: Variation of ionic conductivity at room temperature and T_g value with concentration of LiI for P(MMA-co-EMA) + LiI electrolytes

5.1.3 Temperature dependence of ionic conductivity

Figure 5.5 presents the variation of dielectric loss with frequency at different temperatures for 10 LiI film. The plots of loss tangent with frequency at different temperatures for 20 LiI and 30 LiI films also show similar trend. From Figure 5.5, it can be seen that the tan δ increases with frequency at different temperatures, reaches a maximum value and thereafter decreases. The tan δ at lower frequency is due to the free charge build up at the interface between the electrolyte and the electrodes. While at higher frequencies, the periodic reversal of the electric field occurs so fast, so that there is no excess ion diffusion in the direction of the field. The polarization which is due to the charge accumulation increases leading to the increase of the tan δ value as the temperature increases, hence enhance the ionic conductivity at high temperature. For the film of 40LiI (Figure 5.6), it does not follow the similar trend as other concentrations, hence make the behaviour for this sample is difficult to understand. Therefore, this study was only done for 3 concentrations of LiI which are 10, 20 and 30. The tan δ peak is also found to shift towards higher frequency with increase in temperature and it suggests a dielectric relaxation process (Fan et al., 2003; Bhargav et al., 2009).

In order to understand the dielectric relaxation process, the relaxation frequency peak ($f_{\max}$) obtained from the maximum peak of tan δ in Figure 5.5 was plotted against temperature, as shown in Figure 5.7.

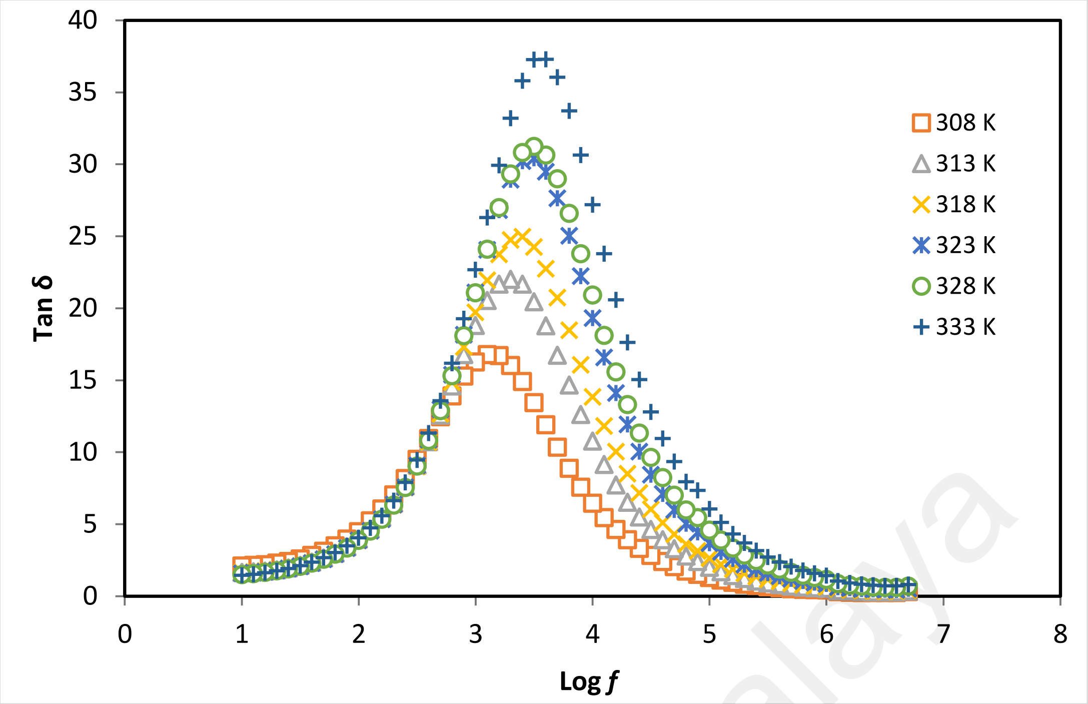

Figure 5.5: Variation of loss tangent with log frequency at different temperatures for 10 LiI polymer electrolyte film.

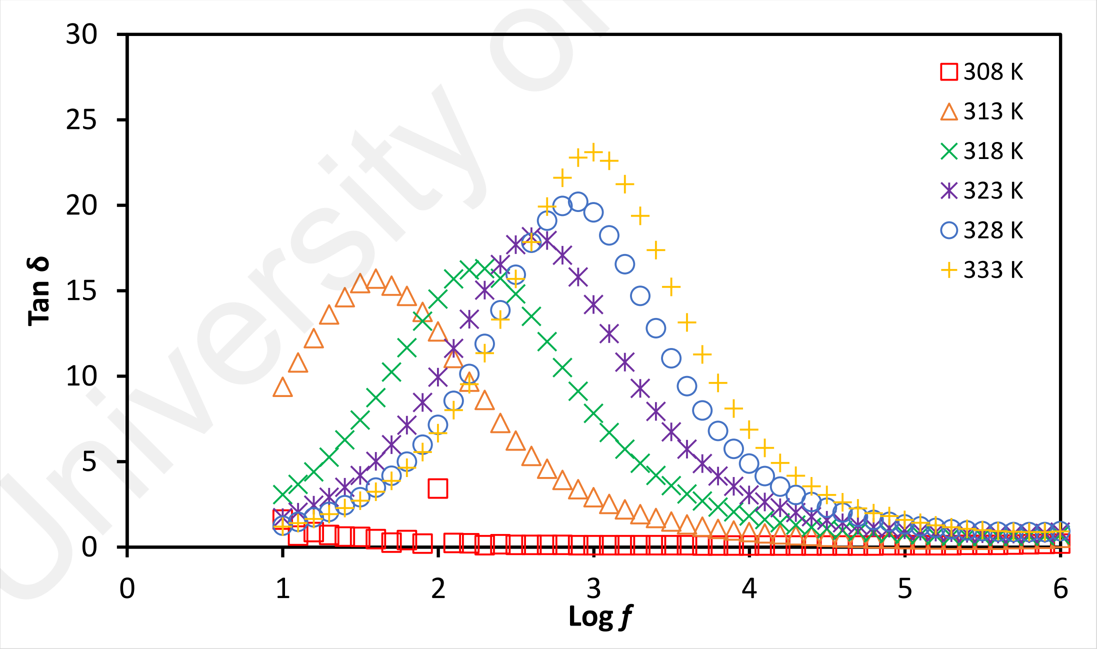

Figure 5.6: Variation of loss tangent with log frequency at different temperatures for 40 LiI polymer electrolyte film

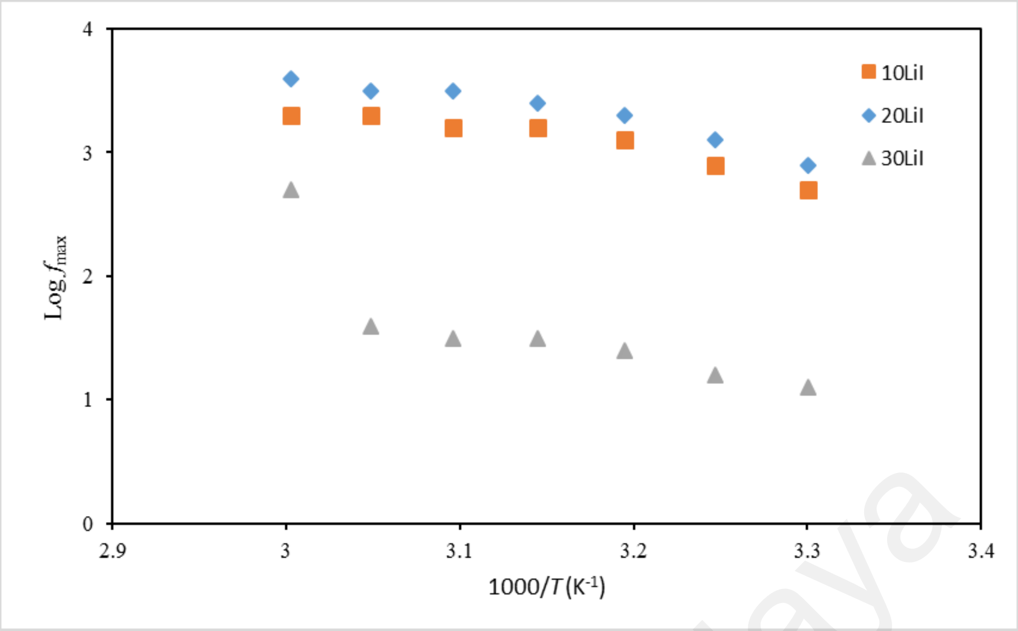

Figure 5.7: Log frequency relaxation peak of P(MMA-co-EMA) + LiI polymer electrolytes films at different temperatures

The plots show that the f_{max} increases with temperature and are in accordance with the non-Debye behaviour (Winie & Arof, 2004). Moreover, from the plot, activation energy of migration mobile ions, E_a can be determined using the following equation (5.1):

$$f_{max} = f_0 exp\left(\frac{-E_a}{K(T)}\right) \tag{5.1}$$

where f_0 is constant and k is the Boltzmann constant.

E_a is also known as the energy required to provide a conductive condition for the migration of ions in the polymer electrolytes system. Furthermore, from the f_{max} value, relaxation times, τ were calculated using equation (5.2):

$$2\pi f_{max}\tau = 1 \tag{5.2}$$

The calculated E_a and τ value for the three different concentrations of LiI are presented in Table 5.2. The trends of E_a versus concentration and τ versus concentration of the electrolytes are consistent with that of the conductivity versus LiI content This means that the conductivity depends on the E_a and τ. (Winie & Arof, 2004; Amir et al., 2011)

Table 5.2: Relaxation time, τ and activation energy, E_a determined from frequency relaxation peak, f_{max} of P (MMA-co-EMA) + LiI

Polymer electrolyte	**τ at ambient temperature (s)**	**E_a (eV)**
10 LiI	3.18×10^{-4}	0.45
20 LiI	2.01×10^{-4}	0.39
30 LiI	1.27×10^{-2}	0.81
40 LiI	-	-

5.1.4 Ionic and Li^+ ion transference number

Figure 5.8 shows the plot of normalized current versus time for 20 LiI polymer electrolyte film. The total ionic transference number shown in this plot is 0.98. This suggests that ions are the dominant charge transport in this polymer electrolyte film (Subba et al., 2003; Saikia & Kumar, 2004). This means that both cations (Li^+) and anions (I^-) may contribute to conductivity since both types of ions are coordinated with the polymer chains as shown in Figure 5.3.

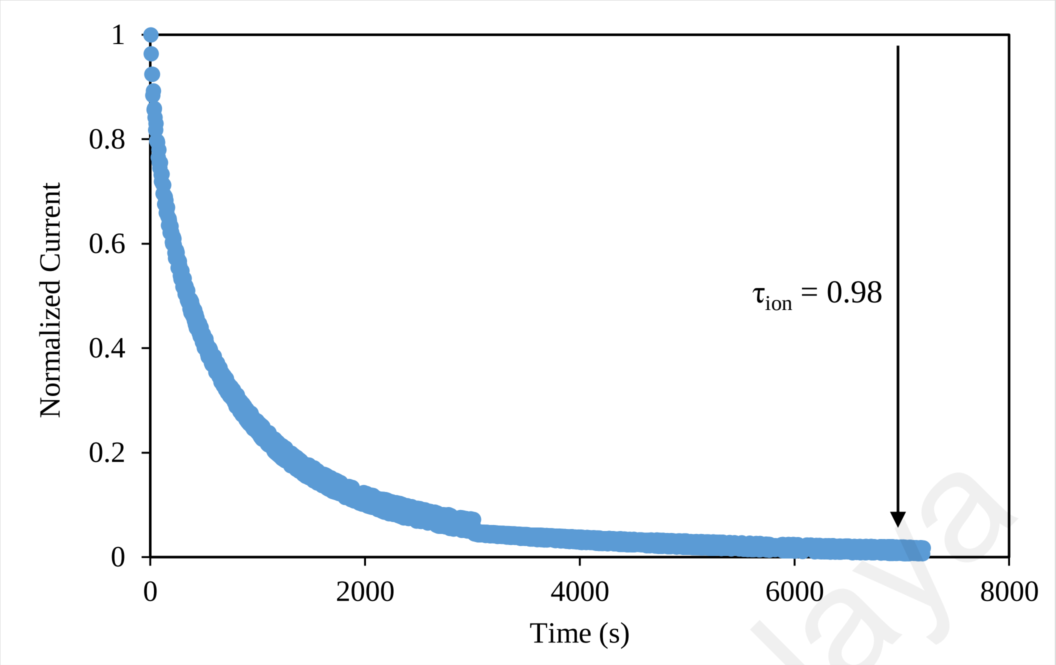

Figure 5.8: Normalized current versus time for 20 LiI polymer electrolyte film

Presented in Table 5.3 are the Li^+ ion transference numbers for various concentrations of LiI. The Li^+ ion transference number values (t_{Li^+}) were calculated using equation 3.8. From the table, it can be seen that t_{Li^+} for all concentrations of LiI are below 0.3. The low value of t_{Li^+} maybe due to small size of Li^+ ions which makes the ions strongly interact with the lone pair electrons of oxygen atoms, which act as electron-donor atoms in the structure of the polymer host, hence decrease the mobility of Li^+ ions (Hiller et al., 2011). Therefore, this result indicates that the majority of ions that contribute to ionic conductivity is not Li^+ ions but most possibly I^- ions (Ali et al., 2006; Bhargav et al., 2009).

Table 5.3: Lithium ion transference numbers of P (MMA-co-EMA) + LiI electrolytes

Polymer electrolytes	**Transport number of Li$^+$ (t_{Li^+})**
10 LiI	0.20
20 LiI	0.30
30 LiI	0.10
40 LiI	0.05

5.1.5 DSSC Performance

In order to fabricate DSSCs, two samples; 30 LiI and 20 LiI which possess the lowest and highest t_{Li^+} respectively. This was done in order to study the effect of Li$^+$ ion transport number in DSSC application. Even though 40 LiI exhibits the lowest t_{Li^+}, it cannot be chosen for fabrication in DSSC because from the temperature dependent conductivity study earlier, its conductivity does not follow any specific trend at elevated temperatures. The DSSC were then tested under illumination of light. Photocurrent density–voltage (*J*–*V*) curves of DSSC employing 20 LiI and 30 LiI as electrolyte membranes are shown in Figure 5.9. The photovoltaic parameters such as J_{sc}, V_{oc}, *FF* and η were obtained from the intersection of current and voltage from the *J*-*V* curves under illumination (Rahman et al., 2007). FTO/TiO$_2$-dye/20 LiI-I$_2$/Pt DSSC gives the photovoltaic efficiency, η of 0.45% with J_{sc} of 4.60 mA cm^{-2}, V_{oc} of 0.30 V and FF of 0.33. Meanwhile, FTO/TiO$_2$-dye/30 LiI-I$_2$/Pt DSSC exhibits an η of 0.10% with J_{sc} of 0.95 mA cm^{-2}, V_{oc} of 0.29 V and *FF* of 0.35. These show that even though I$^-$ ions is important for redox couple in DSSC system, the t_{Li^+} of the electrolyte systems should not be too low because the smaller size of cations can penetrate easily into the dye coated

TiO_2 film and form ambipolar Li^+-e^- with the electrons in the conduction band of TiO_2. This will increases the transport speed of electrons in the TiO_2 network and enhances J_{sc} of the DSSC (Li et al., 2010; Shi et al., 2011; Bella et al., 2013). Therefore, based on the performance of the DSSCs, 20 LiI is a more promising system for application in DSSC.

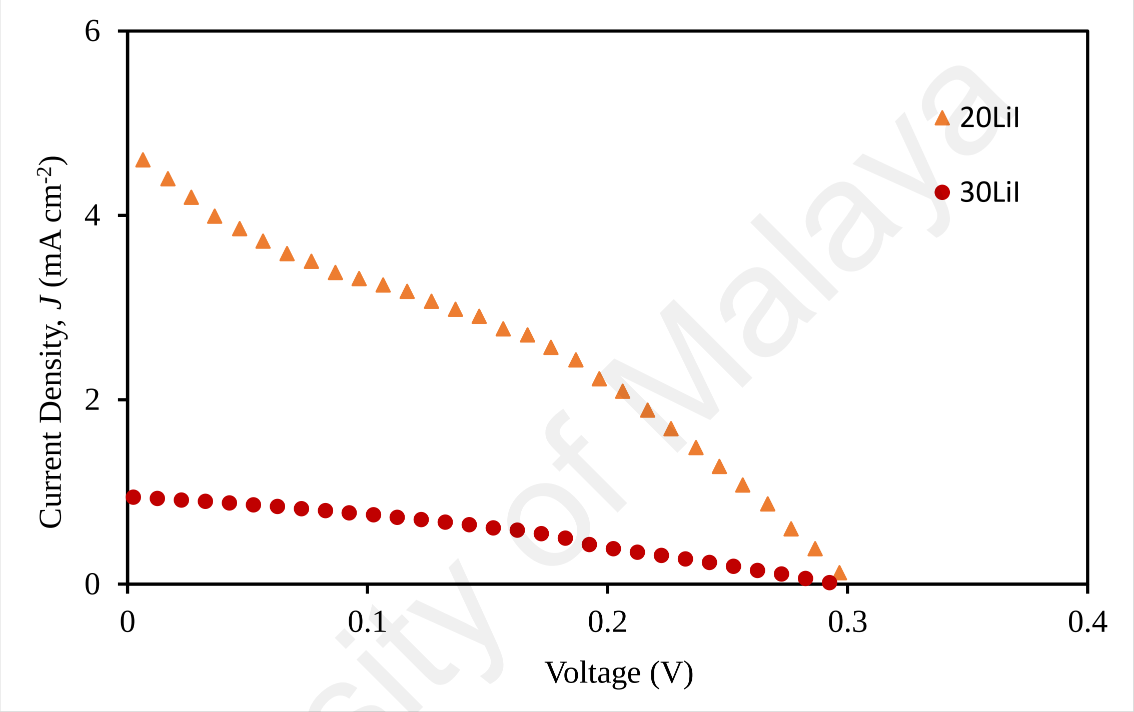

Figure 5.9: *J*-V curves of FTO/TiO_2-dye/P(MMA-co-EMA)-LiI/I_2/Pt assembled with 20 LiI and 30 LiI polymer electrolytes

5.2 P (MMA-co-EMA) + NaI POLYMER ELECTROLYTES SYSTEM

Composition and designation of each P(MMA-co-EMA) + NaI polymer electrolyte films prepared in this study are listed in Table 5.4.

Table 5.4: P(MMA-co-EMA) + NaI polymer electrolytes prepared in this study

P(MMA-co-EMA) + (*x*) NaI (wt%)	**Sample Designation**
10	10 NaI
20	20 NaI
30	30 NaI
40	40 NaI

5.2.1 FTIR Analysis

FTIR spectroscopy was used to study the vibration energy of covalent bonds in the polymer host due to the interactions that occurred when salt was introduced into the polymer (Su'ait et al., 2011). Figure 5.10 shows the FTIR spectra at selected regions of interest. The main regions of interest are the regions for oxygen atoms of the carbonyl group (C=O) located around the wavenumber of 1750–1730 cm^{-1}, ether group (C–O–C) at 1300–1000 cm^{-1} and the methyl group (CH_3) at 1440–1245 cm^{-1} of the MMA and EMA structure in P(MMA-co-EMA). The interaction of sodium iodide with polymer host is similar with P(MMA-co-EMA) + LiI system where with of the presence of polar solvent, iodide salts has been widely used for the cleavage of the C-O bonds in esters and ethers with. (Sako et al., 2001; Chakraborti et al., 2002; Dick et al., 2004). Therefore, the oxygen atoms from carbonyl and ether groups that act as electron donor atoms will form coordinate or dative bonds with sodium ions from the doping salt, while iodide ions to the methyl group that have been as polar group after cleavage with C-O bonds in esters and ethers, hence forming a polymer-salt electrolyte (Sako et al., 2001; Chakraborti et al., 2002; Dick et al., 2004; Pavia et al., 2005; Ahmad et al., 2011). Thus, in these polymer electrolyte system, the sodium iodide is assumed to be fully dissociated into cations and anions, then coordinated with the polymer host structure. Figure 5.10 (a) presents the FTIR spectra of the symmetrical stretching of the carbonyl group, ν(C=O), from the polymer host structure for various concentrations of salt. With the addition of 10 wt%, 20 wt%, 30 wt% and 40 wt% of sodium salt, the peak is shifted from 1725 to 1719 cm^{-1}. The specific vibration mode of ether group (C–O–C) can also be observed in the spectra (b, c, d and e), which shows that the $–CH_3$ asymmetric deformation of P(MMA-co-EMA) from σ($O–CH_3$), the symmetric and asymmetric stretching mode of C–O–C and the asymmetrical stretching mode, ν_{as}(C–O–C), of the ether group at 1447, 1271, 1240 and 1144 cm^{-1}, respectively. With addition of salt, these peaks shifted to lower wavenumbers, which are 1444, 1267, 1236 and 1141 cm^{-1} respectively. CH_3 asymmetric bending at 1434 cm^{-1} is shifted to 1431 cm^{-1}, and the CH_3 symmetric bending at 1239 cm^{-1} to 1236 cm^{-1}. All of the wavenumbers are shifted more than 2 cm^{-1} (Ahmad et al., 2011; Imperiyka et al., 2014). Therefore, these observations are significant to prove the occurrence of complexation between the polymer host and the doping salt. The possible interaction between polymer host with the doping salt is shown in Figure 5.11.

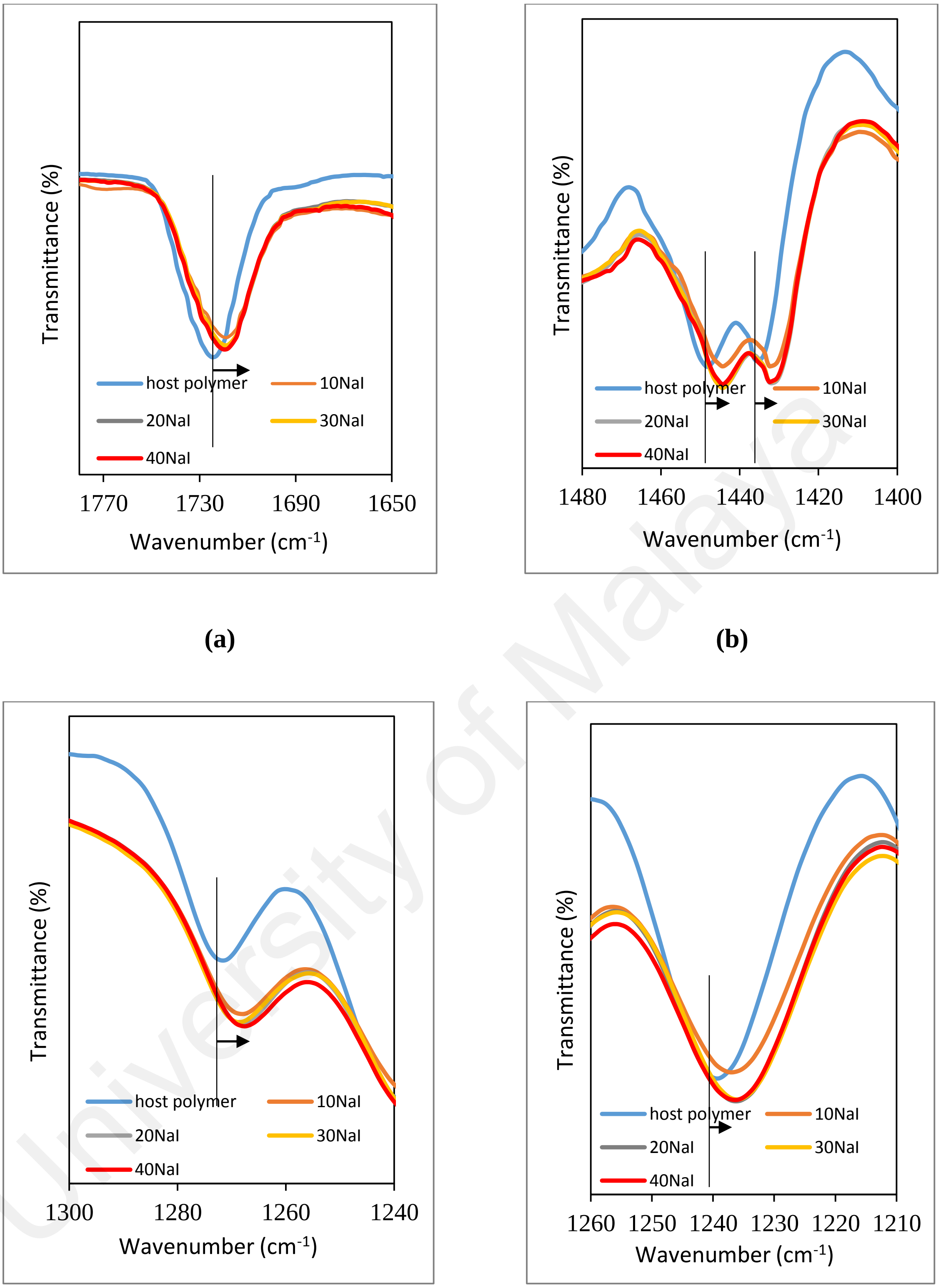
Transmittance (%)
host polymer
10NaI
20NaI
30NaI
40NaI
1770
1730
1690
1650
Wavenumber (cm-1)
1480
1460
1440
1420
1400
1300
1280
1260
1240
1250
1230
1220
1210

(a) **(b)**

(c) **(d)**

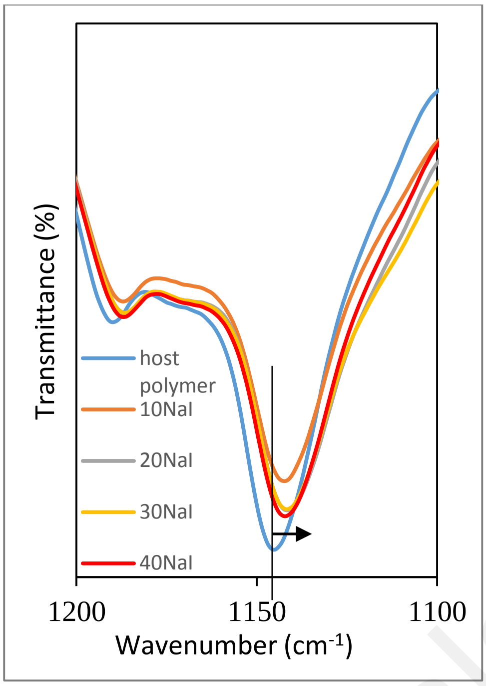

(e)

Figure 5.10: (a–e) FTIR spectra in the spectral region of carbonyl, ether and methyl group of P(MMA-co-EMA) + NaI

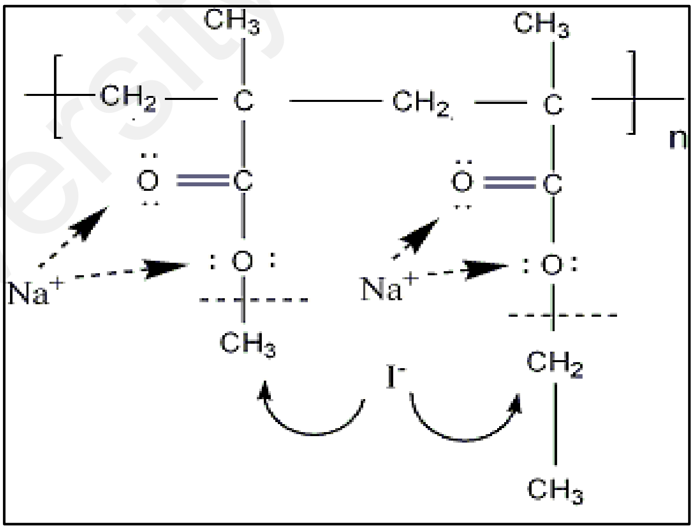

Figure 5.11: Possible interaction of P(MMA-co-EMA) + NaI polymer electrolytes.

5.2.2 Conductivity and Thermal Analysis

Figure 5.12 shows the plots of ionic conductivity and glass transition temperature (T_g) of copolymer electrolytes as a function of sodium salt concentration. The ionic conductivity increases with the increase of the concentration of salt until it reaches the optimum value of 5.19×10^{-6} S·cm^{-1} at 20 NaI. The full dissociation of Na^+ and I^- in the polymer host structure is a factor for the enhancement of the ionic conductivity. The increase in salt content increases the number of mobile ions in the polymer matrix, resulting in the increase of ionic conductivity (Tsuchida et al., 1988; Ramesh & Arof, 2001; De Oliveira et al., 2003). With further increment of the salt concentration (up to 40 wt%), the ionic conductivity starts to decrease. The decrease may be due to the excess dissociation of Na^+ and I^- attributed to the increase of the association rate of the ion, thus leading to the formation of ion clusters. This reduces the number of mobile charge carriers and the mobility of the ions, hence decreasing the ionic conductivity (Wu, 1985; Rajendran et al., 2008; Kumar & Hashmi, 2010; Imperiyka et al., 2013). The content of salt was limited to 40 wt%, since the addition of salt of more than 40 wt% produced sticky films that were difficult to handle.

The trend of T_g versus sodium salt concentration is the same as that of the ionic conductivity. Generally, the conductivity is expected to decrease when the T_g increases (Nagaoka et al., 1984; Kobayashi et al., 1985). But, in this system, the T_g increases with conductivity which may be due to crosslinking that formed between the P(MMA-co-EMA) chain and sodium salts. According to Subban (2004) and Mohammad et al (2013), in the polymer electrolyte system, the crosslinks are well separated in space and can move with respect to each other to a certain extent, thereby contributing to an increase in ionic conductivity (Subban, 2004; Mohammad et al., 2013). Similar observation was reported by other researchers (Le Nest et al., 1992; Song et al., 2002). Besides that, the anions that interact with the polymer may also contribute to the ionic conductivity, as mentioned earlier (Hardy & Shriver, 1985; Johansson et al., 1996).

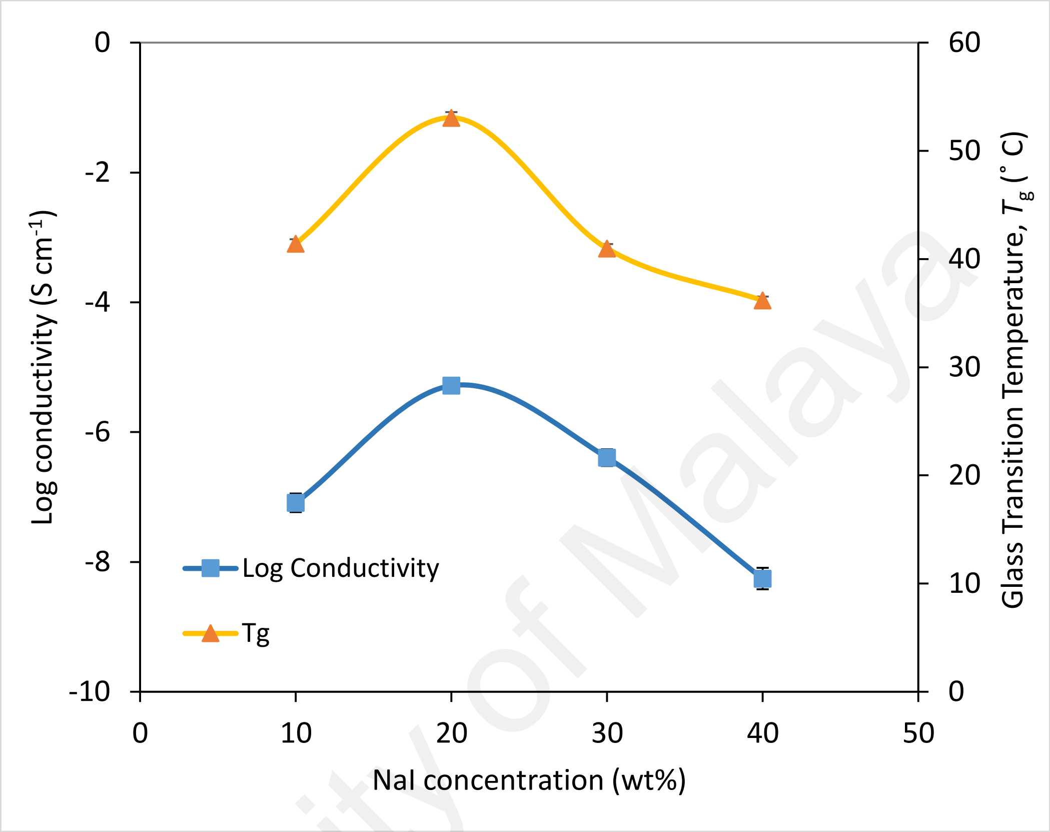

Figure 5.12: Variation of conductivity and T_g of P(MMA-co-EMA) with concentration of NaI.

5.2.3 Temperature Dependent Impedance Analysis

Figure 5.13 shows the plot of loss tangent with frequency at different temperatures for 20 NaI polymer electrolyte film. The plots 10 NaI, 30 NaI and 40 NaI polymer electrolyte films were also plotted and the plots show similar trend. The value of tan δ shows an increasing trend to reach a maximum value before decreasing at high frequency region. As the temperature increases, the frequency at which tan δ_{max} was occurred are shifted towards higher frequencies. The loss peaks and their shifts with temperature indicates that the relaxation time decreases when the temperature increases (Huo & Cebe, 1992; Glatz-Reichenbach et al., 1994; Bhargav et al., 2009). Besides that, from equation 5.2 and 5.3, f_{max} is proportional to P, indicates that P increase with increase the temperature, hence increased the ionic conductivity.

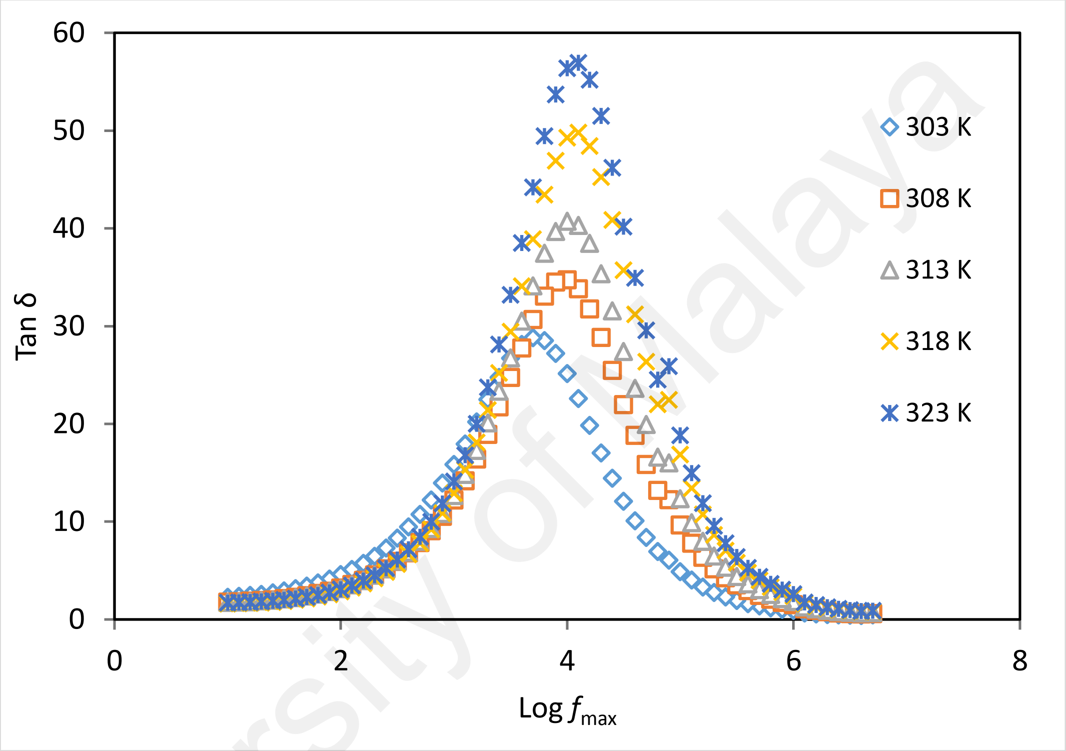

Figure 5.13: Variation of loss tangent with log frequency at different temperatures for 20 NaI polymer electrolyte film

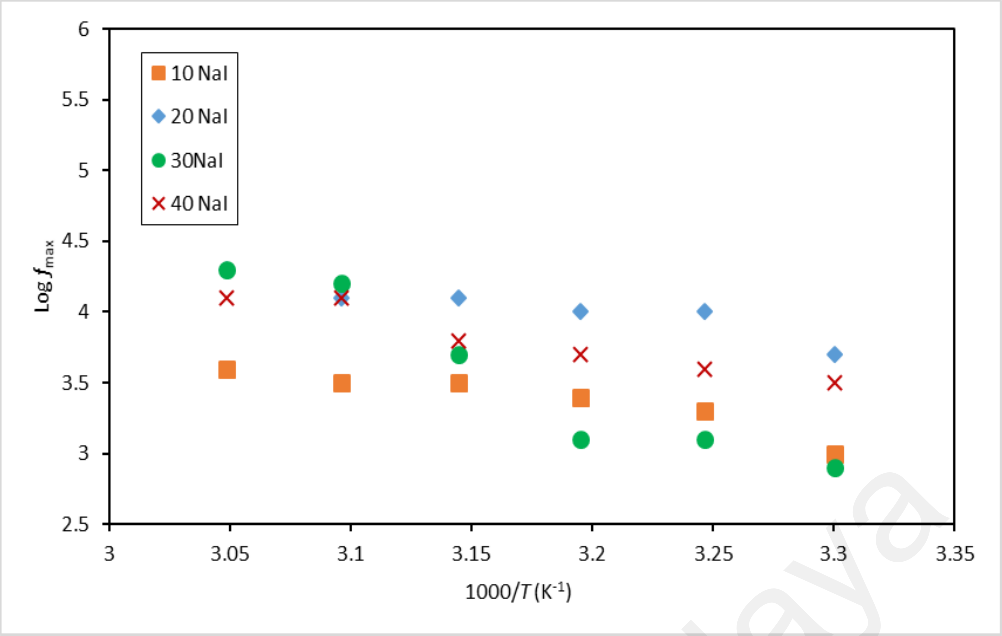

Figure 5.14: Log frequency relaxation peak of P(MMA-co-EMA) + NaI polymer electrolyte films at different temperatures

The frequency at the peak of tan δ in Figure 5.12 is known as a relaxation frequency (f_{max}). The plot of f_{max} are then plotted against temperature and presented in Figure 5.13.

The temperature dependence of relaxation frequency appears thermally activated (Harun et al.; Glatz-Reichenbach et al., 1994; Winie & Arof, 2004) and from the plot, the activation energy of migration mobile ions, E_a can be determined using the equation (6) that showed earlier. Furthermore, from the f_{max} values, the relaxation times at ambient temperature can be determine using equation (5.2).

The calculated E_a and relaxation time, τ values for the four different concentrations of NaI are presented in Table 5.5. As can be seen in the table, the electrolyte that contains 20 wt% of NaI exhibits the lowest E_a compared to other electrolyte films. This indicates that 20 NaI required smallest energy for ions to move in the polymer electrolytes. In addition, the film with 20 NaI also exhibits the lowest τ. This means that the ions travel fastest in this film (Winie & Arof, 2004; Amir et al., 2011). These explain why the 20 NaI film shows the highest conductivity.

In addition, E_a and τ for 20 NaI shows the lower value compared to 20 LiI. This results is expected since the ionic conductivity for 20 NaI is higher compared to 20 LiI. This may be due to the weaker Coulomb force interaction between Na^+ and I^- ions compared to Li^+ and I^- hence enhance the number of mobile free ions (Fuoss & Kraus, 1933; Karo, 1959; Klein et al., 2006; Noor et al., 2015).

Table 5.5: Activation energy, E_a and relaxation time, τ for various concentrations of NaI.

Samples	Activation Energy, E_a (eV)	Relaxation time (s) at ambient temperature, τ
10 NaI	0.42	1.60×10^{-4}
20 NaI	0.38	3.18×10^{-5}
30 NaI	1.22	2.01×10^{-4}
40 NaI	0.52	1.60×10^{-4}

5.2.5 Ionic and Na^+ ion transference Number

The normalized current versus time of 20 NaI is plotted in the graph that is shown in Figure 5.14. From this graph, it shows that the total ionic transference number is 0.98. This suggests that the charge transport that contribute to conductivity in this polymer electrolytes film is predominantly due to ions (Subba et al., 2003; Saikia & Kumar, 2004; Bhargav et al., 2007, 2009). This result is consistent with coordination of both cations (Na^+) and anions (I^-) with polymer host that is shown in Figure 5.10.

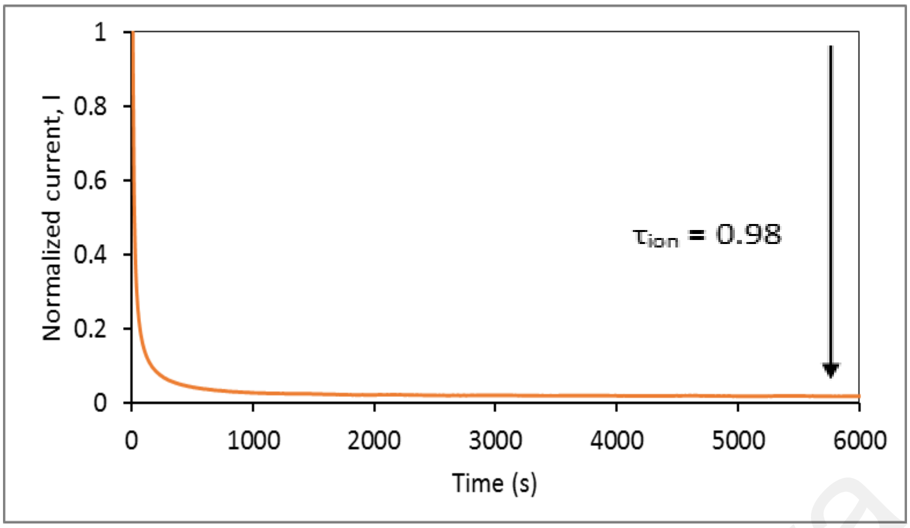

Figure 5.15: Normalized current versus time for 20 NaI polymer electrolyte film

Table 5.6 listed the Na^+ ion transference number values for various NaI concentrations. For high salt concentration (40NaI), the excess dissociation of Na^+ and I^- attributed to the increase of the association rate of the ion, thus leading to the formation of ion clusters. Therefore, the value of sodium transport number cannot be determined. From the table, it can be suggested that the dominant charge carriers contribute for conductivity is most probably due to I^- ions (Zhao et al., 2008; Bhargav et al., 2009). It also shows that the t_{Na^+} for 20NaI is higher compared to t_{Li^+} for 20LiI. This may be due to the size of Na^+ ions which is slightly bigger than Li^+ ions. Therefore, it makes the Na^+ ions loosely interact with the electron donor atom in the polymer host compared to Li^+ ions (Kim & Oh, 2000; Zhao et al., 2008).

Table 5.6: Sodium ion transference number of P (MMA-co-EMA) + NaI

Polymer electrolytes	**Transport number of Na⁺ (t_{Na^+})**
10 NaI	0.35
20 NaI	0.52
30 NaI	0.43
40 NaI	-

5.2.6 Linear Sweep Voltammetry

Film of 20 NaI was chosen for LSV analysis to determine the electrochemical stability of the electrolytes. Figure 5.15 represents the current-voltage response of the polymer electrolyte film which shows that at potentials range from 0 to 2.5 V, the current is small and almost constant. This small current is due to the electron flow that required to maintain a charged double layer at the stainless steel electrode surface. This current is called charging current. As the potential varied beyond 2.5 V, an electrochemical reaction occurs between the surface of the electrode and electrolytes which is, electrons transfer from the electrode surface to the polymer electrolytes film, causing a reduction of the polymer electrolytes and a rapid increase in current. Therefore, the reduction value for this polymer electrolyte film is 2.5 V. This value suggests that this polymer electrolyte is suitable for applications in DSSC (Suri & Mehra, 2007; Imperiyka et al., 2013; Rani et al., 2014).

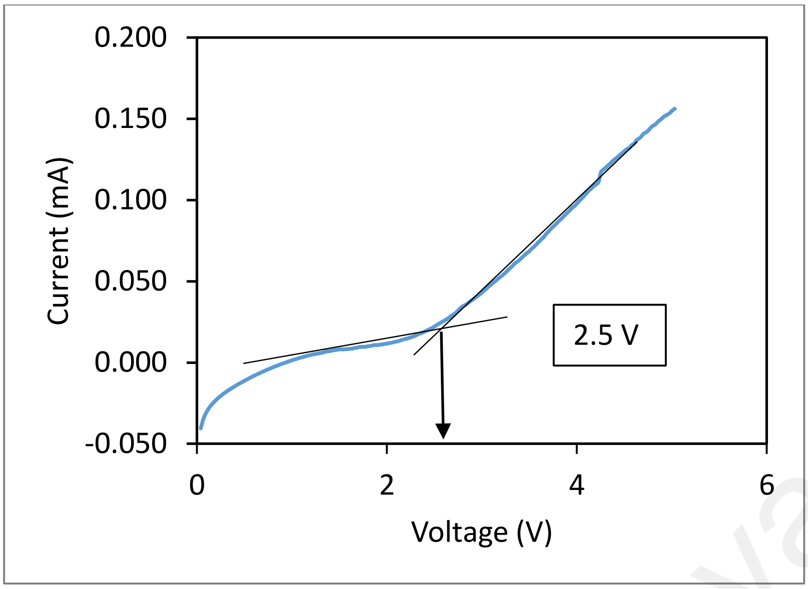

Figure 5.16: Current versus voltage plot of 20 NaI.

5.2.7 *J*–V Measurements

Illustrated in Figure 5.16 is the photocurrent density-voltage (*J*–V) curve of 20 NaI-based DSSC under illumination. The mechanism in the DSSC can be explained as follows. As the dye molecules are struck by light, electrons in the dye are injected into the TiO_2 layer. Then, the electrons are collected by the FTO glass electrode and supplied to the external load. The dye molecules are then electrically reduced to their initial states by electrons transferred from the redox coupling (I^-/I_3^-) in the polymer electrolyte. The oxidized ions in the polymer electrolyte diffuse to the Pt electrode to receive electrons (Ichino et al., 1995).

The photovoltaic parameters, such as J_{sc}, V_{oc}, FF and η, were obtained from the intersection of current and voltage from the *J*–V curves under illumination (Rahman et al., 2007). FTO/TiO_2-dye/20NaI-I_2/Pt DSSC shows a photovoltaic response with a J_{sc} of 2.23 $mA \cdot cm^{-2}$, V_{oc} of 0.76 V, FF of 0.37 and η of 0.62%.

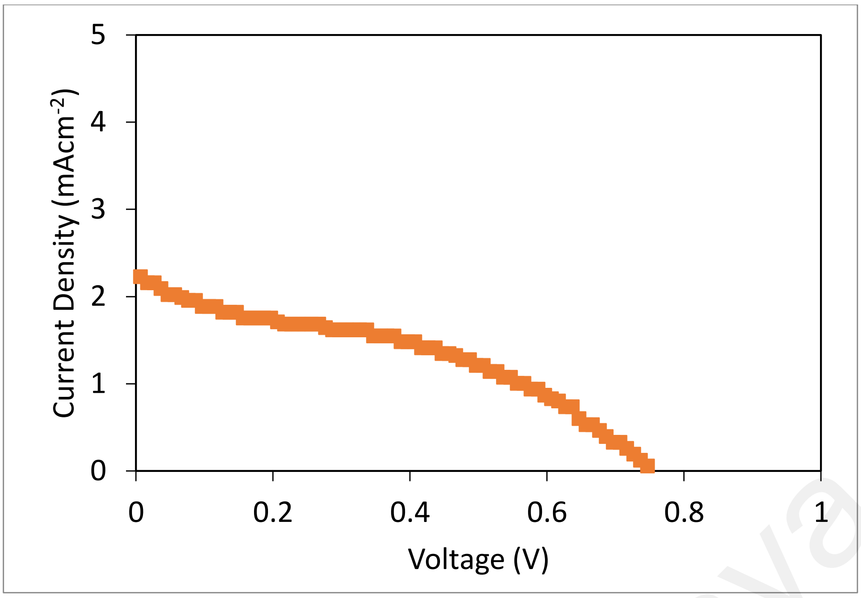

Figure 5.17: *J*-V curve of FTO/TiO_2-dye/20NaI-I_2/Pt DSSC

Comparing the results of DSSCs based on P(MMA-co-EMA) + LiI and P(MMA-co-EMA) + NaI, it can be said that the efficiency of DSSC employing P(MMA-co-EMA) + NaI is higher compared to DSSC employing P(MMA-co-EMA) + LiI. It might be due to the high value of V_{oc} for former compared to the latter. The increase of V_{oc} value is related to the reduction of both the volume concentration of dye adsorbed on the photoelectrode and the I_3^- concentration in the electrolyte (Kim et al., 2005).

According to Nazeeruddin et al (1993), based on equation (5.3), the decrease of the I_3^- concentration retards the back transfer of electrons from the conduction band of TiO_2 to I_3^-, and hence improves the V_{oc} value (Nazeeruddin et al., 1993).

$$V_{oc} = \left(\frac{kT}{q}\right) ln\left(\frac{I_{inj}}{n_{cb}k_{et}[I_3{}^-]}\right) \tag{5.3}$$

where k and T are the Boltzmann constant and absolute temperature, respectively, q is the elementary charge, I_{inj} is the photocurrent resulting from injection, n_{cb} is the electron concentration at the conduction band of TiO_2, k_{et} is the rate constant for the back transfer of electron, and I_3^- is the triiodide concentration.

CHAPTER 6: ADDITION OF IONIC LIQUID FOR DSSC EFFICIENCY ENHANCEMENT

6.0 Introduction

In Chapter 5, the P(MMA-co-EMA) + LiI and P(MMMA-co-EMA) + NaI polymer electrolyte systems with salt ratio of 20 wt% have been found to give the highest conductivity for each system. In order to improve the properties of the polymer electrolytes, various ratio of iodide ionic liquid was added to both polymer electrolytes. Several experimental techniques namely FTIR, DSC, IS and ionic transference number measurement have been employed in order to determine the suitable ratio of electrolytes to be further applied in DSSC. The results of the measurements are presented in the following sections.

6.1 P(MMA-co-EMA) + LiI/NaI + PMII IONIC LIQUID SYSTEM

The compositions and designations of ionic liquid added P(MMA-co-EMA) + 20 LiI and P(MMA-co-EMA) + 20 NaI electrolytes are listed in Table 6.1. Figure 6.1 (a) and (b) shows the example of 6 wt% ionic liquid added P(MMA-co-EMA) + 20 LiI and P(MMA-co-EMA) + 20 NaI polymer electrolyte films. These films are smoother compared to without ionic liquid polymer electrolytes films shown in Figure 5.1 (a) and (b) respectively.

Table 6.1: Designations of PMII ionic liquid added P(MMA-co-EMA) + 20 LiI and P(MMA-co-EMA) + 20 NaI polymer electrolytes.

PMII (wt% ratio)	LiI-PMII	NaI-PMII
2	LiI-2IL	NaI-2IL
4	LiI-4IL	NaI-4IL
6	LiI-6IL	NaI-6IL
8	LiI-8IL	NaI-8IL

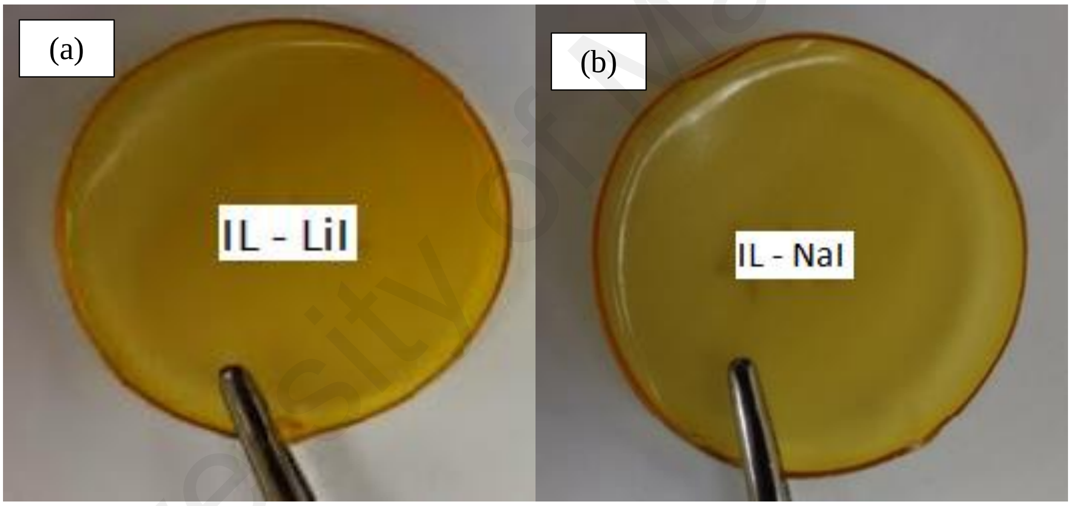

Figure 6.1: PMII ionic liquid (6 wt%) added (a) P(MMA-co-EMA) + 20 LiI and (b) P(MMA-co-EMA) + 20 NaI polymer electrolyte films

6.1.1 FTIR Analysis

Displayed in Figures 6.2 and 6.3 are FTIR spectra of the P(MMA-co-EMA) + LiI and P(MMA-co-EMA) + NaI polymer electrolytes before and after addition of PMII ionic liquid. The figures show several selected regions which are regions for carbonyl group

(C=O) located between the wavenumber 1750 and 1730 cm^{-1}, ether group (C-O-C) at 1300-1000 cm^{-1} and methyl group (CH_3) at 1440-1245 cm^{-1} of the MMA and EMA in P(MMA-co-EMA). In earlier discussion (Chapter 5), the addition of LiI and NaI to the P(MMA-co-EMA) host copolymer resulted in the shifting of the bands to lower wavenumbers. This was due to the coordination of cations and anions from the doping salts with the oxygen atoms and methyl group from the functional groups of host copolymer respectively (Pavia et al., 2005; Ahmad et al., 2011).

Later, with addition of PMII ionic liquid into the P(MMA-co-EMA) + LiI and P(MMA-co-EMA) + NaI polymer electrolytes, the bands are shifted to higher wavenumbers. For PMII added polymer electrolytes containing LiI, the symmetrical stretching of the carbonyl group, ν(C=O) at 1717 cm^{-1} are shifted to 1723 cm^{-1}. The specific vibration mode of ether group (C-O-C) such as –CH_3 asymmetric deformation of P(MMA-co-EMA) from δ(O-CH_3) at 1478 cm^{-1} was shifted to 1483 cm^{-1}, symmetric and asymmetric stretching mode of C-O-C at 1266 and 1234 cm^{-1} respectively are shifted to 1272 and 1242 cm^{-1} and asymmetrical stretching mode, ν_{as}(C-O-C) at 1138 cm^{-1} shifted to 1143 cm^{-1} respectively.

Meanwhile for polymer electrolytes ionic liquid added P(MMA-co-EMA) + NaI system, the band of the symmetrical stretching of the carbonyl group, ν(C=O) at 1717 cm^{-1} is shifted to 1726 cm^{-1}. The specific vibration mode of ether group (C-O-C) such as –CH_3 asymmetric deformation of P(MMA-co-EMA) from δ(O-CH_3) at 1444 cm^{-1}, symmetric and asymmetric stretching mode of C-O-C at 1267 and 1234 cm^{-1} respectively and asymmetrical stretching mode, ν_{as}(C-O-C) at 1138 cm^{-1} are shifted to higher wavenumbers of 1448, 1272, 1239 and 1145 cm^{-1} respectively. The shifting of the bands to the higher wavenumbers for both polymer electrolytes added with ionic liquid are probably due to the strong interaction that occurred between H^+ from the PMII ionic liquid with the oxygen atoms of the copolymer host (Freitas et al., 2009).

Ethyl group, CH_2 scissoring $\delta(CH_2)$ band for ionic liquid added P(MMA-co-EMA) + LiI and P(MMA-co-EMA) + NaI polymer electrolytes was assigned at 1478 and 1480 cm^{-1} respectively is shifted to 1483 and 1486 cm^{-1}. These may be due to the interaction between polymer host with iodide ions from salts and the anions from PMII ionic liquid (Ramesh & Lu, 2008; Ramesh et al., 2014). The possible interaction mechanism between of the host copolymer, doping salt and ionic liquid polymer electrolytes are shown in Figure 6.4 (a) and (b) respectively.

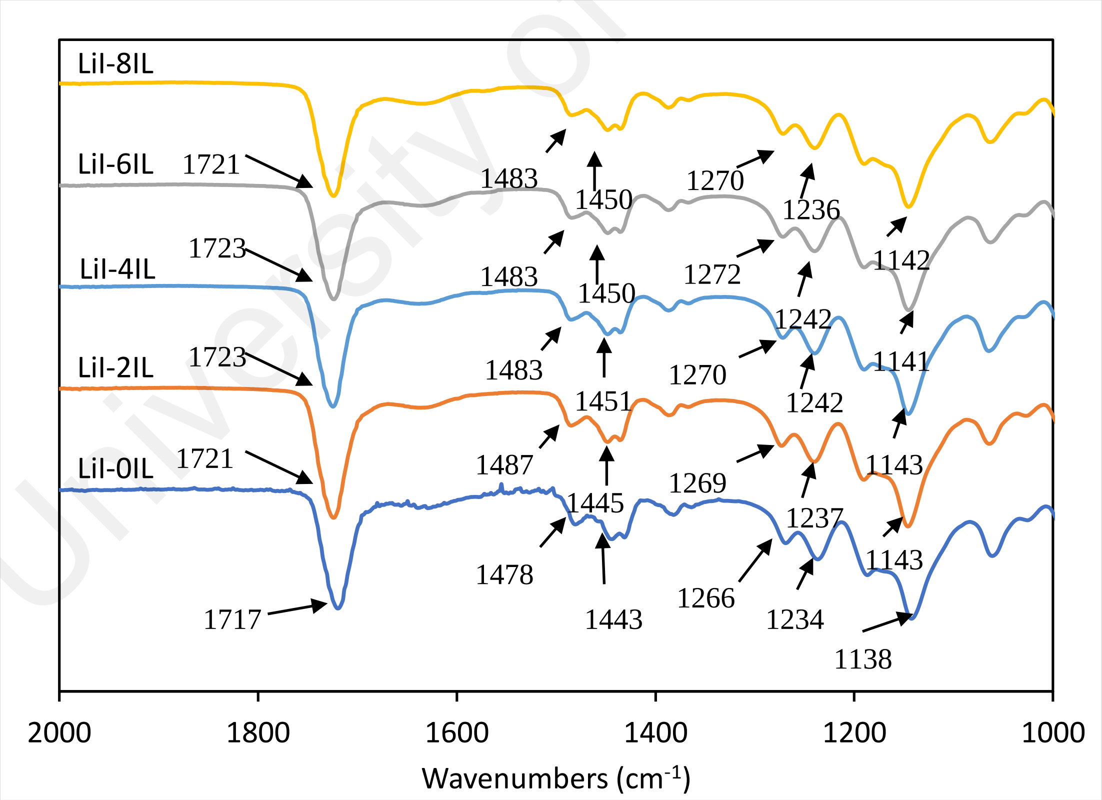

Figure 6.2: FTIR spectra of P(MMA-co-EMA) + LiI + IL

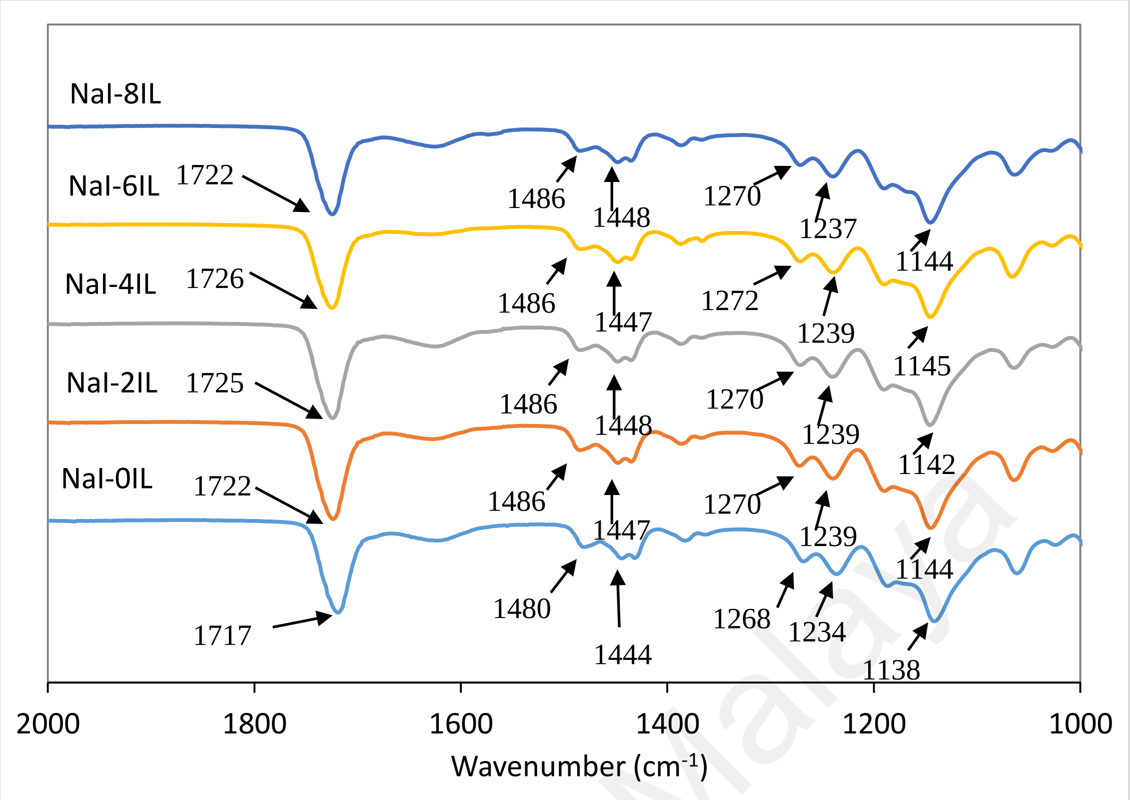

Figure 6.3: FTIR spectra of P(MMA-co-EMA) + NaI + IL

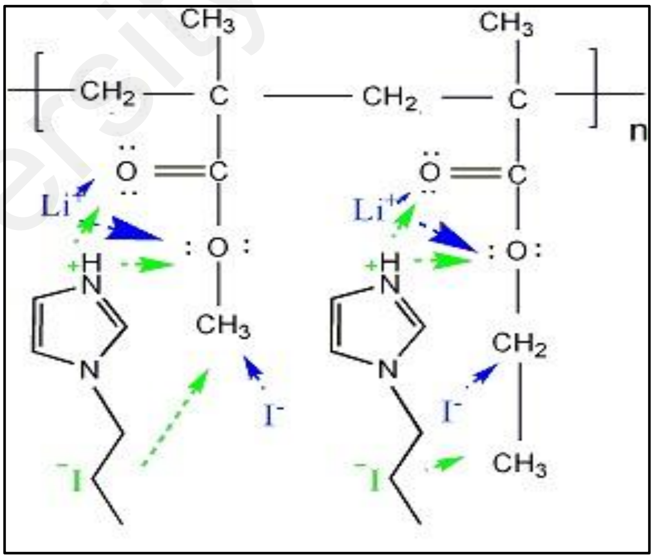

(a)

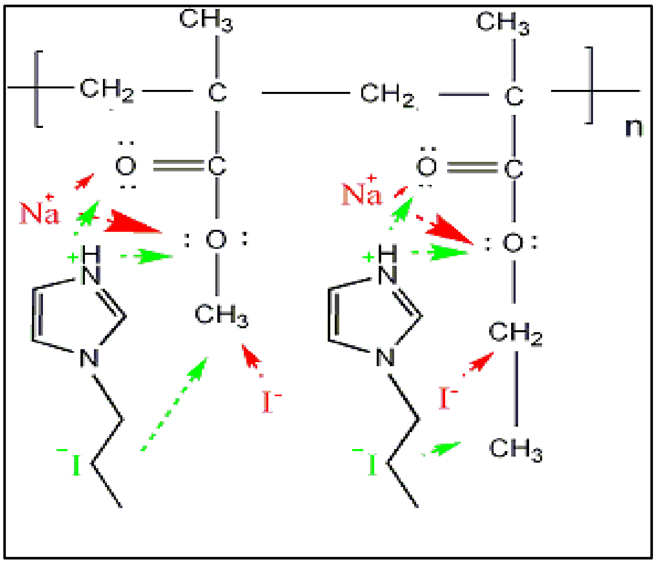

(b)

Figure 6.4: Possible interaction in (a) LiI-IL and (b) NaI-IL polymer electrolytes

6.1.2 Thermal Analysis

DSC thermograms of PMII added P(MMA-co-EMA) + LiI and P(MMA-co-EMA) + NaI with various concentrations of PMII are shown in Figure 6.5 (a) and (b) respectively. The figures demonstrate that the T_g decreases with the increase in PMII concentration up to 6 wt%. It is may be due to the IL molecules have interrupted and weaken the polymer-salt interactions, hence increase the polymer chain segmental mobility resulted in the decrease of T_g (Chiodelli et al., 1988; Silva et al., 2004; Baskaran et al., 2006; Anuar et al., 2012). However, further addition of PMII concentration resulted in an increase in T_g. This phenomenon is believed due to the formation of ion pairs and ion aggregates that could obstruct the orientation of the molecules and hence constrain the flexibility of polymer chains (Thokchom et al., 2005; Liew et al., 2014).

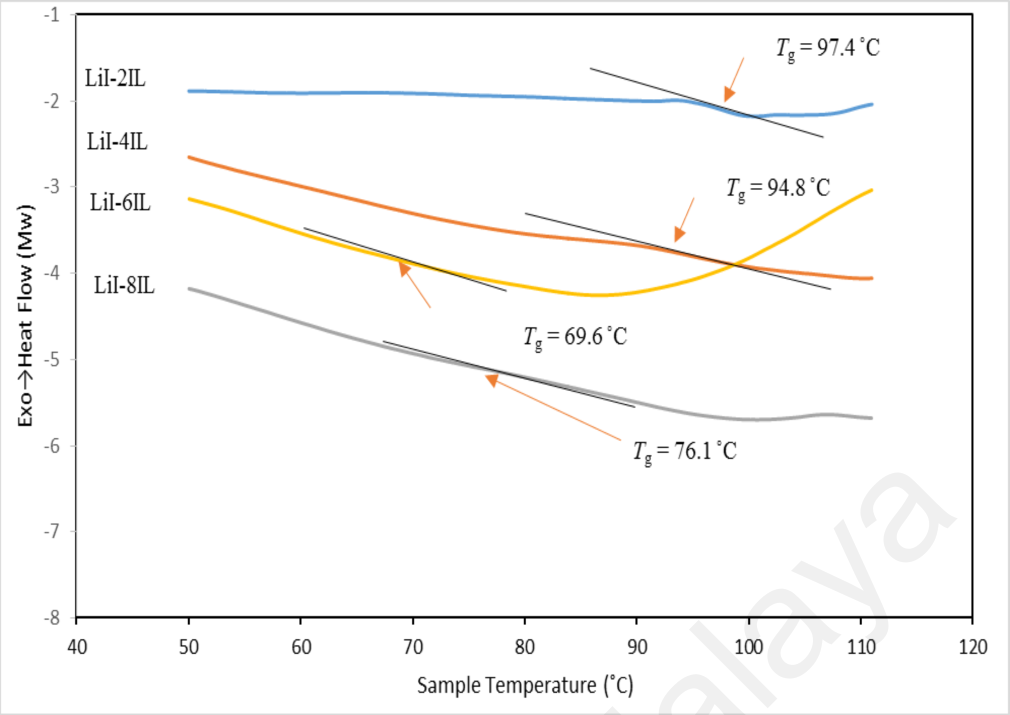

(a)

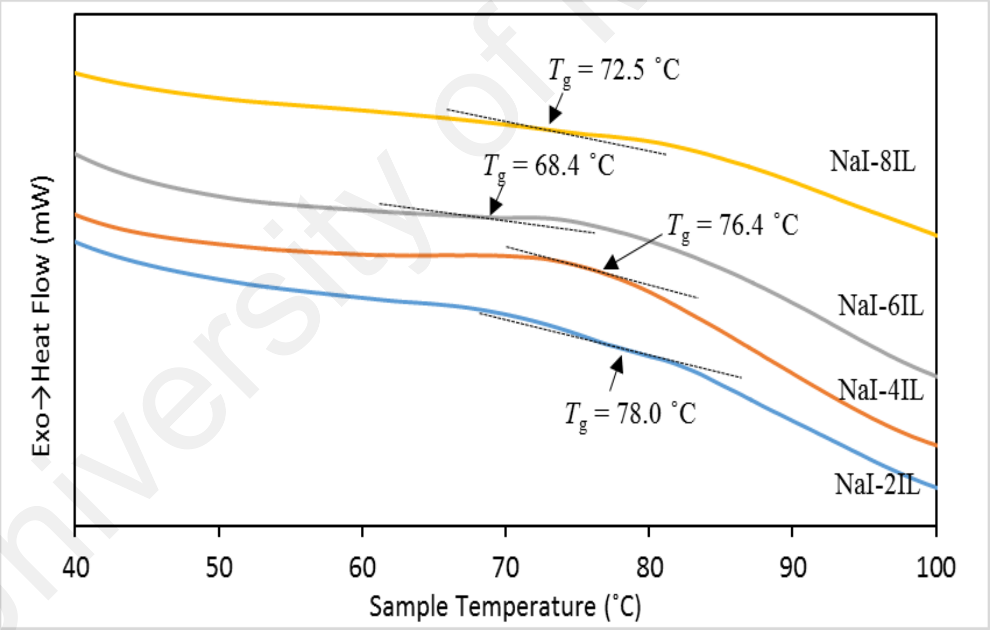

(b)

Figure 6.5: DSC thermograms of (a) LiI-IL and (b) NaI-IL polymer electrolytes

6.1.3 Electrical Analysis

The ionic conductivity behaviour for both P(MMA-co-EMA) + LiI and P(MMA-co-EMA) + NaI added with PMII are presented in Table 6.2. The conductivity of P(MMA-co-EMA) (copolymer host) is in the order of 10^{-11} S cm^{-1} (Chapter 4). Later, with addition of LiI and NaI salt into the copolymer host, the ionic conductivity value is enhanced to the order of 10^{-6} S cm^{-1}. This enhancement was attributed to the increase of the number and mobility of ions in the polymer host matrix. Further effect in ionic conductivity is observed with addition of PMII ionic liquid to polymer electrolytes.

For the P(MMA-co-EMA) + NaI + PMII system, the highest ionic conductivity value is obtained at 6 wt% of PMII with the value of 4.43×10^{-5} S cm^{-1}. The conductivity enhancement upon the addition of ionic liquid concentration for both systems are may be due to the increase of charge carriers and polymer chains segmental mobility as evidenced by the decrease in T_g mentioned earlier (Chaurasia et al., 2014; Ng et al., 2015). As the amount of ionic liquid increased to 6 wt %, an optimum ion concentration is reached whereby ion interactions between polymer, salt and ionic liquid were optimized. At high ionic liquid concentration (8 wt%), the distance between the ions from doping salt and ionic liquid within the polymer host decreases and the ions might have formed ion pairs or ion clusters (Karan et al., 2008; Kunze et al., 2012). This result was similar to the variation of T_g with ionic liquid concentration which decrease the ions mobility and hence decreases the ionic conductivity (Thokchom et al., 2005; Karan et al., 2008). Some researchers have reported that with addition of low viscosity ionic liquid to the polymer electrolytes system increased the ionic conductivity due to additional charge carriers since the ionic liquid composed of cations as well as anions (Bhattacharya et al., 2010; Nagarale et al., 2010; Singh et al., 2010; Singh et al., 2011).

However, in this work the conductivity decreases upon the addition of PMII to the P(MMA-co-EMA) + LiI system. The ionic conductivity values showed no significant decrease when the amount of ionic liquid was increased. The slight decrease in conductivity may be due to the trapping of Li^+ ions by the bulky ions of the ionic liquid. (Calhoun & Voth, 1996; Selvasekarapandian et al., 2006).

Table 6.2: Conductivity of samples with various concentrations of PMII at room temperature

IL Concentration (wt%)	Conductivity, σ (S cm^{-1}) LiI-IL	Conductivity, σ (S cm^{-1}) NaI-IL
2IL	$(2.19 \pm 0.19) \times 10^{-8}$	$(1.56 \pm 0.33) \times 10^{-8}$
4IL	$(2.34 \pm 0.11) \times 10^{-9}$	$(1.22 \pm 0.19) \times 10^{-8}$
6IL	$(8.94 \pm 0.26) \times 10^{-8}$	$(4.43 \pm 0.34) \times 10^{-5}$
8IL	$(4.28 \pm 0.20) \times 10^{-9}$	$(1.90 \pm 0.85) \times 10^{-8}$

6.1.4 Temperature dependence study

Figures 6.7 and 6.8 show the plot of log conductivity against 1000/*T*, for LiI-IL and NaI-IL system. For LiI-IL system, the film of LiI-2IL was not stable at elevated temperature as presented in Figure 6.6 and the phenomenon could not be understandable. Therefore, for LiI-IL system, the temperature dependence study was done only for 3 concentrations of IL which are 4, 6 and 8 wt%. From Figure 6.7 and 6.8, it is observed that the conductivity value increases as the temperature increase. This indicates that the conductivity for both LiI-IL and NaI-IL polymer electrolyte systems are thermally activated due to the improvement of polymer chain segments movement and dissociation of ions in the polymer electrolytes-ionic liquid systems (Rajendran & Uma, 2000; Rajendran et al., 2004; Alias et al., 2005).

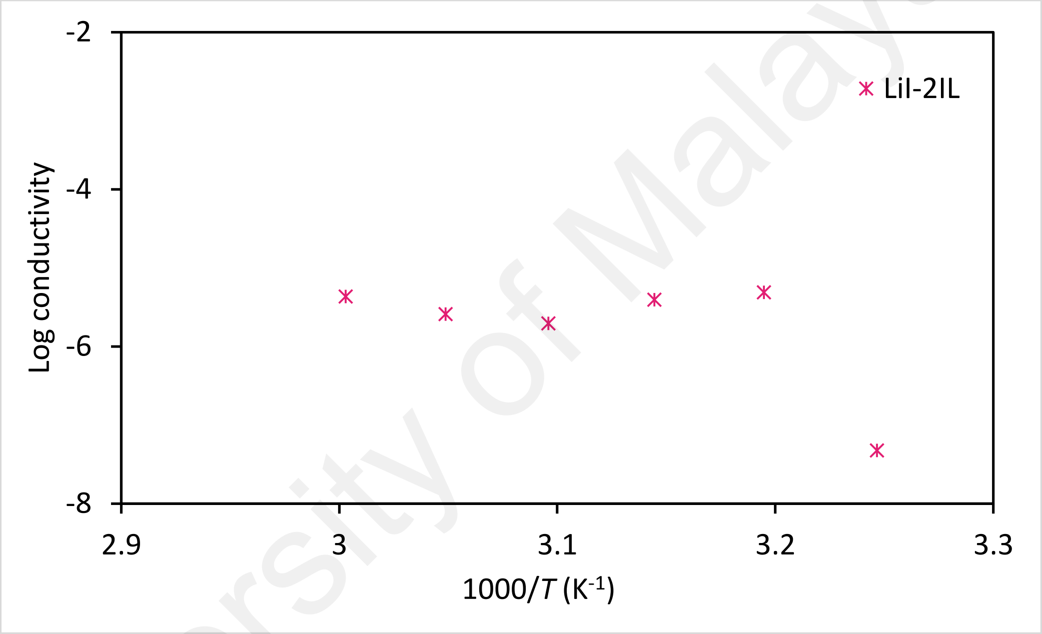

Figure 6.6: Plots of temperature dependence of conductivity for LiI-2IL polymer electrolyte

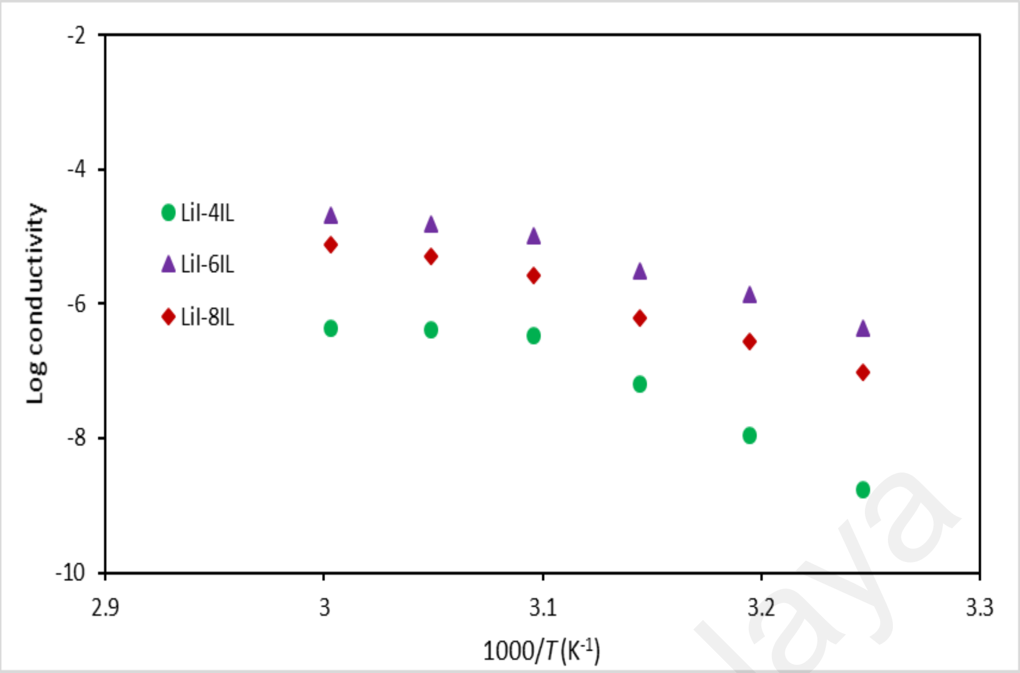

Figure 6.7: Plots of temperature dependence of conductivity for LiI-IL polymer electrolytes

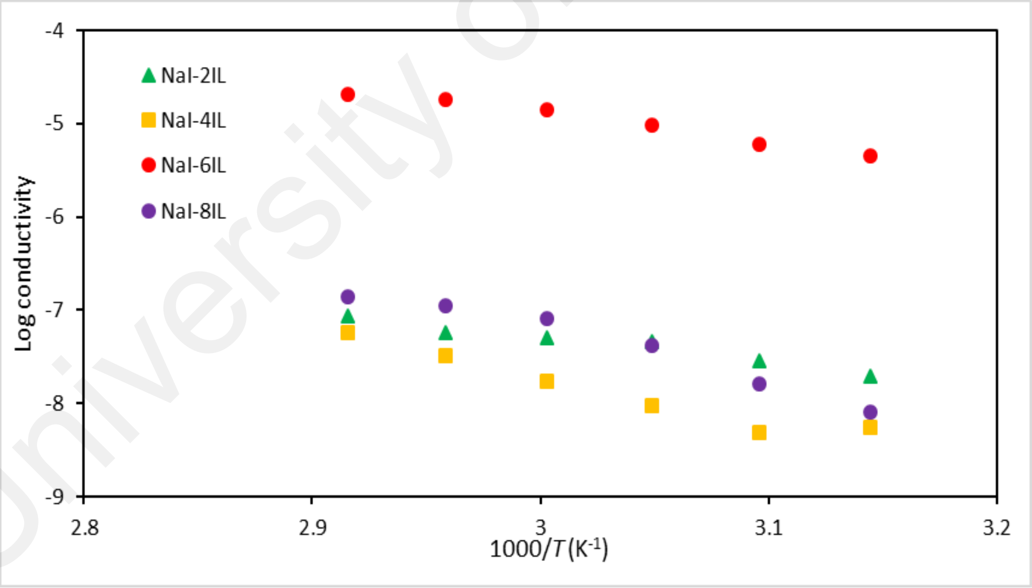

Figure 6.8: Plots of temperature dependence of conductivity for NaI-IL polymer electrolytes

The activation energy, E_a, can be calculated from the slope of the plots in Figure 6.7 and 6.8 using the equation below:

$$\sigma = \sigma_0 exp\left(\frac{-E_\mathrm{a}}{k_B T}\right) \tag{6.1}$$

where σ_0 is the pre-exponantial factor of conductivity, k_B and T are Boltzman constant and absolute temperature respectively.

The E_a values for both LiI-IL and NaI-IL are listed in Table 6.3. Samples with lower value of E_a which are LiI-6IL and NaI-6IL required smaller energy to allow the conducting ions move easily in the polymer matrix, hence increase the ionic conductivity of the sample (Chandra & Chandra, 1994). The trend of the E_a - IL content is the same as the trend of T_g - IL content and consistent with the trend of conductivity - IL content. This shows that the E_a is another factor influencing the conductivity of the studied IL added copolymer electrolytes.

Table 6.3: Activation energy for LiI-IL and NaI-IL

IL Concentration (wt%)	**E_a for LiI-IL (eV)**	**E_a for NaI-IL (eV)**
2IL	-	0.61
4IL	2.04	0.96
6IL	1.41	0.52
8IL	1.63	1.12

6.1.5 Ionic transference number measurement

Total ionic transference number (τ_{ion}) was measured to determine the ionic contribution to the total charge transport. The plots of normalized current versus time for LiI-6IL and NaI-6IL are depicted in Figure 6.9 and 6.10 respectively. The value of τ_{ion} for LiI-6IL and NaI-6IL was calculated using equation (3.7) and the value is 0.99 for both samples. According to Arof (2000), the value of τ_{ion} is approximately to 1 if the ideal electrolytes is predominantly due to ions. Therefore, these results shows that the charge transport for these polymer electrolyte films were predominantly due to ions (Saikia & Kumar, 2004).

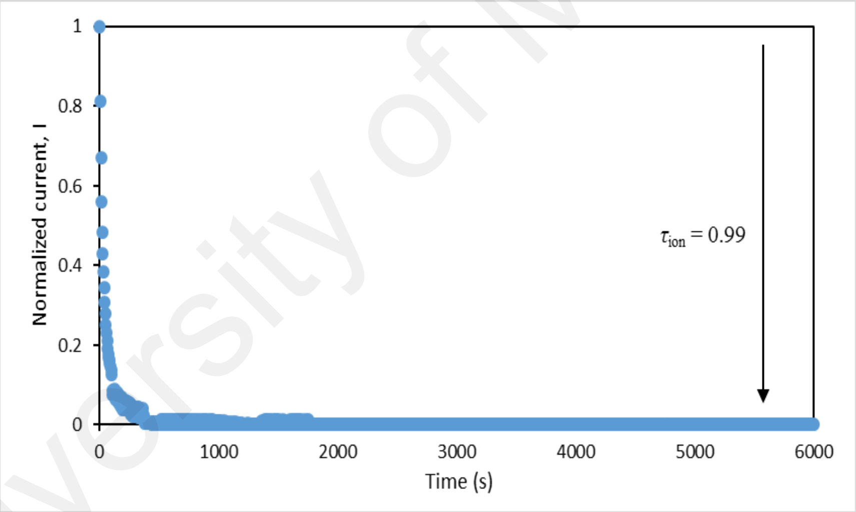

Figure 6.9: Normalized current-time plot of LiI-6 IL polymer electrolyte

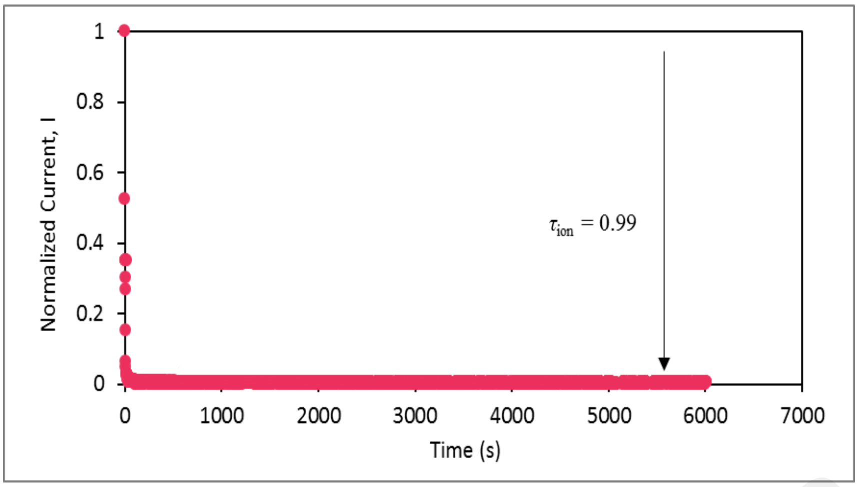

Figure 6.10: Normalized current-time plot of NaI-6 IL polymer electrolyte

6.1.6 DSSC Measurement

The photocurrent density voltage curve of the FTO/ TiO_2-dye/ LiI-6IL-I_2/ Pt is presented in Figure 6.11. The DSSC based on LiI-6IL shows a higher efficiency value, Table 6.4, compared to that of the DSSC fabricated using 20LiI reported in Section 5.1. This behaviour is not predictable since the ionic conductivity of the LiI-6IL is lower than the conductivity of 20LiI. The J_{sc} value for DSSC based LiI-6IL does not have significant effect compared to DSSC based 20LiI. Therefore, the higher efficiency can be related with the higher V_{oc} value of DSSC based LiI-6IL compared to DSSC based 20LiI. The higher V_{oc} value may be due to the negative shift of the conduction band edge of TiO_2 and the suppression of electron recombination at the TiO_2/electrolyte interface. It is assumed that when the electrons are injected into the conduction band of TiO_2 from the dye sensitizer, the cations are likely to be adsorbed on the negative charged TiO_2 particle, forming the electric double layer (Helmholtz layer) at the TiO_2 particle surface. Generally, the potential drop in Helmholtz layer gives a positive shift of conduction band edge of TiO_2 (Redmond & Fitzmaurice, 1993; Lyon & Hupp, 1995; Liu et al., 1998; Cahen et al., 2000). In this case, the PMI^+ cation is bulky, therefore it is less mobile while

Li^+ cations form complex with hard coordination with P(MMA-co-EMA) (the interaction of ions with host polymer is presented in Figure 6.4 (a)) (Armand, 1990), correspondingly decreasing the amount of the absorbed Li^+ on the surface of TiO_2 particle and thereby resulting in the shift of the conduction band edge back to a negative position. Furthermore, this polymer electrolytes membrane might have also served as a passivation layer on the TiO_2 surface, blocking the charge recombination between the electrons in TiO_2 and triiodide in the electrolyte, which resulted in a decrease recombination and increase electron lifetime of the polymer electrolytes.

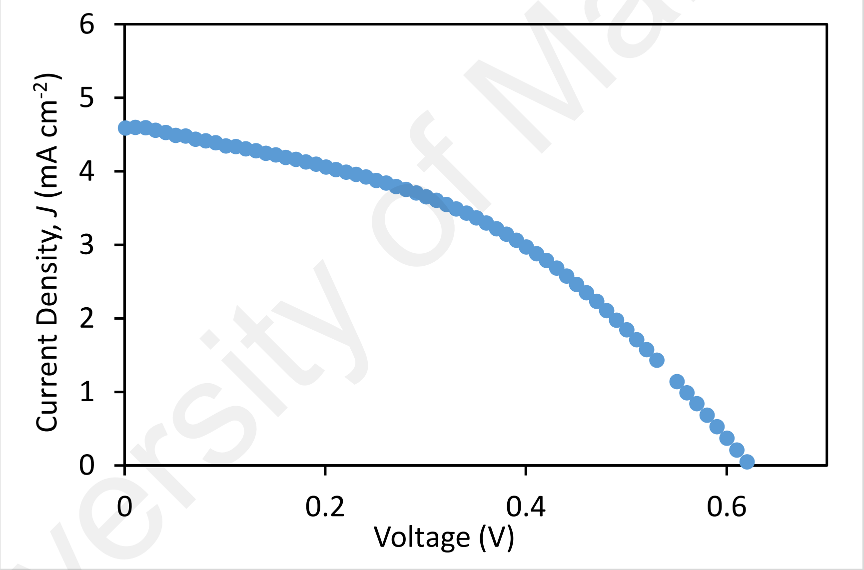

Figure 6.11: *J*–V curve of the dye-sensitized solar cell based LiI-6IL

Figure 6.12 illustrated the photocurrent density voltage curve of FTO/ TiO_2-dye/ NaI-6IL-I_2/ Pt. The efficiency of this DSSC is 1.05% which is higher compared to DSSC based on 20NaI. The higher efficiency value of DSSC based on NaI-6IL is due to the increases of J_{sc} and decreases of V_{oc} value. This behaviour is expected since this electrolyte contained more Na^+ ions (from Na^+ transference number result) and iodide ions (from NaI and PMII), thus the regeneration of the oxidized dye is expected to be more efficient

(Seo et al., 2011). This result is confirmed with the lower value of V_{oc} value compared to that of DSSC employing ionic liquid free polymer electrolyte which is 0.76 V. According to Enright et al (Enright et al., 1994) and Redmond et al (Redmond & Fitzmaurice, 1993), this reduction might be due to the increase concentration of I_3^- hence increasing the recombination reaction between injected electrons and electrolyte. Besides, the intercalation of cations into the TiO_2 structure might have also shifted down the Fermi level of the oxide semiconductor (Freitas et al., 2009).

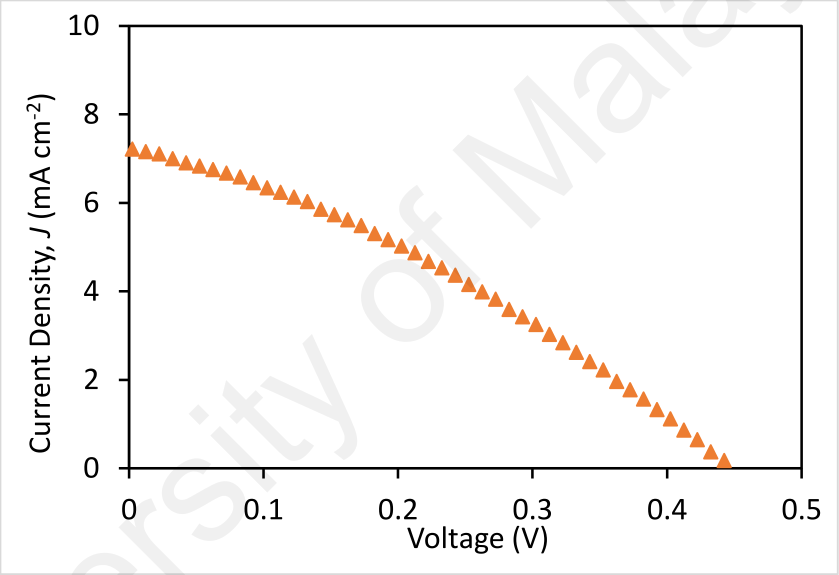

Figure 6.12: *J*–V curve of the dye-sensitized solar cell based NaI-6IL

Table 6.4 lists the results of V_{oc}, J_{sc}, FF and efficiency of DSSC for both based LiI-6IL and NaI-6IL. These results prove that with addition of ionic liquid in to the P(MMA-co-EMA) based polymer electrolytes gave better energy conversion efficiency.

Table 6.4: Parameters of LiI-IL and NaI-IL based DSSCs

DSSC	***V*oc**	***J*sc**	**FF**	**Eff (%)**
LiI_PMII	0.62	4.59	0.42	1.19
NaI_PMII	0.44	7.21	0.33	1.05

CHAPTER 7: CONCLUSIONS AND SUGGESTIONS FOR FUTURE WORK

7.0 Conclusions

New P(MMA-co-EMA) copolymers were successfully obtained using free radical photo-polymerization technique. Five different monomers ratios of 90MMA:10EMA, 70MMA:30EMA, 50MMA:50EMA, 30MMA:70EMA and 10MMA:90EMA were copolymerized. However only three of them, namely 90MMA:10EMA, 70MMA:30EMA and 50MMA:50EMA could form flexible free standing films. The formation of the copolymers was confirmed by the disappearance of reactive double bond peaks of $C=CH_2$ at 939 cm^{-1} and C=C peak at 1636 cm^{-1} in the FTIR spectra indication the combination between $C-CH_2$ from MMA and EMA monomers. This was supported by the presence of a single peak in the DMA curves. Among those three ratios, 90MMA:10EMA exhibited the lowest molecular weight bulk resistivity and glass transition temperature value indicating greatest copolymer chain flexibility that is favourable for ions transport. Therefore, 90MMA:10EMA copolymer was the most promising to be used as host in polymer electrolytes.

Addition of LiI and NaI into the 90MMA:10EMA copolymer host gave significant effects to the optical, thermal and electrical properties. The formation of P(MMA-co-EMA) – salt complex was indicated by the interactions between the cations and anions from the salts with oxygen atoms and methyl group of the copolymer host respectively. This was evidenced by the shifting of FTIR bands of carbonyl (C=O) group located around 1750-1730 cm^{-1}, ether (C-O-C) and methyl (CH_3) group located around 1500-1000 cm^{-1} towards lower wavenumbers.

The ionic conductivity of the P(MMA-co-EMA) + LiI system increased with the increase of LiI concentration but decreased at high loading of LiI. The highest ionic conductivity was achieved at 20 wt% of LiI with the value of 1.3×10^{-6} S cm^{-1}. This trend is opposite to that of the T_g – LiI concentration. The increase in ionic conductivity was due to the increase in flexibility of the polymer chain, as evidenced by the decrease in T_g, that helped in enhancing the mobility of Li^+ and I^- ions. This was supported by the decrease in activation energy and relaxation time. However, the decrease in ionic conductivity with addition of more than 20 wt% LiI was ascribed to the formation of ion pairs or ion clusters which reduced the number of free ions. The charges transport in the electrolyte system was predominantly due to ions. All of the P(MMA-co-EMA) + LiI electrolytes exhibited low Li^+ ion transport number indicating that the majority of ions that contributed to ionic conductivity was not Li^+ ions but most possibly I^- ions and 20LiI sample exhibited the highest Li^+ transport number.

Unlike the P(MMA-co-EMA) + LiI, the σ - NaI content of the P(MMA-co-EMA)-NaI polymer electrolyte system showed the same trend as that of the T_g – NaI content. The sample containing 20 wt% of NaI exhibited the highest ionic conductivity value of 5.19 × 10^{-6} S cm^{-1}. The conductivity increase observed for samples containing $\leq$ 20 wt% of NaI might be due to the crosslinking effect between NaI and P(MMA-co-EMA) chains. On the other hand, the decrease in conductivity for sample containing more than 20 wt% NaI was attributable to the formation ion pairs or ion clusters which reduced the number of free ions leading to the decrease in ionic conductivity. Ionic transference number of

20NaI polymer electrolyte samples suggested that the charge transport in the electrolyte system was predominantly due to ions. Besides that, all the P(MMA-co-EMA) + NaI displayed low Na^+ ion transport number (<0.5) suggested that the majority of ions that contributed to ionic conductivity was most probably due to I^- ions not Na^+ ions.

Comparatively, polymer electrolytes of P(MMA-co-EMA) + NaI exhibited higher ionic conductivity, lower activation energy and relaxation time. This was ascribed to the bigger size of Na^+ compared to Li^+, implying lower Coulomb interaction force between Na^+ and I^- compared to that between Li^+ and I^-. Therefore, the Na^+ and I^- ions were easier to be dissociated leading to higher number of free mobile ions that contributed to ionic conductivity. The bigger size of Na^+ also made the Na^+ ions loosely interact with the electron donor atoms in the polymer host compared to Li^+ ions and thus gave greater contribution to conductivity as indicated by the higher Na^+ ion transport number compared to Li^+ ion.

PMII ionic liquid of various concentrations was added into the P(MMA-co-EMA) + 20LiI and P(MMA-co-EMA) + 20NaI polymer electrolytes. FTIR spectra for both polymer electrolytes added with ionic liquid showed that the bands of carbonyl, ether and methyl groups were shifted to the higher wavenumbers. This was due to the strong interaction that occurred between H^+ from the PMII ionic liquid with the oxygen atoms of the copolymer host and iodide ions with the methyl groups.

The addition of ionic liquid increased the conductivity by one order magnitude of the NaI-IL system. The highest ionic conductivity values was obtained at 6 wt% of PMII for NaI-IL system with ionic conductivity values of 4.43×10^{-5} S cm^{-1}. The increase in conductivity was believed due to the plasticizing effect of ionic liquid which increased the segmental mobility of the polymer chains as evidenced by the decrease in T_g. The decrease of conductivity of the polymer electrolyte containing high content of PMII ionic liquid might be due to the decrease of the distance between ions from doping salt and ionic liquid, due to high content of ions, within the polymer host resulting in the formation of ion pairs or ion clusters.

Meanwhile, for the LiI-IL system, the conductivity decreased by two orders of magnitude. This may be due to the entrapment of Li^+ ions by the bulky PMI^+ ions of ionic liquid that decreased the mobility of the ions. The size of Na^+ is bigger compared to Li^+ as such the chances of Na^+ ions to be trapped by the PMI^+ was smaller. This was consistent with the results of E_a, which was another factor that affected the conductivity. The Li-IL exhibited higher E_a compared to the NaI-IL system indicating that the ions in the latter system were more readily to move in the system.

Transference number measurement demonstrated that both LiI-6IL and NaI-6IL polymer electrolytes were ionic conductors. The obtained transference number values are about the same with those without ionic liquid, LiI and NaI systems. This demonstrated that the IL did not contributed additional ions but only acted as a plasticizing agent. The low cationic transference number for P(MMA-co-EMA) + LiI and P(MMA-co-EMA) + NaI systems, <0.5, indicated that the majority mobile ions in these polymer electrolyte systems were I^- anions. This means that both the P(MMA-co-EMA) + LiI and P(MMA-co-EMA) + NaI polymer electrolytes can act as redox mediator (I^-/I_3^-) making them suitable for DSSC application.

DSSC based on P(MMA-co-EMA) + 20LiI and P(MMA-co-EMA) + 20NaI polymer electrolytes exhibited the energy conversion efficiency of 0.45% and 0.62% respectively. The higher efficiency of DSSC based on the 20NaI polymer electrolytes membrane might be due to the high value of V_{oc}. This was ascribed to the decrease of I_3^- concentrations that retarded the back transfer of electrons from the conduction bands of TiO_2 to I_3^-. The DSSC efficiencies increased to 1.19% and 1.05% for LiI-6IL and NaI-6IL respectively with addition of ionic liquid into the systems. This was attributed to the increased iodide ions content (from salt and ionic liquid) in the polymer electrolyte systems. Therefore, this observation proved that the DSSC efficiency can be enhanced by adding ionic liquid into the polymer electrolyte systems.

7.1 Suggestions for future work

Solid polymer electrolytes studied in this work were found suitable for application in dye sensitized solar cells. Further work should be done in order to improve the properties of these solid polymer electrolytes such as conductivity and mechanical stability for long term use in DSSC application. The improvement may be achieved by several approaches as follows:

i. Acrylic monomer may be copolymerized with other suitable monomers in order to improve the mechanical stability of the host polymer for long term usage.
ii. Other types of more suitable salts and ionic liquids that can act as redox couple for DSSC application may be used to act as dopant and plasticizers respectively.
iii. Other types of metal oxides need to be considered as alternative photo-electrodes in order to improve the performance of the P(MMA-co-EMA) based DSSCs.

REFERENCES

Abdelrazek, E. (2007). Influence of $FeCl_3$ filler on the structure and physical properties of polyethyl-methacrylate films. *Physica B: Condensed Matter, 400*(1), 26-32.

Agapov, A. L., and Sokolov, A. P. (2011). Decoupling Ionic Conductivity from Structural Relaxation: A Way to Solid Polymer Electrolytes? *Macromolecules, 44*(11), 4410-4414.

Agarwala, S., Thummalakunta, L. N. S. A., Cook, C. A., Peh, C. K. N., Wong, A. S. W., Ke, L., and Ho, G. W. (2011). Co-existence of LiI and KI in filler-free, quasi-solid-state electrolyte for efficient and stable dye-sensitized solar cell. *Journal of Power Sources, 196*(3), 1651-1656.

Ahmad, A., Isa, K. M., and Osman, Z. (2011). Conductivity and structural studies of plasticized polyacrylonitrile (PAN)-lithium triflate polymer electrolyte films. *Sains Malaysiana, 40*(7), 691-694.

Ahmad, A., Rahman, M., Su'ait, M., and Hamzah, H. (2011). Study of MG49-PMMA Based Solid Polymer Electrolyte. *Open Materials Science Journal, 5*.

Ali, A., Yahya, M., Bahron, H., and Subban, R. (2006). Electrochemical studies on polymer electrolytes based on poly (methyl methacrylate)-grafted natural rubber for lithium polymer battery. *Ionics, 12*(4-5), 303-307.

Alias, Y., Ling, I., and Kumutha, K. (2005). Structural and electrochemical characteristics of 49% PMMA grafted polyisoprene-$LiCF_3SO_3$-PC based polymer electrolytes. *Ionics, 11*(5-6), 414-417.

Amir, S. N., Othman, R., Subban, R. H. Y., and Mohamed, N. S. (2011). Ionic conductivity of PEMA-$LiClO_4$ polymer electrolytes. *Sains Malaysiana, 40*(7), 701-705.

Andrzejewska, E. (2001). Photopolymerization kinetics of multifunctional monomers. *Progress in Polymer Science, 26*(4), 605-665.

Anuar, N. K., Subban, R. H. Y., and Mohamed, N. S. (2012). Properties of PEMA-NH4CF3SO3 added to BMATSFI ionic liquid. *Materials, 5*(12), 2609-2620.

Armand, M. (1990). Polymers with ionic conductivity. *Advanced Materials, 2*(6-7), 278-286.

Arof, A., Mohamed, N., Subban, R., Hashim Ali, S., and Yahya, M. (2000). *Electrochemical Power Sources: Materials and Characterization*. Malaysia: Universiti Malaya.

Ashton, A. Q. (2013). Iron Compounds—Advances in Research and Application. *Atlanta, Georgia: Scholarly-Editions.*

Bach, U., Lupo, D., Comte, P., Moser, J., Weissörtel, F., Salbeck, J., . . . Grätzel, M. (1998). Solid-state dye-sensitized mesoporous TiO_2 solar cells with high photon-to-electron conversion efficiencies. *Nature, 395*(6702), 583-585.

Bai, Y., Cao, Y., Zhang, J., Wang, M., Li, R., Wang, P., . . . Gratzel, M. (2008). High-performance dye-sensitized solar cells based on solvent-free electrolytes produced from eutectic melts. *Nat Mater, 7*(8), 626-630.

Balakrishnan, V. V., Abidin, Z., Nasir, K., Jamari, S., Saidon, N., Lee, S., . . . Yahya, R. (2013). The characteristics of a coating system containing lawsone dye colorant and PMMA-acrylic polyol blended resin. *Pigment & Resin Technology, 42*(2), 128-136.

Balducci, A., Jeong, S. S., Kim, G. T., Passerini, S., Winter, M., Schmuck, M., . . . Tran, N. (2011). Development of safe, green and high performance ionic liquids-based batteries (ILLIBATT project). *Journal of Power Sources, 196*(22), 9719-9730.

Bandara, T., Dissanayake, M., Jayasundara, W., Albinsson, I., and Mellander, B.-E. (2012). Efficiency enhancement in dye sensitized solar cells using gel polymer electrolytes based on a tetrahexylammonium iodide and MgI_2 binary iodide system. *Physical Chemistry Chemical Physics*, *14*(24), 8620-8627.

Bard, A. J., and Faulkner, L. R. (1980). *Electrochemical methods: fundamentals and applications* (Vol. 2): Wiley New York.

Bari, D., Wrachien, N., Tagliaferro, R., Brown, T. M., Reale, A., Di Carlo, A., . . . Cester, A. (2012). Reliability study of dye-sensitized solar cells by means of solar simulator and white LED. *Microelectronics Reliability, 52*(9), 2495-2499.

Baskaran, R., Selvasekarapandian, S., Kuwata, N., Kawamura, J., and Hattori, T. (2006). Conductivity and thermal studies of blend polymer electrolytes based on PVAc–PMMA. *Solid State Ionics, 177*(26–32), 2679-2682.

Basri, N., Ibrahim, S., and Mohamed, N. (2011). *PVDF-HFP/PVC Blend Based Lithium Ion Conducting Polymer Electrolytes.* Paper presented at the Advanced Materials Research.

Bella, F., and Bongiovanni, R. (2013). Photoinduced polymerization: an innovative, powerful and environmentally friendly technique for the preparation of polymer electrolytes for dye-sensitized solar cells. *Journal of Photochemistry and Photobiology C: Photochemistry Reviews, 16*, 1-21.

Bella, F., Imperiyka, M., and Ahmad, A. (2014). Photochemically produced quasi-linear copolymers for stable and efficient electrolytes in dye-sensitized solar cells. *Journal of Photochemistry and Photobiology A: Chemistry, 289*(0), 73-80.

Bella, F., Ozzello, E. D., Bianco, S., and Bongiovanni, R. (2013). Photo-polymerization of acrylic/methacrylic gel–polymer electrolyte membranes for dye-sensitized solar cells. *Chemical Engineering Journal, 225*, 873-879.

Bella, F., Ozzello, E. D., Sacco, A., Bianco, S., and Bongiovanni, R. (2014). Polymer electrolytes for dye-sensitized solar cells prepared by photopolymerization of PEG-based oligomers. *International Journal of Hydrogen Energy, 39*(6), 3036-3045.

Bella, F., Pugliese, D., Nair, J. R., Sacco, A., Bianco, S., Gerbaldi, C., . . . Bongiovanni, R. (2013). A UV-crosslinked polymer electrolyte membrane for quasi-solid dye-sensitized solar cells with excellent efficiency and durability. *Physical Chemistry Chemical Physics, 15*(11), 3706-3711.

Benkö, G., Kallioinen, J., Korppi-Tommola, J. E., Yartsev, A. P., and Sundström, V. (2002). Photoinduced ultrafast dye-to-semiconductor electron injection from nonthermalized and thermalized donor states. *Journal of the American Chemical Society, 124*(3), 489-493.

Bershteĭn, V. A., and Egorov, V. M. (1994). *Differential scanning calorimetry of polymers: physics, chemistry, analysis, technology*: Prentice Hall.

Bhargav, P. B., Mohan, V. M., Sharma, A. K., and Rao, V. V. R. N. (2007). Structural and electrical studies of sodium iodide doped poly(vinyl alcohol) polymer electrolyte films for their application in electrochemical cells. *Ionics, 13*(3), 173-178.

Bhargav, P. B., Mohan, V. M., Sharma, A. K., and Rao, V. V. R. N. (2009). Investigations on electrical properties of (PVA:NaF) polymer electrolytes for electrochemical cell applications. *Current Applied Physics, 9*(1), 165-171.

Bhattacharya, B., Lee, J. Y., Geng, J., Jung, H.-T., and Park, J.-K. (2009). Effect of cation size on solid polymer electrolyte based dye-sensitized solar cells. *Langmuir, 25*(5), 3276-3281.

Bhattacharya, B., Nagarale, R., and Singh, P. K. (2010). Effect of sodium-mixed anion doping in PEO-based polymer electrolytes. *High Performance Polymers, 22*(4), 498-512.

Boonsin, R., Sudchanham, J., Panusophon, N., Sae-Heng, P., Sae-Kung, C., and Pakawatpanurut, P. (2012). Dye-sensitized solar cell with poly (acrylic acid-co-acrylonitrile)-based gel polymer electrolyte. *Materials Chemistry and Physics, 132*(2), 993-998.

Bruce, P. G., Evans, J., and Vincent, C. A. (1988). Conductivity and transference number measurements on polymer electrolytes. *Solid State Ionics, 28–30, Part 2*(0), 918-922.

Bruce, P. G., Evans, J., and Vincent, C. A. (1988). Conductivity and transference number measurements on polymer electrolytes. *Solid State Ionics, 28*, 918-922.

Cahen, D., Hodes, G., Grätzel, M., Guillemoles, J. F., and Riess, I. (2000). Nature of photovoltaic action in dye-sensitized solar cells. *The Journal of Physical Chemistry B, 104*(9), 2053-2059.

Calhoun, A., and Voth, G. A. (1996). Electron transfer across the electrode/electrolyte interface: Influence of redox ion mobility and counterions. *Journal of Physical Chemistry, 100*(25), 10746-10753.

Campbell, I. M. (1994). *Introduction to synthetic polymers*: Oxford University Press, USA.

Cappel, U. B., Karlsson, M. H., Pschirer, N. G., Eickemeyer, F., Schöneboom, J., Erk, P., . . . Hagfeldt, A. (2009). A broadly absorbing perylene dye for solid-state dye-sensitized solar cells. *The Journal of Physical Chemistry C, 113*(33), 14595-14597.

Capuano, F., Croce, F., and Scrosati, B. (1991). Composite polymer electrolytes. *Journal of the Electrochemical Society, 138*(7), 1918-1922.

Caramori, S., Cristino, V., Boaretto, R., Argazzi, R., Bignozzi, C. A., and Di Carlo, A. (2010). New components for dye-sensitized solar cells. *International Journal of Photoenergy, 2010*.

Chakraborti, A. K., Sharma, L., and Nayak, M. K. (2002). Influence of hydrogen bonding in the activation of nucleophiles: PhSH-(catalytic) KF in N-methyl-2-pyrrolidone as an efficient protocol for selective cleavage of alkyl/aryl esters and aryl alkyl ethers under nonhydrolytic and neutral conditions. *The Journal of organic chemistry, 67*(8), 2541-2547.

Chandra, S., and Chandra, A. (1994). Solid state ionics: Materials aspect. Proceedings-*National Academy of Sciences India Section A*, *64*, 141-141.

Charlesby, A. (1965). Solid-state polymerization induced by radiation. *Reports on Progress in Physics, 28*(1), 463.

Chaurasia, S., Singh, R., and Chandra, S. (2014). Ionic liquid assisted modification in ionic conductivity, phase transition temperature and crystallization kinetics behaviour of polymer poly (ethylene oxide). *Solid State Ionics, 262*, 790-794.

Chen, Z., Hu, J., Tang, M., and Tian, Q. (2011). *The application of inorganic nanomaterials in dye-sensitized solar cells*: INTECH Open Access Publisher.

Chiodelli, G., Ferloni, P., Magistris, A., and Sanesi, M. (1988). Ionic conduction and thermal properties of poly (ethylene oxide)-lithium tetrafluoroborate films. *Solid State Ionics, 28-30*(PART 2), 1009-1013.

Coutts, T. J., Mason, T. O., Perkins, J., and Ginley, D. S. (1999). *Transparent conducting oxides: status and opportunities in basic research.* Paper presented at the Photovoltaics for the 21st Century: Proceedings of the International Symposium.

Cowie, J., MacCallum, J., and Vincent, C. (1987). Polymer Electrolyte Reviews-1: Elsevier, London.

Cowie, J., and Spence, G. (1998). Ion conduction in macroporous polyethylene film doped with electrolytes. *Solid State Ionics, 109*(1), 139-144.

Croce, F., Appetecchi, G., Persi, L., and Scrosati, B. (1998). Nanocomposite polymer electrolytes for lithium batteries. *Nature, 394*(6692), 456-458.

Croce, F., Persi, L., Ronci, F., and Scrosati, B. (2000). Nanocomposite polymer electrolytes and their impact on the lithium battery technology. *Solid State Ionics, 135*(1), 47-52.

Danley, R. L., Reader Jr, J. R., and Schaefer, J. W. (1998). Differential scanning calorimeter: Google Patents.

De Oliveira, H., dos Santos, M., Dos Santos, C., and De Melo, C. (2003). Electrical properties of PVA/PPY blends. *Synthetic metals, 135*, 447-448.

Decker, C. (1996). Photoinitiated crosslinking polymerisation. *Progress in Polymer Science, 21*(4), 593-650.

Dick, A. R., Hull, K. L., and Sanford, M. S. (2004). A highly selective catalytic method for the oxidative functionalization of CH bonds. *Journal of the American Chemical Society, 126*(8), 2300-2301.

Ding, Y., Zhang, P., Long, Z., Jiang, Y., Xu, F., and Di, W. (2009). The ionic conductivity and mechanical property of electrospun P(VdF-HFP)/PMMA membranes for lithium ion batteries. *Journal of Membrane Science, 329*(1), 56-59.

Dissanayake, M., Thotawatthage, C., Senadeera, G., Bandara, T., Jayasundera, W., and Mellander, B.-E. (2012). Efficiency enhancement by mixed cation effect in dye-sensitized solar cells with PAN based gel polymer electrolyte. *Journal of Photochemistry and Photobiology A: Chemistry, 246*, 29-35.

Dissanayake, M. A. K. L., Jayathissa, R., Seneviratne, V. A., Thotawatthage, C. A., Senadeera, G. K. R., and Mellander, B. E. (2014). Polymethylmethacrylate (PMMA) based quasi-solid electrolyte with binary iodide salt for efficiency enhancement in TiO2 based dye sensitized solar cells. *Solid State Ionics, 265*, 85-91.

Dissanayake, M. A. K. L., Thotawatthage, C. A., Senadeera, G. K. R., Bandara, T. M. W. J., Jayasundara, W. J. M. J. S. R., and Mellander, B. E. (2013). Efficiency enhancement in dye sensitized solar cells based on PAN gel electrolyte with Pr_4NI + MgI_2 binary iodide salt mixture. *Journal of Applied Electrochemistry, 43*(9), 891-901.

Drobny, J. G. (2010). *Radiation technology for polymers*: CRC press.

Eh, A. L. S., Lu, X., and Lee, P. S. (2015). Advances in Polymer Electrolytes for Electrochromic Applications. *Electrochromic Materials and Devices*, 289-310.

Elmér, A. M., Wesslén, B., Sommer-Larsen, P., West, K., Hassander, H., and Jannasch, P. (2003). Ion conductive electrolyte membranes based on co-continuous polymer blends. *Journal of Materials Chemistry, 13*(9), 2168-2176.

Enright, B., Redmond, G., and Fitzmaurice, D. (1994). Spectroscopic determination of flatband potentials for polycrystalline TiO_2 electrodes in mixed solvent systems. *The Journal of Physical Chemistry, 98*(24), 6195-6200.

Fan, L., Dang, Z., Nan, C.-W., and Li, M. (2002). Thermal, electrical and mechanical properties of plasticized polymer electrolytes based on PEO/P (VDF-HFP) blends. *Electrochimica Acta, 48*(2), 205-209.

Fan, L., Dang, Z., Wei, G., Nan, C.-W., and Li, M. (2003). Effect of nanosized ZnO on the electrical properties of (PEO) 16 $LiClO_4$ electrolytes. *Materials Science and Engineering: B, 99*(1), 340-343.

Frechet, J. M., Henmi, M., Gitsov, I., Aoshima, S., Leduc, M. R., and Grubbs, R. B. (1995). Self-condensing vinyl polymerization: an approach to dendritic materials. *Science-New York Then Washington-*, 1080-1080.

Freitas, F. S., Freitas, J. N. d., Ito, B. I., Paoli, M.-A. D., and Nogueira, A. F. (2009). Electrochemical and structural characterization of polymer gel electrolytes based on a PEO copolymer and an imidazolium-based ionic liquid for dye-sensitized solar cells. *ACS Applied Materials & Interfaces*, *1*(12), 2870-2877.

Fukui, A., Komiya, R., Yamanaka, R., Islam, A., and Han, L. (2006). Effect of a redox electrolyte in mixed solvents on the photovoltaic performance of a dye-sensitized solar cell. *Solar Energy Materials and Solar Cells*, *90*(5), 649-658.

Fuoss, R. M., and Kraus, C. A. (1933). Properties of electrolytic solutions. III. The dissociation constant. *Journal of the American Chemical Society*, *55*(3), 1019-1028.

Garnett, J. L. (1995). Radiation curing-twenty five years on. *Radiation Physics and Chemistry*, *46*(4-6 PART 2), 925-930.

Gerbaldi, C., Nair, J. R., Ahmad, S., Meligrana, G., Bongiovanni, R., Bodoardo, S., and Penazzi, N. (2010). UV-cured polymer electrolytes encompassing hydrophobic room temperature ionic liquid for lithium batteries. *Journal of Power Sources*, *195*(6), 1706-1713.

Giribabu, L., and Kanaparthi, R. K. (2013). Are porphyrins an alternative to ruthenium (II) sensitizers for dye-sensitized solar cells? *Current Science(Bangalore)*, *104*(7), 847-855.

Glatz-Reichenbach, J. K., Sorriero, L., and Fitzgerald, J. J. (1994). Influence of crosslinking on the molecular relaxation of an amorphous copolymer near its glass-transition temperature. *Macromolecules*, *27*(6), 1338-1343.

Gong, J., Liang, J., and Sumathy, K. (2012). Review on dye-sensitized solar cells (DSSCs): fundamental concepts and novel materials. *Renewable and Sustainable Energy Reviews*, *16*(8), 5848-5860.

Grätzel, M. (2001). Photoelectrochemical cells. *Nature*, *414*(6861), 338-344.

Grätzel, M. (2003). Dye-sensitized solar cells. *Journal of Photochemistry and Photobiology C: Photochemistry Reviews*, *4*(2), 145-153.

Grätzel, M. (2005). Dye-sensitized solid-state heterojunction solar cells. *MRS Bulletin*, *30*(01), 23-27.

Gray, F. M. (1991). *Solid polymer electrolytes*: VCH New Tork etc.

Günes, S., and Sariciftci, N. S. (2008). Hybrid solar cells. *Inorganica Chimica Acta, 361*(3), 581-588.

Guo, P., Guan, W., Liang, L., and Yao, P. (2008). Self-assembly of pH-sensitive random copolymers: Poly (styrene-co-4-vinylpyridine). *Journal of Colloid and Interface Science, 323*(2), 229-234.

Hagfeldt, A., Boschloo, G., Sun, L., Kloo, L., and Pettersson, H. (2010). Dye-sensitized solar cells. *Chemical Reviews, 110*(11), 6595-6663.

Hagfeldt, A., and Grätzel, M. (2000). Molecular photovoltaics. *Accounts of Chemical Research, 33*(5), 269-277.

Han, D., Zhu, L., Chen, Y., Li, W., and Feng, L. (2013). Synthesis and characterization of acrylic latex: Effects of fluorine and silicon components on properties of the latex copolymers. *Journal of Fluorine Chemistry, 156*, 38-44.

Hara, K., Kurashige, M., Dan-oh, Y., Kasada, C., Shinpo, A., Suga, S., . . . Arakawa, H. (2003). Design of new coumarin dyes having thiophene moieties for highly efficient organic-dye-sensitized solar cells. *New Journal of Chemistry, 27*(5), 783-785.

Hara, K., Sato, T., Katoh, R., Furube, A., Ohga, Y., Shinpo, A., . . . Arakawa, H. (2003). Molecular design of coumarin dyes for efficient dye-sensitized solar cells. *The Journal of Physical Chemistry B, 107*(2), 597-606.

Hardin, B. E., Snaith, H. J., and McGehee, M. D. (2012). The renaissance of dye-sensitized solar cells. *Nature Photonics, 6*(3), 162-169.

Hardy, L. C., and Shriver, D. F. (1985). Preparation and electrical response of solid polymer electrolytes with only one mobile species. *Journal of the American Chemical Society, 107*(13), 3823-3828.

Harrison, C., Park, M., Chaikin, P., Register, R. A., Adamson, D. H., and Yao, N. (1998). Depth profiling block copolymer microdomains. *Macromolecules, 31*(7), 2185-2189.

Harun, M. H., Saion, E., Kassim, A., Hussain, M. Y., Mustafa, I. S., and Omer, M. A. A. Temperature dependence of ac electrical conductivity of PVA-PPy-$FeCl_3$ composite polymer films.

Hatta, F., Yahya, M., Ali, A., Subban, R., Harun, M., and Mohamad, A. (2005). Electrical conductivity studies on PVA/PVP-KOH alkaline solid polymer blend electrolyte. *Ionics, 11*(5-6), 418-422.

Hiller, M. M., Gentschev, A.-C., Amereller, M., Gores, H., Winter, M., and Wiemhöfer, H. D. (2011). Salt-in-polymer electrolytes based on polysiloxanes for lithium-ion cells: ionic transport and electrochemical stability. *ECS Transactions, 33*(28), 3-15.

Hirata, N., Kroeze, J. E., Park, T., Jones, D., Haque, S. A., Holmes, A. B., and Durrant, J. R. (2006). Interface engineering for solid-state dye-sensitised nanocrystalline solar cells: the use of an organic redox cascade. *Chemical Communications*(5), 535-537.

Hou, X., and Siow, K. S. (2000). Mechanical properties and ionic conductivities of plasticized polymer electrolytes based on ABS/PMMA blends. *Polymer, 41*(24), 8689-8696.

Huo, P., and Cebe, P. (1992). Temperature-dependent relaxation of the crystal-amorphous interphase in poly (ether ether ketone). *Macromolecules, 25*(2), 902-909.

Hutchinson, R. A., and Penlidis, A. (2008). *Free-radical polymerization: Homogeneous systems*: Blackwell Publishing Ltd: Oxford, UK.

Ibrahim, S., Ahmad, A., and Mohamed, N. (2015). Synthesis and characterization of castor oil-based polyurethane for potential application as host in polymer electrolytes. *Bulletin of Materials Science, 38*(5), 1155-1161.

Ichino, T., Takeshima, Y., Takeshima, M., and Nishi, S. (1995). NTT Co. *Japanese Patent Publication*(07), 335258.

Imperiyka, M., Ahmad, A., Hanifah, S., and Bella, F. (2014). A UV-prepared linear polymer electrolyte membrane for dye-sensitized solar cells. *Physica B: Condensed Matter, 450*, 151-154.

Imperiyka, M., Ahmad, A., Hanifah, S., Mohamed, N., and Rahman, M. (2013). Investigation of plasticized UV-curable glycidyl methacrylate based solid polymer electrolyte for photoelectrochemical cell (PEC) application. *International Journal of Hydrogen Energy*.

Imperiyka, M., Ahmad, A., Hanifah, S., and Rahman, M. (2013). Potential of UV-Curable Poly (Glycidyl Methacrylate-co-Ethyl Methacrylate)-Based Solid Polymer Electrolyte For Lithium Ion Battery Application. *Int. J. Electrochem. Sci, 8*, 10932-10945.

Imperiyka, M., Ahmad, A., Hanifah, S., Rahman, M., and Mohamed, N. (2014). Preparation and Characterization of Ultraviolet-cured Polymer Electrolyte Poly (glycidyl methacrylate-co-methyl methacrylate). *Journal of New Materials for Electrochemical Systems, 17*(4), 213-217.

Imperiyka, M., Ahmad, A., Hanifah, S., and Rahman, M. Y. A. (2013). *Role of salt concentration lithium perchlorate on ionic conductivity and structural of (glycidyl methacrylate-co-ethyl methacrylate)(70/30) based on a solid polymer electrolyte.* Paper presented at the Advanced Materials Research.

Imperiyka, M., Ahmad, A., Hanifah, S., and Rahman, M. Y. A. (2013). Role of salt concentration lithium perchlorate on ionic conductivity and structural of (Glycidyl Methacrylate-co-Ethyl Methacrylate)(70/30) based on a solid polymer electrolyte. *Advanced Materials Research, 626*, 454-458.

Imperiyka, M., Ahmad, A., Hanifah, S. A., and Rahman, M. Y. A. (2014). Preparation and Characterization of Polymer Electrolyte of Glycidyl Methacrylate-Methyl Methacrylate-$LiClO_4$ Plasticized with Ethylene Carbonate. *International Journal of Polymer Science, 2014*, 7.

Jamil, M., Ali, A., Husnain, I., Mushtaq, W., Iqbal, N., and Khan, Z. S. (2015). *Effect of calcination on the particle size of nano-Nb_2O_5 for development as photo-anode material in advanced generation DSSCs.* Paper presented at the Power Generation System and Renewable Energy Technologies (PGSRET), 2015.

Jena, A., Mohanty, S. P., Kumar, P., Naduvath, J., Gondane, V., Lekha, P., . . . Bhargava, P. (2012). Dye sensitized solar cells: a review. *Transactions of the Indian Ceramic Society, 71*(1), 1-16.

Johansson, A., Gogoll, A., and Tegenfeldt, J. (1996). Diffusion and ionic conductivity in Li (CF_3SO_3) PEG_{10} and LiN (CF_3SO_2)$_2$ PEG_{10}. *Polymer, 37*(8), 1387-1393.

Kalaignan, G. P., and Kang, M.-S. (2006). Effects of compositions on properties of PEO–KI–I_2 salts polymer electrolytes for DSSC. *Solid State Ionics, 177*(11), 1091-1097.

Kalal, J., Švec, F., and Maroušek, V. (1974). *Reactions of epoxide groups of glycidyl methacrylate copolymers.* Paper presented at the Journal of Polymer Science: Polymer Symposia.

Kang, D.-W., Kim, D.-W., Jo, S. I., and Sohn, H.-J. (2002). Preparation and characterization of gel polymer electrolytes based on methyl methacrylate–styrene copolymers. *Journal of Power Sources, 112*(1), 1-7.

Kannan, M. (2012). Studies on thermoplastic polyurethanes based blends.

Karan, N. K., Pradhan, D. K., Thomas, R., Natesan, B., and Katiyar, R. S. (2008). Solid polymer electrolytes based on polyethylene oxide and lithium trifluoro- methane sulfonate (PEO–$LiCF_3SO_3$): Ionic conductivity and dielectric relaxation. *Solid State Ionics, 179*(19–20), 689-696.

Karo, A. M. (1959). Lattice Vibrations in Alkali Halide Crystals. I. Lithium and Sodium Halides. *The Journal of Chemical Physics, 31*(6), 1489-1499.

Kawano, R., and Watanabe, M. (2003). Equilibrium potentials and charge transport of an I^-/I_3^- redox couple in an ionic liquid. *Chemical Communications*(3), 330-331.

Kim, C. S., and Oh, S. M. (2000). Importance of donor number in determining solvating ability of polymers and transport properties in gel-type polymer electrolytes. *Electrochimica Acta, 45*(13), 2101-2109.

Kim, D.-W., Jeong, Y.-B., Kim, S.-H., Lee, D.-Y., and Song, J.-S. (2005). Photovoltaic performance of dye-sensitized solar cell assembled with gel polymer electrolyte. *Journal of Power Sources, 149*, 112-116.

Kim, D.-W., Kim, Y.-R., Park, J.-K., and Moon, S.-I. (1998). Electrical properties of the plasticized polymer electrolytes based on acrylonitrile-methyl methacrylate copolymers. *Solid State Ionics, 106*(3–4), 329-337.

Kim, S., Kim, D., Choi, H., Kang, M.-S., Song, K., Kang, S. O., and Ko, J. (2008). Enhanced photovoltaic performance and long-term stability of quasi-solid-state dye-sensitized solar cells via molecular engineering. *Chemical Communications*(40), 4951-4953.

Klein, R. J., Zhang, S., Dou, S., Jones, B. H., Colby, R. H., and Runt, J. (2006). Modeling electrode polarization in dielectric spectroscopy: ion mobility and mobile ion concentration of single-ion polymer electrolytes. *Journal of Chemical Physics, 124*(14), 144903-144903.

Kobayashi, N., Uchiyama, M., Shigehara, K., and Tsuchida, E. (1985). Ionically high conductive solid electrolytes composed of graft copolymer-lithium salt hybrids. *The Journal of Physical Chemistry, 89*(6), 987-991.

Kong, F.-T., Dai, S.-Y., and Wang, K.-J. (2007). Review of recent progress in dye-sensitized solar cells. *Advances in OptoElectronics, 2007*.

Kuang, D., Klein, C., Ito, S., Moser, J. E., Humphry-Baker, R., Evans, N., . . . Grätzel, M. (2007). High-Efficiency and Stable Mesoscopic Dye-Sensitized Solar Cells Based on a High Molar Extinction Coefficient Ruthenium Sensitizer and Nonvolatile Electrolyte. *Advanced Materials, 19*(8), 1133-1137.

Kubo, W., Kitamura, T., Hanabusa, K., Wada, Y., and Yanagida, S. (2002). Quasi-solid-state dye-sensitized solar cells using room temperature molten salts and a low molecular weight gelator. *Chemical Communications*(4), 374-375.

Kumar, D., and Hashmi, S. (2010). Ion transport and ion–filler-polymer interaction in poly (methyl methacrylate)-based, sodium ion conducting, gel polymer electrolytes dispersed with silica nanoparticles. *Journal of Power Sources, 195*(15), 5101-5108.

Kunze, M., Karatas, Y., Wiemhöfer, H.-D., and Schönhoff, M. (2012). Correlations of ion motion and chain motion in salt-in-polysiloxane-g-oligoether electrolytes. *Macromolecules, 45*(20), 8328-8335.

Latif, F., Aziz, M., Katun, N., Ali, A. M. M., and Yahya, M. Z. (2006). The role and impact of rubber in poly(methyl methacrylate)/lithium triflate electrolyte. *Journal of Power Sources, 159*(2), 1401-1404.

Le Nest, J. F., Callens, S., Gandini, A., and Armand, M. (1992). A new polymer network for ionic conduction. *Electrochimica Acta, 37*(9), 1585-1588.

Lee, J.-J., Ahammad, A. S., Lee, J. K., Rahman, M. M., Nath, N. D., and Sarker, S. (2011). *Metal oxides and their composites for the photoelectrode of dye sensitized solar cells*: INTECH Open Access Publisher.

Lee, J.-K., and Yang, M. (2011). Progress in light harvesting and charge injection of dye-sensitized solar cells. *Materials Science and Engineering: B, 176*(15), 1142-1160.

Lee, S. V., Usop, R., Noral Hadi, A., Mazni, N. A., Majid, S. R., Arof, A., . . . Balakrishnan, V. (2015). Comparison study on the effect of acid and nitrate salt on the properties of poly (vinyl alcohol) coating doped with dye consist of anthocyanin. *Pigment & Resin Technology, 44*(4).

Lenzmann, F., Krueger, J., Burnside, S., Brooks, K., Grätzel, M., Gal, D., . . . Cahen, D. (2001). Surface photovoltage spectroscopy of dye-sensitized solar cells with TiO_2, Nb_2O_5, and $SrTiO_3$ nanocrystalline photoanodes: Indication for electron injection from higher excited dye states. *The Journal of Physical Chemistry B, 105*(27), 6347-6352.

Lewandowski, A., Zajder, M., Frąckowiak, E., and Béguin, F. (2001). Supercapacitor based on activated carbon and polyethylene oxide–KOH–H_2O polymer electrolyte. *Electrochimica Acta, 46*(18), 2777-2780.

Lewis, N. S. (2007). Toward cost-effective solar energy use. *Science, 315*(5813), 798-801.

Li, B., Wang, L., Kang, B., Wang, P., and Qiu, Y. (2006). Review of recent progress in solid-state dye-sensitized solar cells. *Solar Energy Materials and Solar Cells, 90*(5), 549-573.

Li, G., Li, Z., Zhang, P., Zhang, H., and Wu, Y. (2008). Research on a gel polymer electrolyte for Li-ion batteries. *Pure and Applied Chemistry, 80*(11), 2553-2563.

Li, Q., Wu, J., Tang, Z., Xiao, Y., Huang, M., and Lin, J. (2010). Application of poly (acrylic acid-g-gelatin)/polypyrrole gel electrolyte in flexible quasi-solid-state dye-sensitized solar cell. *Electrochimica Acta, 55*(8), 2777-2781.

Li, R., Liu, D., Zhou, D., Shi, Y., Wang, Y., and Wang, P. (2010). Influence of the electrolyte cation in organic dye-sensitized solar cells: lithium versus dimethylimidazolium. *Energy & Environmental Science, 3*(11), 1765-1772.

Li, Z., Zhou, Y., Sun, R., Xiong, Y., Xie, H., and Zou, Z. (2014). Nanostructured SnO_2 photoanode-based dye-sensitized solar cells. *Chinese Science Bulletin, 59*(18), 2122-2134.

Liew, C.-W., Ramesh, S., and Arof, A. K. (2014). Good prospect of ionic liquid based-poly(vinyl alcohol) polymer electrolytes for supercapacitors with excellent electrical, electrochemical and thermal properties. *International Journal of Hydrogen Energy, 39*(6), 2953-2963.

Lin, D., Liu, W., Liu, Y., Lee, H. R., Hsu, P.-C., Liu, K., and Cui, Y. (2015). High ionic conductivity of composite solid polymer electrolyte via in situ synthesis of monodispersed SiO_2 nanospheres in poly (ethylene oxide). *Nano Letters*.

Lin, L.-Y., Lee, C.-P., Vittal, R., and Ho, K.-C. (2011). Improving the durability of dye-sensitized solar cells through back illumination. *Journal of Power Sources, 196*(3), 1671-1676.

Liu, B., Wang, R., Mi, W., Li, X., and Yu, H. (2012). Novel branched coumarin dyes for dye-sensitized solar cells: significant improvement in photovoltaic performance by simple structure modification. *Journal of Materials Chemistry, 22*(30), 15379-15387.

Liu, H., Avrutin, V., Izyumskaya, N., Özgür, Ü., and Morkoç, H. (2010). Transparent conducting oxides for electrode applications in light emitting and absorbing devices. *Superlattices and Microstructures, 48*(5), 458-484.

Liu, X., Kim, J.-S., Wu, J., and Eisenberg, A. (2005). Bowl-Shaped Aggregates from the Self-Assembly of an Amphiphilic Random Copolymer of Poly (styrene-co-methacrylic acid). *Macromolecules, 38*(16), 6749-6751.

Liu, Y., Hagfeldt, A., Xiao, X.-R., and Lindquist, S.-E. (1998). Investigation of influence of redox species on the interfacial energetics of a dye-sensitized nanoporous TiO_2 solar cell. *Solar Energy Materials and Solar Cells, 55*(3), 267-281.

Luo, X., Hu, X., Zhao, X., Goh, S., and Li, X. (2003). Miscibility and interactions in blends and complexes of poly (4-methyl-5-vinylthiazole) with proton-donating polymers. *Polymer, 44*(18), 5285-5291.

Lyon, L. A., and Hupp, J. T. (1995). Energetics of semiconductor electrode/solution interfaces: EQCM evidence for charge-compensating cation adsorption and intercalation during accumulation layer formation in the titanium dioxide/acetonitrile system. *The Journal of Physical Chemistry, 99*(43), 15718-15720.

Macdonald, J. R., and Barsoukov, E. (2005). Impedance spectroscopy: theory, experiment, and applications. *History, 1*, 8.

Mahesh, D., and Rajesh, J. (2012). TiO_2 Microstructure, Fabrication of thin Film Solar Cells and Introduction to Dye Sensitized Solar Cells. *Research Journal of Recent Sciences, 2277*, 2502.

Martens, C. R. (1961). *Alkyd resins* (Vol. 21): Reinhold Publishing Corporation.

Mastroianni, S., Lanuti, A., Brown, T. M., Argazzi, R., Caramori, S., Reale, A., and Di Carlo, A. (2012). Reverse bias degradation in dye solar cells. *Applied Physics Letters, 101*(12), 123302.

Mauritz, K. A. (1989). Dielectric relaxation studies of ion motions in electrolyte-containing perfluorosulfonate ionomers. 4. Long-range ion transport. *Macromolecules, 22*(12), 4483-4488.

Meng, Q.-B., Takahashi, K., Zhang, X.-T., Sutanto, I., Rao, T., Sato, O., . . . Uragami, M. (2003). Fabrication of an efficient solid-state dye-sensitized solar cell. *Langmuir, 19*(9), 3572-3574.

Mobarak, N. N., and Abdullah, M. P. (2010). Synthesis and characterization of several lauryl chitosan derivatives. *Malaysian Journal of Analytical Sciences, 14*(2), 82-99.

Mobarak, N. N., Ahmad, A., Abdullah, M. P., Ramli, N., and Rahman, M. Y. A. (2013). Conductivity enhancement via chemical modification of chitosan based green polymer electrolyte. *Electrochimica Acta, 92*, 161-167.

Mohammad, S., Zainal, N., Ibrahim, S., and Mohamed, N. (2013). Conductivity enhancement of (epoxidized natural rubber 50)/poly (ethyl methacrylate)–ionic liquid-ammonium triflate. *Int. J. Electrochem. Sci, 8,* 6145-6153.

Mohmeyer, N., Kuang, D., Wang, P., Schmidt, H.-W., Zakeeruddin, S. M., and Grätzel, M. (2006). An efficient organogelator for ionic liquids to prepare stable quasi-solid-state dye-sensitized solar cells. *Journal of Materials Chemistry, 16*(29), 2978-2983.

Nagaoka, K., Naruse, H., Shinohara, I., and Watanabe, M. (1984). High ionic conductivity in poly (dimethyl siloxane-co-ethylene oxide) dissolving lithium perchlorate. *Journal of Polymer Science: Polymer Letters Edition, 22*(12), 659-663.

Nagarale, R., Shin, W., and Singh, P. K. (2010). Progress in ionic organic-inorganic composite membranes for fuel cell applications. *Polymer Chemistry, 1*(4), 388-408.

Nair, J., Gerbaldi, C., Meligrana, G., Bongiovanni, R., Bodoardo, S., Penazzi, N., . . . Gentili, V. (2008). UV-cured methacrylic membranes as novel gel–polymer electrolyte for Li-ion batteries. *Journal of Power Sources, 178*(2), 751-757.

Narayan, M. R. (2012). Review: dye sensitized solar cells based on natural photosensitizers. *Renewable and Sustainable Energy Reviews, 16*(1), 208-215.

Nasirtabrizi, M. H., Mohebalizadeh, S., and Parchehbaf Jadid, A. (2011). Glycidyl methacrylate polymers containing indole groups: synthesis and characterization. *Iran Polym J, 20*(7), 579-586.

Nazeeruddin, M. K., Kay, A., Rodicio, I., Humphry-Baker, R., Müller, E., Liska, P., . . . Grätzel, M. (1993). Conversion of light to electricity by cis-X_2bis (2, 2'-bipyridyl-4, 4'-dicarboxylate) ruthenium (II) charge-transfer sensitizers (X= Cl^-, Br^-, I^-, CN^-, and SCN^-) on nanocrystalline titanium dioxide electrodes. *Journal of the American Chemical Society, 115*(14), 6382-6390.

Negro, S. O., Alkemade, F., and Hekkert, M. P. (2012). Why does renewable energy diffuse so slowly? A review of innovation system problems. *Renewable and Sustainable Energy Reviews, 16*(6), 3836-3846.

Ng, H., Ramesh, S., and Ramesh, K. (2015). Efficiency improvement by incorporating 1-methyl-3-propylimidazolium iodide ionic liquid in gel polymer electrolytes for dye-sensitized solar cells. *Electrochimica Acta*.

Ng, L., and Mohamad, A. (2008). Effect of temperature on the performance of proton batteries based on chitosan–NH_4NO_3–EC membrane. *Journal of Membrane Science, 325*(2), 653-657.

Nogueira, A., Longo, C., and De Paoli, M.-A. (2004). Polymers in dye sensitized solar cells: overview and perspectives. *Coordination Chemistry Reviews, 248*(13), 1455-1468.

Nogueira, A. F., De Paoli, M.-A., Montanari, I., Monkhouse, R., Nelson, J., and Durrant, J. R. (2001). Electron transfer dynamics in dye sensitized nanocrystalline solar cells using a polymer electrolyte. *The Journal of Physical Chemistry B, 105*(31), 7517-7524.

Noor, S. A. M., Bayley, P. M., Forsyth, M., and MacFarlane, D. R. (2013). Ionogels based on ionic liquids as potential highly conductive solid state electrolytes. *Electrochimica Acta, 91*, 219-226.

Noor, S. A. M., Howlett, P. C., MacFarlane, D. R., and Forsyth, M. (2013). Properties of sodium-based ionic liquid electrolytes for sodium secondary battery applications. *Electrochimica Acta, 114*, 766-771.

Noor, S. A. M., Yoon, H., Forsyth, M., and MacFarlane, D. R. (2015). Gelled ionic liquid sodium ion conductors for sodium batteries. *Electrochimica Acta, 169*, 376-381.

O'Regan, B., and Grätzel, M. (1991). A low-cost, high-efficiency solar cell based on dye-sensitized colloidal TiO_2 films. *Nature, 353*(6346), 737-740.

Oh, B., Sun, Y. K., and Kim, D. W. (2001). Electrochemical properties of gel polymer electrolytes prepared by poly (vinyl acetate) copolymers. *BULLETIN-KOREAN CHEMICAL SOCIETY, 22*(10), 1136-1140.

Omar, A., and Abdullah, H. (2014). Electron transport analysis in zinc oxide-based dye-sensitized solar cells: A review. *Renewable and Sustainable Energy Reviews, 31*, 149-157.

Pal, S., Roy, S. G., and De, P. (2014). Synthesis via RAFT polymerization of thermo-and pH-responsive random copolymers containing cholic acid moieties and their self-assembly in water. *Polymer Chemistry, 5*(4), 1275-1284.

Patel, M. G., Patel, H. J., Patel, K. H., Patel, R. M., and Vidyanagar, V. (2008). Synthesis and Characterization of Novel Acrylic Copolymers: Determination of Monomer Reactivity Ratios and Antimicrobial Activity. *Malaysian Polymer Journal, 3*(1), 14-26.

Patel, R. J., Patel, Z. R., and Patel, K. H. (2012). Novel Acrylic copolymers based on Schiff base: Synthesis, characterization and antimicrobial activity. *Journal of Chemical & Pharmaceutical Research, 4*(12).

Pavia, D. L., Lampman, G., Kriz, G., and Engel, R. (2005). *Introduction to organic laboratory techniques: a small scale approach* (Vol. 6): Thomson Brooks/Cole Belmont, CA.

Pomposo, J., De Juana, R., Mugica, A., Cortazar, M., and Gomez, M. (1996). Binary poly (ethylene oxide)/poly (methyl methacrylate-co-ethyl methacrylate) blends: Miscibility predictions from model compound mixtures vs experimental phase behavior. *Macromolecules, 29*(22), 7038-7046.

Prabakaran, K., Mohanty, S., and Nayak, S. (2015). PEO/PVdF–HFP electrolytes for natural dye sensitized solar cell applications: effect of modified nano-TiO_2 on electrochemical and photovoltaic performance. *Journal of Materials Science: Materials in Electronics, 26*(6), 3887-3897.

Preat, J., Jacquemin, D., and Perpète, E. A. (2010). Towards new efficient dye-sensitised solar cells. *Energy & Environmental Science, 3*(7), 891-904.

Qin, Y., and Peng, Q. (2012). Ruthenium sensitizers and their applications in dye-sensitized solar cells. *International Journal of Photoenergy, 2012*.

Rahman, M., Salleh, M., Talib, I., and Yahaya, M. (2007). Light intensity and temperature dependence on performance of a photoelectrochemical cells of ITO/TiO_2/PVC-$LiClO_4$/graphite. *Ionics, 13*(4), 241-244.

Rajendran, S., Prabhu, M. R., and Rani, M. U. (2008). Ionic conduction in poly (vinyl chloride)/poly (ethyl methacrylate)-based polymer blend electrolytes complexed with different lithium salts. *Journal of Power Sources, 180*(2), 880-883.

Rajendran, S., Ramesh Prabhu, M., and Usha Rani, M. (2008). Characterization of PVC/PEMA based polymer blend electrolytes. *Int J Electrochem Sci, 3*, 282-290.

Rajendran, S., Sivakumar, M., and Subadevi, R. (2004). Investigations on the effect of various plasticizers in PVA-PMMA solid polymer blend electrolytes. *Materials letters, 58*(5), 641-649.

Rajendran, S., and Uma, T. (2000). Lithium ion conduction in PVC-$LiBF_4$ electrolytes gelled with PMMA. *Journal of Power Sources, 88*(2), 282-285.

Ramesh, S., and Arof, A. (2001). Ionic conductivity studies of plasticized poly (vinyl chloride) polymer electrolytes. *Materials Science and Engineering: B, 85*(1), 11-15.

Ramesh, S., and Lu, S.-C. (2008). Effect of nanosized silica in poly(methyl methacrylate)–lithium bis(trifluoromethanesulfonyl)imide based polymer electrolytes. *Journal of Power Sources, 185*(2), 1439-1443.

Ramesh, S., Uma, O., Shanti, R., Yi, L. J., and Ramesh, K. (2014). Preparation and characterization of poly (ethyl methacrylate) based polymer electrolytes doped with 1-butyl-3-methylimidazolium trifluoromethanesulfonate. *Measurement, 48*, 263-273.

Rani, M. S. A., Rudhziah, S., Ahmad, A., and Mohamed, N. S. (2014). Biopolymer Electrolyte Based on Derivatives of Cellulose from Kenaf Bast Fiber. *Polymers, 6*(9), 2371-2385.

Ratner, M., MacCallum, J., and Vincent, C. (1987). Polymer electrolyte reviews. *Elsevier, London*, 173-236.

Ratner, M. A., and Shriver, D. F. (1988). Ion transport in solvent-free polymers. *Chemical Reviews, 88*(1), 109-124.

Reddy, G. J., Reddy, M. M., Reddy, G. R., Naidu, S. V., and Reddy, A. R. (2010). Poly (n-phenyl methacrylamide-co-ethyl methacrylate): synthesis, characterization and determination of reactivity ratios. *Malays Polym J, 5*, 68-80.

Redmond, G., and Fitzmaurice, D. (1993). Spectroscopic determination of flatband potentials for polycrystalline titania electrodes in nonaqueous solvents. *The Journal of Physical Chemistry, 97*(7), 1426-1430.

Riley, M., Fedkiw, P. S., and Khan, S. A. (2002). Transport properties of lithium hectorite-based composite electrolytes. *Journal of the Electrochemical Society, 149*(6), A667-A674.

Roy, S. G., Bauri, K., Pal, S., Goswami, A., Madras, G., and De, P. (2013). Synthesis, characterization and thermal degradation of dual temperature-and pH-sensitive RAFT-made copolymers of N, N-(dimethylamino) ethyl methacrylate and methyl methacrylate. *Polymer International, 62*(3), 463-473.

Rudhziah, S., Muda, N., Ibrahim, S., Rahman, A., and Mohamed, N. (2011). Studies on Proton Conducting Polymer Electrolytes Based on PVDF-HFP and PVDF-HFP/PEMA Blend.

Rudhziah, S., Rani, M. S. A., Ahmad, A., Mohamed, N. S., and Kaddami, H. (2015). Potential of blend of kappa-carrageenan and cellulose derivatives for green polymer electrolyte application. *Industrial Crops and Products, 72*, 133-141.

Sagane, F., Abe, T., Iriyama, Y., and Ogumi, Z. (2005). Li^+ and Na^+ transfer through interfaces between inorganic solid electrolytes and polymer or liquid electrolytes. *Journal of Power Sources, 146*(1), 749-752.

Saikia, D., and Kumar, A. (2004). Ionic conduction in P(VDF-HFP)/PVDF–(PC + DEC)–$LiClO_4$ polymer gel electrolytes. *Electrochimica Acta, 49*(16), 2581-2589.

Saikia, D., Wu, H.-Y., Pan, Y.-C., Lin, C.-P., Huang, K.-P., Chen, K.-N., . . . Kao, H.-M. (2011). Highly conductive and electrochemically stable plasticized blend polymer electrolytes based on PVdF-HFP and triblock copolymer PPG-PEG-PPG diamine for Li-ion batteries. *Journal of Power Sources*, *196*(5), 2826-2834.

Sako, M., Kihara, T., Okada, K., Ohtani, Y., and Kawamoto, H. (2001). Reductive Cleavage of Heteroaryl C-Halogen Bonds by Iodotrimethylsilane. Facile and Regioselective Dechlorination of Antibiotic Pyrrolnitrin. *The Journal of organic chemistry, 66*(10), 3610-3612.

Sao, C. N. (2009). *Dye-sensitized solar cells based on perylene derivatives.*

Sariciftci, N., Smilowitz, L., Heeger, A. J., and Wudl, F. (1992). Photoinduced electron transfer from a conducting polymer to buckminsterfullerene. *Science, 258*(5087), 1474-1476.

Schwanitz, K. C. N. (2008). *The TiO2/Dye/Electrolyte Interface in the Dye Sensitized Solar Cell: A Synchrotron Induced Photoelectron Spectroscopy Study*. TU Darmstadt.

Scrosati, B. (1993). *Applications of electroactive polymers* (Vol. 75): Springer.

Scrosati, B., Neat, R., and Scrosati, B. (1997). Applications of Electroactive Polymers, 1993. *Gray, FM," Polymer Electrolytes*.

Selvasekarapandian, S., Baskaran, R., Kamishima, O., Kawamura, J., and Hattori, T. (2006). Laser Raman and FTIR studies on Li^+ interaction in PVAc–$LiClO_4$ polymer electrolytes. *Spectrochimica Acta Part A: Molecular and Biomolecular Spectroscopy*, *65*(5), 1234-1240.

Seo, D. W., Parvez, M. K., Lee, S. H., Kim, J. H., Kim, S. R., Lim, Y. D., and Kim, W. G. (2011). Synthesis of acetyl imidazolium-based electyrolytes and application for dye-sensitized solar cells. *Electrochimica Acta*, *57*, 285-289.

Seo, Y. G., Woo, K., Kim, J., Lee, H., and Lee, W. (2011). Rapid fabrication of an inverse opal TiO2 photoelectrode for DSSC using a binary mixture of TiO_2 nanoparticles and polymer microspheres. *Advanced Functional Materials, 21*(16), 3094-3103.

Shi, J., and Vincent, C. A. (1993). The effect of molecular weight on cation mobility in polymer electrolytes. *Solid State Ionics, 60*(1), 11-17.

Shi, Y., Wang, Y., Zhang, M., and Dong, X. (2011). Influences of cation charge density on the photovoltaic performance of dye-sensitized solar cells: lithium, sodium, potassium, and dimethylimidazolium. *Physical Chemistry Chemical Physics, 13*(32), 14590-14597.

Shukla, N., Thakur, A. K., Shukla, A., and Marx, D. T. (2014). Ion Conduction Mechanism in Solid Polymer Electrolyte: An Applicability of Almond-West Formalism. *Int. J. Electrochem. Sci, 9*, 7644-7659.

Sichina, W. (2000). Measurement of T_g by DSC. *PerkinElmer, Application note*.

Silva, M. M., Barros, S. C., Smith, M. J., and MacCallum, J. R. (2004). Characterization of solid polymer electrolytes based on poly(trimethylenecarbonate) and lithium tetrafluoroborate. *Electrochimica Acta, 49*(12), 1887-1891.

Singh, P. K., Bhattacharya, B., Mehra, R., and Rhee, H.-W. (2011). Plasticizer doped ionic liquid incorporated solid polymer electrolytes for photovoltaic application. *Current Applied Physics, 11*(3), 616-619.

Singh, P. K., Jadhav, N. A., Mishra, S., Singh, U., and Bhattacharya, B. (2010). Application of ionic liquid doped solid polymer electrolyte. *Ionics, 16*(7), 645-648.

Singh, P. K., Kim, K.-W., and Rhee, H.-W. (2008). Electrical, optical and photoelectrochemical studies on a solid PEO-polymer electrolyte doped with low viscosity ionic liquid. *Electrochemistry Communications, 10*(11), 1769-1772.

Singh, P. K., Kim, K. W., and Rhee, H. W. (2009). Ionic liquid (1-methyl 3-propyl imidazolium iodide) with polymer electrolyte for DSSC application. *Polymer Engineering and Science, 49*(5), 862-865.

Sivakumar, M., Subadevi, R., Rajendran, S., Wu, H.-C., and Wu, N.-L. (2007). Compositional effect of PVdF–PEMA blend gel polymer electrolytes for lithium polymer batteries. *European Polymer Journal, 43*(10), 4466-4473.

Slobodian, P., Svoboda, P., Riha, P., Boruta, R., and Saha, P. (2012). Synthesis of PMMA-co-PMAA Copolymer Brush on Multi-Wall Carbon Nanotubes. *Journal of Surface Engineered Materials and Advanced Technology, 2*(03), 221.

Smitha, B., Sridhar, S., and Khan, A. A. (2005). Solid polymer electrolyte membranes for fuel cell applications—a review. *Journal of Membrane Science, 259*(1–2), 10-26.

Song, M.-K., Cho, J.-Y., Cho, B. W., and Rhee, H.-W. (2002). Characterization of UV-cured gel polymer electrolytes for rechargeable lithium batteries. *Journal of Power Sources, 110*(1), 209-215.

Soykan, C., Ahmedzade, M., and Coşkun, M. (2000). Copolymers of phenacyl methacrylate with glycidyl methacrylate: synthesis, characterization and monomer reactivity ratios. *European Polymer Journal, 36*(8), 1667-1675.

Stadler, A. (2012). Transparent conducting oxides—An up-to-date overview. *Materials, 5*(4), 661-683.

Strub, H. (2008). Photopolymerisation: développements industriels. *L'Actualité chimique*(317), 22-24.

Su'ait, M., Ahmad, A., Hamzah, H., and Rahman, M. (2009). Preparation and characterization of PMMA–MG49–$LiClO_4$ solid polymeric electrolyte. *Journal of Physics D: Applied Physics, 42*(5), 055410.

Su'ait, M. S., Ahmad, A., Badri, K. H., Mohamed, N. S., Rahman, M. Y. A., Ricardo, C. L. A., and Scardi, P. (2014). The potential of polyurethane bio-based solid polymer electrolyte for photoelectrochemical cell application. *International Journal of Hydrogen Energy, 39*(6), 3005-3017.

Su’ait, M., Ahmad, A., Hamzah, H., and Rahman, M. (2011). Effect of lithium salt concentrations on blended 49% poly (methyl methacrylate) grafted natural rubber and poly (methyl methacrylate) based solid polymer electrolyte. *Electrochimica Acta, 57*, 123-131.

Su’ait, M., Rahman, M., and Ahmad, A. (2015). Review on polymer electrolyte in dye-sensitized solar cells (DSSCs). *Solar Energy, 115*, 452-470.

Subba, R. C. V., Sharma, A., and Narasimha, R. V. (2003). Conductivity and discharge characteristics of polyblend (PVP+ PVA+ KIO_3) electrolyte. *Journal of Power Sources, 114*(2), 338-345.

Subban, R. H. Y. (2004). *Some properties of plasticized and composite PVC-based polymer electrolytes and $LiCoO_2$/PVC-$LiCF_3SO_3$-SiO_2/MCMB electrochemical cells* (PhD Thesis), University of Malaya.

Sundaram, N. K., Musthafa, O. M., Lokesh, K., and Subramania, A. (2008). Effect of porosity on PVdF-co-HFP–PMMA-based electrolyte. *Materials Chemistry and Physics, 110*(1), 11-16.

Suri, P., and Mehra, R. M. (2007). Effect of electrolytes on the photovoltaic performance of a hybrid dye sensitized ZnO solar cell. *Solar Energy Materials and Solar Cells, 91*(6), 518-524.

Szczepanski, C. R., Pfeifer, C. S., and Stansbury, J. W. (2012). A new approach to network heterogeneity: polymerization induced phase separation in photo-initiated, free-radical methacrylic systems. *Polymer, 53*(21), 4694-4701.

Szczepanski, C. R., and Stansbury, J. W. (2015). Modification of linear prepolymers to tailor heterogeneous network formation through photo-initiated polymerization-induced phase separation. *Polymer, 70*, 8-18.

Tang, Z., Liu, Q., Tang, Q., Wu, J., Wang, J., Chen, S., . . . Lin, J. (2011). Preparation of PAA-g-CTAB/PANI polymer based gel-electrolyte and the application in quasi-solid-state dye-sensitized solar cells. *Electrochimica Acta, 58*, 52-57.

Tarascon, J.-M., Gozdz, A., Schmutz, C., Shokoohi, F., and Warren, P. (1996). Performance of Bellcore's plastic rechargeable Li-ion batteries. *Solid State Ionics, 86*, 49-54.

Tennakone, K., Kumara, G., Kumarasinghe, A., Wijayantha, K., and Sirimanne, P. (1995). A dye-sensitized nano-porous solid-state photovoltaic cell. *Semiconductor Science and Technology, 10*(12), 1689.

Thokchom, J. S., Chen, C., Abraham, K. M., and Kumar, B. (2005). High conductivity electrolytes in the PEOx : LLLLLL iN($SO_2CF_2CF_3$)$_2$ -Al_2O_3 system. *Solid State Ionics, 176*(23-24), 1887-1893.

Thomas, S., Deepak, T., Anjusree, G., Arun, T., Nair, S. V., and Nair, A. S. (2014). A review on counter electrode materials in dye-sensitized solar cells. *Journal of Materials Chemistry A, 2*(13), 4474-4490.

Tsuchida, E., Ohno, H., and Kobayashi, N. (1988). Single-ion conduction in poly [(oligo (oxyethylene) methacrylate)-co-(alkali-metal methacrylates)]. *Macromolecules, 21*(1), 96-100.

Venkatesh, G., Gilbert, R., and Fornes, R. (1985). Fourier transform infra-red spectroscopy of nylon-6 blends: binary blends with poly (methyl methacrylate) and ethylene vinyl ester/alcohol copolymer. *Polymer, 26*(1), 45-49.

Wagner, J. B., and Wagner, C. (1957). Electrical conductivity measurements on cuprous halides. *The Journal of Chemical Physics, 26*(6), 1597-1601.

Wang, J. (2006). *Analytical electrochemistry*: John Wiley & Sons.

Wang, P., Zakeeruddin, S. M., Moser, J.-E., Humphry-Baker, R., and Grätzel, M. (2004). A solvent-free, $SeCN^-/(SeCN)_3^-$ based ionic liquid electrolyte for high-efficiency dye-sensitized nanocrystalline solar cells. *Journal of the American Chemical Society, 126*(23), 7164-7165.

Weerasinghe, H. C., Huang, F., and Cheng, Y.-B. (2013). Fabrication of flexible dye sensitized solar cells on plastic substrates. *Nano Energy, 2*(2), 174-189.

Winie, T., and Arof, A. (2004). Dielectric behaviour and AC conductivity of $LiCF_3SO_3$ doped H-chitosan polymer films. *Ionics, 10*(3-4), 193-199.

Wright, P. V. (1975). Electrical conductivity in ionic complexes of poly (ethylene oxide). *British Polymer Journal, 7*(5), 319-327.

Wu, J., Lan, Z., Hao, S., Li, P., Lin, J., Huang, M., . . . Huang, Y. (2008). Progress on the electrolytes for dye-sensitized solar cells. *Pure and Applied Chemistry, 80*(11), 2241-2258.

Wu, J., Lan, Z., Lin, J., Huang, M., Hao, S., and Fang, L. (2007). Influence of solvent on the poly (acrylic acid)-oligo-(ethylene glycol) polymer gel electrolyte and the performance of quasi-solid-state dye-sensitized solar cells. *Electrochimica Acta, 52*(24), 7128-7135.

Wu, J., Lan, Z., Lin, J., Huang, M., and Li, P. (2007). Effect of solvents in liquid electrolyte on the photovoltaic performance of dye-sensitized solar cells. *Journal of Power Sources, 173*(1), 585-591.

Wu, S. (1985). Phase structure and adhesion in polymer blends: a criterion for rubber toughening. *Polymer, 26*(12), 1855-1863.

Würfel, P., and Würfel, U. (2009). *Physics of solar cells: from basic principles to advanced concepts*: John Wiley & Sons.

Xia, J., Masaki, N., Jiang, K., and Yanagida, S. (2006). Deposition of a thin film of TiO_x from a titanium metal target as novel blocking layers at conducting glass/TiO_2 interfaces in ionic liquid mesoscopic TiO_2 dye-sensitized solar cells. *The Journal of Physical Chemistry B, 110*(50), 25222-25228.

Yagci, Y., Jockusch, S., and Turro, N. J. (2010). Photoinitiated polymerization: advances, challenges, and opportunities. *Macromolecules, 43*(15), 6245-6260.

Yagci, Y., Nuyken, O., and Graubner, V. (2005). In Encyclopedia of Polymer Science and Technology, ; Kroschwitz, JI, Ed: Wiley: New York.

Yamazaki, M., Soji, Y., Yoshimura, S., Nishio, K., and Saito, T. (1995). Sanyo Electric Co. *Japanese Patent Publication*(07), 320781.

Yan, L., Zhang, G., Liu, G., Ji, J., and Li, W. (2006). Emulsifier-free synthesis and self-assembly of an amphiphilic poly (styrene-co-acrylic acid) copolymer. *Journal of Applied Polymer Science, 100*(5), 3718-3726.

Yang, J. M., Wang, H. Z., and Yang, C. C. (2008). Modification and characterization of semi-crystalline poly (vinyl alcohol) with interpenetrating poly (acrylic acid) by UV radiation method for alkaline solid polymer electrolytes membrane. *Journal of Membrane Science, 322*(1), 74-80.

Yang, S., Kou, H., Wang, J., Xue, H., and Han, H. (2010). Tunability of the band energetics of nanostructured $SrTiO_3$ electrodes for dye-sensitized solar cells. *The Journal of Physical Chemistry C, 114*(9), 4245-4249.

Yang, Y., Zhang, J., Zhou, C., Wu, S., Xu, S., Liu, W., . . . Zhao, X.-z. (2008). Effect of Lithium Iodide Addition on Poly (ethylene oxide)− Poly (vinylidene fluoride) Polymer-Blend Electrolyte for Dye-Sensitized Nanocrystalline Solar Cell. *The Journal of Physical Chemistry B, 112*(21), 6594-6602.

Yella, A., Lee, H.-W., Tsao, H. N., Yi, C., Chandiran, A. K., Nazeeruddin, M. K., . . . Grätzel, M. (2011). Porphyrin-sensitized solar cells with cobalt (II/III)–based redox electrolyte exceed 12 percent efficiency. *Science, 334*(6056), 629-634.

Yu, L., Dean, K., and Li, L. (2006). Polymer blends and composites from renewable resources. *Progress in Polymer Science, 31*(6), 576-602.

Zadora, G., and Brożek-Mucha, Z. (2003). SEM–EDX—a useful tool for forensic examinations. *Materials Chemistry and Physics, 81*(2–3), 345-348.

Zafer, C., Kus, M., Turkmen, G., Dincalp, H., Demic, S., Kuban, B., . . . Icli, S. (2007). New perylene derivative dyes for dye-sensitized solar cells. *Solar Energy Materials and Solar Cells, 91*(5), 427-431.

Zhang, Z., Zhou, B., Ge, W., Xiong, B., Zheng, Q., and Cai, W. (2005). Charge recombination in dye-sensitized nanoporous TiO_2 solar cell. *Chinese Science Bulletin, 50*(21), 2408-2412.

Zhao, J., Wang, L., He, X., Wan, C., and Jiang, C. (2008). Determination of Lithium-Ion Transference Numbers in $LiPF_6$–PC Solutions Based on Electrochemical Polarization and NMR Measurements. *Journal of the Electrochemical Society, 155*(4), A292-A296.

LIST OF PUBLICATIONS, CONFERENCES AND AWARDS

PAPERS PUBLISHED

1. Dzulkurnain, N. A., Hanifah, S. A., Ahmad, A., & Mohamed, N. S. (2015). Characterization of Random Methacrylate Copolymers Synthesized Using Free-Radical Bulk Polymerization Method. *Int. J. Electrochem. Sci*, *10*, 84-92.

2. Dzulkurnain, N. A., Ahmad, A., & Mohamed, N. S. (2015). P (MMA-EMA) Random Copolymer Electrolytes Incorporating Sodium Iodide for Potential Application in a Dye-Sensitized Solar Cell. *Polymers*, *7*(2), 266-280.

3. Dzulkurnain, N.A., Ahmad, A. and Mohamed, N.S. (2016), Addition of 1 methyl-3 propyl imidazolium iodide into polymer electrolyte system for enhancement in dye sensitized solar cell efficiency. *Science of Advanced Materials*, *8*(1), 41-46.

PRESENTATION IN CONFERENCE

1. Dzulkurnain, N. A., Ahmad, A. and Mohamed, N. S. (2016), Comparative study on the properties of lithium and sodium salts containing P(MMA-co-EMA) polymer electrolytes and DSSC performance. Presented at 11th Annual International Electromaterials Science Symposium, Melbourne, Australia, 10 to 12 February 2016.
2. Dzulkurnain, N. A., Ahmad, A. and Mohamed, N. S. (2015), Preparation and characterization of ionic liquid based polymer electrolytes for application in dye sensitized solar cell. Presented at Materials Challenges in Alternative & Renewable Energy 2015, MCARE 2015, Jeju, Korea, 24 to 27 February 2015.

3. Dzulkurnain, N. A., Ahmad, A. and Mohamed, N. S. (2014), Structural and electrical properties of poly (methyl methacryate-co-ethyl methacrylate) based polymer electrolytes. Accepted for oral presentation in the 28th Regional Conference on Solid State Science and Technology, RCSSST 2014, Cameron Highland, Malaysia, 25 to 27 November 2015.

4. Dzulkurnain, N. A., Ahmad, A. and Mohamed, N. S. (2014), Characterization of P(MMA-EMA) Random Copolymer Electrolytes Incorporated with Sodium Iodide. Presented at XIV International Symposium on Polymer Electrolytes 2014, ISPE 14, Geelong, Australia, 24 – 29 August 2014.

AWARDS

1. **Silver Award** on Invention, Innovation & Design Exposition 2015 (IIDEX2015).

2. **'Student Travel Award'** ,The XIV International Symposium on Polymer Electrolytes 2014, Melbourne, Australia.